610-3

Copyright © 1968
Jet Propulsion Laboratory
California Institute of Technology

Prepared Under Contract No. NAS 7-100
National Aeronautics & Space Administration

REPRODUCED BY
NATIONAL TECHNICAL
INFORMATION SERVICE
U. S. DEPARTMENT OF COMMERCE
SPRINGFIELD, VA. 22161

FACILITY FORM 602

N 68 36667 (ACCESSION NUMBER)	(THRU)
123 (PAGES)	0 (CODE)
CR-97216 (NASA CR OR TMX OR AD NUMBER)	30 (CATEGORY)

JET PROPULSION LABORATORY
CALIFORNIA INSTITUTE OF TECHNOLOGY
PASADENA, CALIFORNIA

128

NOTICE

THIS DOCUMENT HAS BEEN REPRODUCED FROM THE BEST COPY FURNISHED US BY THE SPONSORING AGENCY. ALTHOUGH IT IS RECOGNIZED THAT CERTAIN PORTIONS ARE ILLEGIBLE, IT IS BEING RELEASED IN THE INTEREST OF MAKING AVAILABLE AS MUCH INFORMATION AS POSSIBLE.

MARINER MARS 1971

ORBITER STUDY REPORT

Technical Document 610-3

1 February 1968

John Casani

John R. Casani, Chairman
Mariner Mars 1971 Study Committ

JET PROPULSION LABORATORY
CALIFORNIA INSTITUTE OF TECHNOLOGY
PASADENA, CALIFORNIA

610-3

CONTENTS

Preceding page blank

610-3

I. INTRODUCTION

During December 1966, a very brief study was conducted at the Jet Propulsion Laboratory at the request of NASA Headquarters to investigate the feasibility of a Mars orbiter mission in 1971, using a spacecraft based heavily on the Mariner Mars 1969 design. The results of this study, which were presented to Headquarters on 20 December 1966, indicated that a very interesting orbiter mission could be flown in 1971. Furthermore, the mission could be supported with spacecraft subsystems of the Mariner 1969 design, except for propulsion.

The prospect of an additional delay in the Voyager Program in the summer of 1967 provided the motivation to re-examine the Mariner 1971 orbiter and in October the study was reactivated. The objective of this latter effort was to update the earlier work, based on a better definition of the Mariner 1969 design. Specifically, it was desired to more fully develop the mission design and orbiter coverage capability and to better identify the nature and scope of those changes that would be required to the Mariner 1969 equipment. A further objective of the study was to develop an orbiter mission of maximum scientific value which could be implemented for a minimum expenditure of resources.

The JPL Lunar and Planetary Projects Office established a very definitive and specific set of guidelines to be followed during the study, designed to permit the fullest exploitation of existing hardware and technology and thus to capitalize on the investment that had already been made on past Mariner and other NASA programs. These guidelines, prompted by cost-effective considerations, established a very constraining set of boundary conditions within which the study was executed. They are repeated herewith:

(1) Use existing Mariner 1969 hardware to the maximum extent practical.

(2) Base the mission on the use of the Atlas (SLV-3C)/Centaur launch vehicle and the Mariner 1969 nose fairing.

(3) Assume a payload consisting of the Mariner 1969 television and infrared radiometer.

(4) Base the date-return capability on the availability of one 85-foot net and a single 210-foot antenna.

Although the basic study effort was directed to the Mariner 1971 orbiter, it was felt that some thought should be given to related mission capabilities. Results of this investigation are reported in the Appenix to this study report.

II. SUMMARY

A. Mission Objectives

A dual Mariner Mission flown to Mars during the period May-November 1971 and injected into a 90-day orbiting phase would yield scientific data significantly improved over that possible from the 1969 Mars flyby. A growth version of the 1969 spacecraft design could be used with essentially the same mission objectives and mission plan as for Mariner Mars 1969. Orbit injection takes place when the seasonal variation in darkening is at a near maximum in the high southerly latitudes of the planet, and conditions are optimum for a meaningful survey of Mars. The injection energy and orbit insertion velocity requirements for the Mars 1971 orbiter mission yield extremely attractive payload capabilities <u>vis-a-vis</u> the requirements for the Mars 1973 or 1975 orbiter missions. Further discussion related to the preference for the 1971 opportunity may be found in Appendix A.

The science experiments chosen for the purpose of this study comprise an infrared radiometer, a television subsystem for visual imaging, and a radio occultation investigation. This particular payload was chosen primarily on the basis of cost effectiveness as an example of what mission capability was available using existing hardware developments. The combination of photographic exploration and infrared radiometry offers the most promise for identifying and classifying the major surface features of the planet. Correlated data from these experiments could help answer the two primary questions about the Martian surface: (1) Has it evolved in a steady-state development or is it only one phase of an episodic history that may have included liquid water in the past, and (2) What are the causes and nature of the seasonal variations in the light and dark areas?

Information on surface temperatures obtained from high-sensitivity infrared radiometry would help identify the nature of the ground features and improve our understanding of heat exchange between the surface and the atmosphere. An infrared radiometer experiment boresighted with television scanning will yield a temperature map correlated with topological or cloud features observed visually by the television subsystem, which will photograph some 40 million square miles or 72% of the planet's surface.

The radio occultation experiment conducted during the orbital phase will help refine our estimate of the density of the lower atmosphere and the ionosphere, and provide information on diurnal, seasonal, and latitudinal variations. Construction of a refractivity profile will permit inferring of atmospheric pressure and mass density. In addition, the occultation experiment will aid in determining the radius of the planet with a precision approximating one kilometer. These data, in conjunction with knowledge of the planet's gravitational field, are necessary to evolve a strong theory of the internal structure of Mars.

With these scientific considerations as a base, the Mariner 1971 Mars orbiter mission objectives are: to obtain imagery of seasonal darkening and to construct surface temperature maps of the dark areas; to obtain seasonal, diurnal, and nocturnal measurements of the pressure and density of the atmosphere and the electron density profile of the ionosphere; and simultaneously to obtain precise measurements of the radius at many points to determine the figure of the planet.

B. Mission Plan

The Mariner 1971 mission is similar in many respects to that of 1969. Two spacecraft are launched from separate pads, using the Atlas (SLV-3C)/ Centaur vehicle and a minimum 6-day separation. The 1,971-pound weight would limit the launch period to 30 days: 4 May to 4 June 1971, and an injection energy of $C_3 = 10\ km^2/sec^2$ is required.

If launched on 4 May, the first spacecraft arrives at Mars on 14 November 1971 after a 194-day flight time; the second spacecraft encounters the planet on 21 November. The launch vehicle Figure of Merit (FOM) of 2-3 m/sec would require only a 10 m/sec propellant allocation for the trajectory correction maneuvers.

Launch is northeast at an azimuth of about 70° in order to obtain launch windows of approximately 1-hour duration. The parking orbit coast time ranges from a minimum of 116 seconds to a maximum of 25 minutes. Upon arrival at the planet, orbital insertion is performed, followed by two propulsion starts to establish the correct orbit.

At encounter, the communication distance of the first spacecraft is 120 million km, the Sun-Mars distance about 211 million km. The selection of 14 November as the earliest arrival date is based on approach velocity considerations.

Three days before orbital insertion, a series of far-encounter television operations begins. Three identical photographic sequences are executed--one each day to take 32 narrow-angle pictures, which are recorded and played back to the 210-foot antenna at Goldstone. Pictures would be obtained of three complete planetary rotations at the rate of one picture each 10° of rotation, with resolutions varying from 22 km/tv line to 2 km/tv line.

Nominal orbital parameters are: a 12-hour period with periapsis altitude of 2,090 km, apoapsis of 16,484 km, and an inclination to the Martian equatorial plane of 60 degrees. The orbital inclination should be as large as possible in order to obtain a wide range of latitude coverage.

Following a one-day orbit, the first trim maneuver adjusts the periapsis altitude and phase; a second trim maneuver then corrects the orbital period to 12 hours, synchronous with the Goldstone zenith. After the orbital adjustments, the television sequences start. Initially, 68 pictures are recorded each day, with photo sequences alternating between opposite sides of the planet. A complete photographic circuit or set in longitude would require 18 days.

During the first 54 days in orbit, 3,672 pictures are taken--1,836 at high resolution (55 m/tv line)--recorded in split channels on both digital and analog recorders, and played back at 16,200 bps. Following this period, the final trim maneuver lowers the periapsis altitude to 1,000 km, the playback rate is reduced to 8,100 bps, and the daily photo rate is reduced to 34.

The first 54 days will produce three complete sets of pictures in a latitudinal range of approximately -60° to 17°. Two more sets of photographs will be taken after the final periapsis trim maneuver, extending the latitudinal coverage to 41° north and producing another 1,224 pictures after 90 days in orbit. The approximately 5,000 pictures returned from the orbiting mission in 90 days require optimum utilization of the 210-foot antenna capability, with both analog and digital recorders played back after each photographic pass.

Significant seasonal changes would have occurred after 90 days in orbit; these changes could be observed by resuming contiguous television coverage, or by re-photographing selected areas of interest.

C. Orbital Conditions

The Mariner 1971 orbit is constrained by several conditions. Orbital insertion must not occur while the planet occults Earth in relation to the spacecraft, in order to permit the sending of backup commands and to obtain telemetry data on this critical event. The orbital period should provide a sufficient number of television sequences and the orbital tracks should be equally spaced from side-to-side in longitude for overlap and contiguous coverage of large areas of the surface. At 16,200 bps, one readout will require approximately 3 hours; proper orbital sequencing will guarantee two readouts per view period.

The orbit should provide short-duration Earth occultation over a wide range of latitudes and solar illumination angles. Finally, it would be desirable from reliability considerations, although not necessary, to avoid Canopus occultation so as not to lose the roll attitude reference and to avoid Sun occultation so as not to require battery charging.

D. Spacecraft System

The Mariner 1971 spacecraft uses the 1969 design to the maximum, with the basic bus and electronics essentially unchanged. Configurational modifications are largely limited to those necessary to integrate a new propulsion subsystem and a new high-gain antenna support and deployment structure. The 1969 nose fairing and Centaur mechanical interfaces are incorporated, except that the spacecraft adapter is redesigned to account for distribution of the larger weight.

The 1969 octagonal bus, the scan platform, and the four solar panels are used in the 1971 spacecraft. The weight is estimated at 1,971 pounds, an increase of some 1,089 over 1969 in the launch configuration. The propulsion subsystem accounts for 92% of this increase; the structure increases from 200 to 300 pounds, the attitude control subsystem from 62 to 82 pounds. About 67 pounds are eliminated from the science payload by omission of the ultraviolet and infrared spectrometers.

The 1969 power subsystem satisfies the 1971 requirements. About 450 watts are available during interplanetary cruise, and 400 watts at the end of the 90-day orbital phase. The maximum normal load is 348 watts during television playback.

Of the 1969 subsystems used in the 1971 design, the following are unchanged: radio, flight command, central computer and sequencer (CC&S), scan control, television, and infrared radiometer. Varying degrees of modification are made to the flight telemetry, attitude control, pyrotechnics, cabling, data automation, data storage, and temperature control subsystems.

A modified 1969 high-gain antenna structure has been designed with a 48-inch circular aperture and integral reinforcement. Steppable in a single degree of freedom, this antenna enables pointing within 1 degree of Earth while the spacecraft is in Mars orbit. The low-gain antenna is the 1969 wave guide with a new aperture design, relocated on an outrigger structure and stowed during launch like the high-gain antenna.

The traveling wave tube is operated in a 20-watt mode only for orbital playback of television data. In order to photograph the surface over a 60-90-day period, the 1969 data storage and flight telemetry subsystems are modified to deliver data at a rate of 8,100 bps over the 210-foot antenna. Playback will start at the 16,200-bps rate, then switch to the lower rate at the end of the first 54 days in orbit, when increasing communications distance degrades system performance. The scan platform is adjusted by the CC&S according to a preprogrammed sequence, or by Earth-originated commands; adjustments can be made after each television picture, if necessary.

Only minor modifications are made to the attitude control subsystem: the primary Sun sensors are relocated on the propulsion structure and the gas supply is increased by incorporating two additional Mariner 1969 tanks. Otherwise, integration of the attitude control subsystem remains unchanged.

The propulsion subsystem incorporates three low-thrust bipropellant engines, all gimballed and mounted for control of the thrust vector along the roll axis of the spacecraft. The new design makes maximum use of existing hardware, where feasible. The single propulsion unit is employed both for trajectory correction and orbit insertion and trim maneuvers. Propellants are stored in four tanks on top of the octagonal bus structure; two of the tanks are for fuel and two for oxidizer. The system also includes two pressure tanks.

III. MISSION CHARACTERISTICS

A. Introduction

This section develops the scientific rationale and objectives for the visual imaging, surface temperature investigation, and radio occultation experiments, from which the mission objectives for Mariner 1971 are deduced. The mission profile, including encounter phase and orbiting phase photographic sequences, is delineated. Data return and surface coverage capabilities are discussed.

B. Scientific Objectives*

1. Visual Imaging

Scientific objectives for Martian photographic exploration can be derived from two sources: (1) The National Academy of Sciences (NAS) Summer Study of 1965 published a section on Mars entitled: "Recommended Priorities in the Early Stages of Investigation"; and (2) The Mariner IV television experiment produced new scientific information about the planet which has led to a sharpening of scientific objectives for future Martian photographic explorations. The Mariner Mars 1969 television experiment will provide still further refinement.

* The objectives and supporting rationale presented herein were taken in large part from "Proposal for the Photographic Exploration of Mars--Visual Imaging Experiment for Mariner Mars 1969", by Prof. R.B. Leighton of California Institute of Technology.

The NAS study cites a high priority for "photographic three-color reconnaissance of surface and clouds". In addition, it stipulates as a specific objective "...the identification and classification of major physiographic and surficial features of the planet, including a distinction between permanent and variable surface features over a significant fraction of the planetary surface. Particular attention should be paid to determining differences in environmental conditions from place to place." Photographic exploration of the planet, particularly when combined with boresighted, high-sensitivity infrared radiometry to determine surface temperature, is the most promising way to accomplish the identification and classification of the major surficial features of Mars, and also to help determine the differences in environmental conditions from place to place.

The Mariner IV television experiment indicated that the Mars surface is more lunar-like than had been thought. However, it left unanswered two very important questions which are directly pertinent to the future biological exploration of the planet: (1) Is the present surface the result of a more or less steady-state condition that has prevalied for a very long period of of time; Or is the present surface condition the most recent in an episodic history which may have included at one time a much denser atmosphere, perhaps with liquid water on the planet itself? (2) What is the difference between the light and dark areas of Mars which undergo seasonal transitions in albedo and, possibly, also in color?

Both of these questions can be investigated quite significantly within the context of a 1971 Mars orbiter television experiment. As a consequence, then, the primary scientific objectives of a photographic experiment for the 1971

Mars orbiting mission assisted by a boresighted infrared experiment, would be:

(1) To determine the general physiography over much of the planet at a resolution significantly better than that obtainable from the Earth's surface, and to topographically categorize the basic light and dark areas and perhaps learn more about why they undergo seasonal variations.

(2) To further explore, both geographically and in resolution, this unknown planetary surface for additional clues as to its origin.

(3) To obtain sufficient coverage at a suitable resolution to distinguish, on the basis of crater morphology and other criteria, between an episodic and a continuous history.

Although these objectives are, in fact, the same as delineated for the 1969 Mariner Mars flyby mission, there is a vast difference in the quantity and quality of information return expected from a Mars 1971 Orbiter. In particular, in 1971 a fortuitous timing match occurs between the optimum arrival time based on trajectory and performance considerations, and the peak of the seasonal variation in darkening in the southern hemisphere (Fig. 1*). Here it is seen that arrival on 14 November 1971, at a heliocentric longitude of 17°, corresponds to very nearly the maximum experienced darkening for a range of latitudes from -60° to +20°. Furthermore, in the subsequent 90-day

* From Reference 1, an article by J. H. Focas: "Seasonal Evolution of the Fine Structure of the Dark Areas of Mars," Planetary and Space Science, Vol. 9, pgs. 371-381, Jan.-Feb. 1962.

610-3

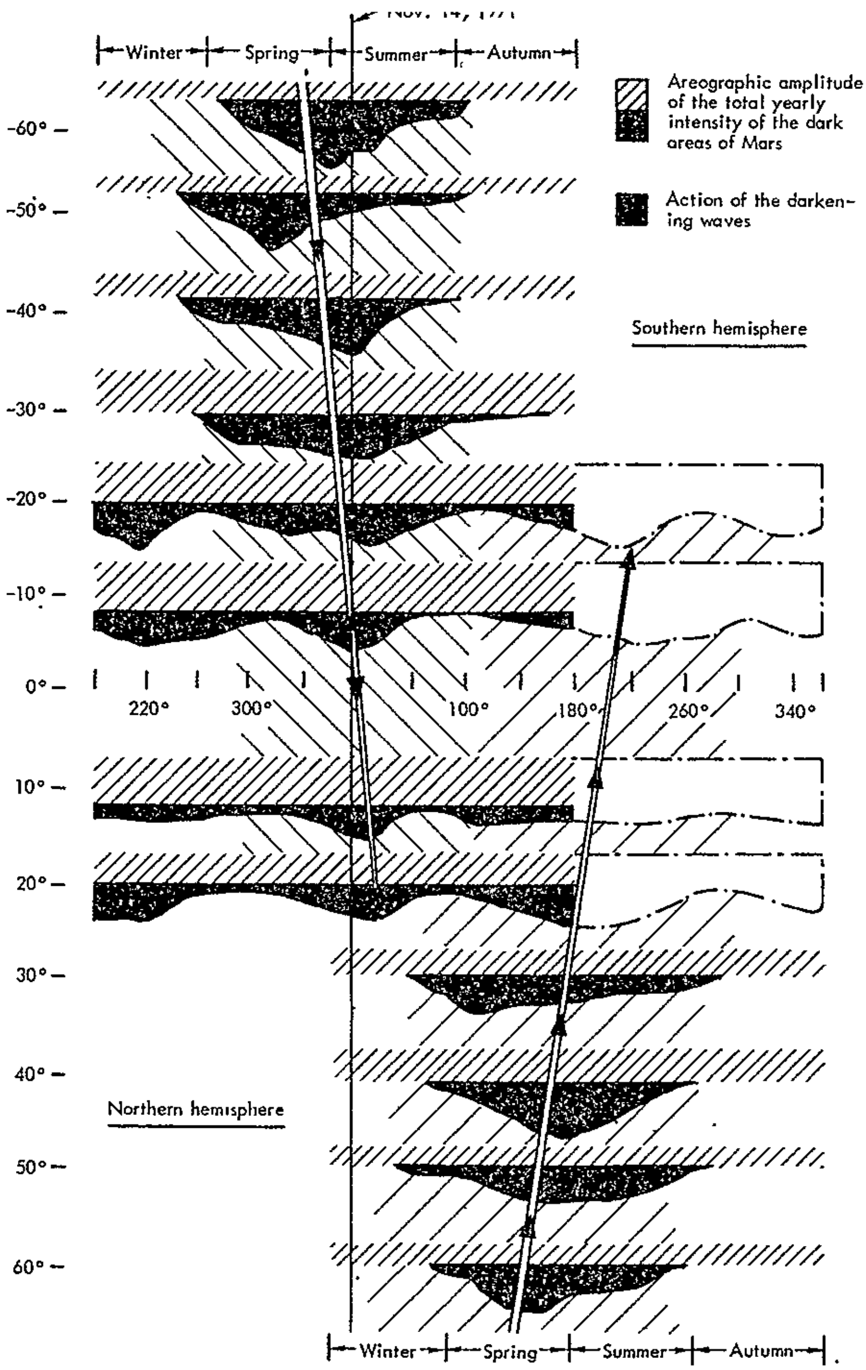

a. Lineated areas show the average intensity of all individual dark areas contained within the corresponding areographic latitudes.
For all areas: limit minimum Bs/Bc = 0.80 = (reference intensity)
For individual areas not included the action of the darkening waves, limit maxima of Bs/Bc = 0.55-0.67

b. Black areas show the action of the darkening waves (increase of the average intensity)
For individual areas:
limit maxima of Bs/Bc = 0.43-0.56

c. Arrows show the propagation of the darkening waves issued alternately at half martian year intervals from the two poles, crossing the equator and fading at 25° areogr. lat. of the opposite hemisphere.

d. Circumpolar and temperate areas are activated by one wave. Equatorial areas are activated by two waves. They are permanently the darkest areas of the planet.

Figure 1. Areographic Amplitude of the Intensity of the Dark Areas of Mars

orbital period, these areas undergo nearly their full change in lighting intensity.

As will be shown below, this change in darkening in the southern hemisphere corresponds nicely to the most readily attainable orbital and photographic coverage properties. Thus, the first scientific objective--learning why the dark areas undergo seasonal variations--can probably be very well satisfied. In contrast, due to the short duration of its photographic mission, there is little likelihood of obtaining information on seasonal variations from Mariner Mars 1969.

2. Surface Temperature*

The value of surface temperature measurements in conjunction with photographic coverage has already been cited. The nature of special features detected in television images, such as the light areas observed around some craters in Mariner pictures, could be ascertained on the basis of simultaneous temperature determinations, establishing whether they were true ground features or remnants of CO_2 or H_2O ices. The identification of cloud features of various kinds would also be facilitated by means of temperature discrimination.

The results of the Mariner IV radio occultation experiment have firmly established the very tenuous nature of the Martian atmosphere, the low temperatures prevailing at layers near the surface, and the predominance of CO_2 as

* The objective and supporting rationale presented herein were taken in large part from Reference 2: "A Proposal for a Surface Temperature Measurement from the Mariner Mission to Mars 1969", by G. Neugebauer of California Institute of Technology.

an atmospheric constituent. At the same time, the results have raised some novel problems regarding the meteorology and climatology of Mars. For example, it is now difficult to reconcile the amount of water vapor reported from spectroscopic observations from Earth with atmosphere temperatures below 180°K.

As pointed out by Leighton and Murray, the entire problem of the constitution of the polar capse of Mars should also be reconsidered, since the caps, if the vapor pressure of H_2O is as low as the Mariner IV data indicate, cannot be formed entirely by H_2O ice and still have the observed dimensions and rates of change. Because the major constituent of the atmosphere can at times be snowed out at sufficiently high latitudes, the ground temperatures can obviously have a major influence on the local and global properties of the atmosphere.

Knowledge of the ground temperature of Mars is important, not only for the understanding of the heat-exchange processes between solid surface and atmosphere, but also because of the information it provides about the nature of the ground itself. The use of lunar temperatures, measured from Earth during a lunation period or a lunar eclipse, to study the thermal properties of the materials on the lunar surface, is well known. In a similar manner, temperature determinations of the Martian ground carried out across and beyond the terminator during the orbit would provide a measure of the thermal inertia $(k\rho c)^{1/2}$ of the surface materials in Mars.

The scientific objective of the surface temperature experiment is then:

> To measure the infrared radiation emitted from the areas of Mars scanned by the television system to obtain a temperature mapping which can be correlated with topological or cloud features observed visually.

3. Radio Occultation Investigation of the Atmosphere of Mars*

Mariner IV and V have demonstrated that the effects of refraction by the atmosphere and the ionosphere of a planet on the frequency, phase, and amplitude of a radio signal received from a probe before and after occultation by the planet, can be used to infer their structure. Similar measurements with an occulting orbiter would yield improved determinations of the density profile of the lower atmosphere, as well as the electron density profile of the ionosphere over a large number of locations on the surface of the planet, thus providing information on diurnal, seasonal, and latitudinal variations. In addition, a precise measurement of the radius of Mars would be obtained at a large number of points, thus defining the physical figure of the planet.

Refraction in the ionosphere and the neutral atmosphere affect the radio signal both en route to the spacecraft and after being coherently retransmitted by the spacecraft transponder. The changes in frequency and phase of the signal that are thus introduced can then be very precisely measured on Earth when the trajectory of the spacecraft is known to a sufficient degree of precision. The changes resulting from refraction can also be measured at the spacecraft, coded, and telemetered to Earth. These changes can then be used to construct the refractivity profile of the Martian ionosphere and atmosphere, which in turn can be reduced to a profile of electron density in

---

* The objectives and supporting rationale presented herein were taken in large part from Reference 7: "Radio Occultation Investigations of the Atmosphere of Mars," Technical Report No. 32-1157, A. Kliore and D. A. Tito, Jet Propulsion Laboratory, May 1967.

the ionosphere and the number density in the neutral atmosphere. However, this method suffers from increased complexity aboard the spacecraft and lacks precision.

In order to obtain the pressure and mass density, the composition and temperature of the neutral atmosphere must be known. However, the refractivity profile provides measurement of the local scale height, which yields the mean molecular weight when the temperature is known from other measurements, thus allowing the pressure and mass density to be inferred.

In addition, the exact observation of the times of extinction and reappearance of the signal, when correlated with trajectory and atmospheric density information, can yield the radius of the planet at the points of tangency with a precision of approximately 1 kilometer. In conjunction with a measurement of the Martian gravitational field, these measurements are necessary for the formulation of a strong theory for the internal structure of Mars.

The scientific objectives of the radio occultation investigation of the atmosphere of Mars is then:

> To obtain seasonal, diurnal, and nocturnal measurements of the pressure and density of the atmosphere of Mars and of the electron density profile of the ionosphere; and simultaneously to obtain precise measurements of the radius of Mars at many points to determine its figure.

C. Mission Objectives

From the scientific rationale and objectives given above, a rather specific set of mission objectives evolves for Mariner 1971:

(1) To conduct orbiting missions to Mars for the purpose of obtaining imagery of the seasonal darkening and surface temperature maps of the dusky areas.

(2) To obtain seasonal, diurnal, and nocturnal measurements of the pressure and density of the atmosphere of Mars and of the electron density profile of the ionosphere; and simultaneously to obtain precise measurements of the radius of Mars at many points to determine its figure.

D. Mission Plan

The mission plan for a Mariner Mars Orbiter in 1971 would be similar in many respects to the Mariner Mars 1969 plan. The two spacecraft would be launched from separate pads (36A and 36B) at Cape Kennedy, using the Atlas (SLV-3C)/Centaur boost vehicle. Due to the larger injected weight (1,971 pounds), however, the launch period would be limited to 30 days--4 May to 4 June 1971. A minimum separation between first and second launches would be about six days to allow for evaluation of the first launch and the first midcourse maneuver. Depending on the availability of launch crews and equipment, the minimum separation between launches may have to be increased to approximately 10 days because of launch schedule considerations.

The parking orbit ascent trajectories tentatively chosen require northeast launch azimuths of about 70°. The resulting injections over North Africa, however, are unfavorable from tracking and telemetry considerations. Alternately, use of yawed direct-ascent trajectories launched to the southeast (108°) would result in more favorable tracking and telemetry coverage. Final choice of ascent mode is contingent on detailed trajectory design studies.

If launched at the beginning of the period on 4 May 1971, the first spacecraft would arrive at Mars on 14 November 1971, after a flight time of 194 days. The second spacecraft would be set to arrive a week later on 21 November, to permit sufficient time to thoroughly establish the orbit and operational activity of the first spacecraft. Each spacecraft would have the capability of executing multiple midcourse maneuvers.

Three days prior to orbital insertion, far-encounter television operations would be initiated. This operation consists of three identical sequences (one each day) which utilize the narrow-angle camera to take 32 pictures in a 21-hour period, or one picture each 39 minutes. These pictures are recorded on the analog recorder and played back for 2.7 hours via the 16.2 Kbps link to the Goldstone 210-foot antenna once each day. Pictures of three complete planet rotations are obtained at the rate of one picture each 10° of rotation. These pictures have resolutions varying from 22 km/tv line to 2 km/tv line and provide an excellent large-scale picture set for correlation with the pictures taken during orbital operations.

Insertion into a nominal 12-hour (Goldstone synchronous) orbit occurs by applying retro thrust at Goldstone zenith time to achieve a ΔV of 1571 m/s. The resulting orbit would have a nominal periapsis altitude of 2,090 km, apoapsis altitude of 16,484 km, and be inclined to the Martian equatorial plane at an angle of 60 degrees. After orbital insertion, tracking for one day (two orbits) would be required to determine the orbit, followed by the first trim maneuver to adjust periapsis altitude and phase. A waiting period of one to six orbits, depending on period error, would be required for periapsis to occur at Goldstone zenith. A second trim maneuver would then be performed to adjust the period to 12 hours, synchronous with Goldstone zenith.

Orbital television operations would then commence. Initially, two complete tape loads (68 pictures total) would be recorded each day. Since the orbital period is 12 hours, the planet rotates a little less than one-half revolution per orbit. Thus, photographic sequences alternate between opposite sides of the planet, coupled with a small shift in longitude. A complete circuit in longitude would be completed each 18 days.

Three complete sets of pictures in the latitudinal range of approximately -60° to 17° would be taken in 54 days. These sets would be contiguous planet coverage (0-360° longitude) at a maximum resolution of 550 m/tv line. A total 3,672 pictures would be obtained, of which 1,836 are high resolution; i.e., 55 m/tv line.

After 54 days, due to increasing Earth-Mars distance, telecommunication performance would have degraded so that a reduction to 8,100-bps playback rate would be required. Picture recording would consequently be reduced to 34 pictures per day. Also at this time, due to a northerly shifting of the lighting band and resulting increase in observation altitude, a trim maneuver would be performed to lower periapsis altitude to 1,000 km.

After the maneuver, two more picture sets (i.e., complete 360° circuits in longitude) would be recovered, extending latitudinal coverage to 41° north and adding another 1,224 pictures after 90 days in orbit. At that time, significant seasonal changes would have occurred in the southern hemisphere. To observe these changes, one of two choices could be made: (1) resume contiguous coverage, or (2) based on examination of previously obtained photography, re-photograph selected sites of interest (spot coverage).

E. Television Coverage and Data Return

Performance characteristics of the television and data return systems are given in Tables 1 and 2; Figure 2 is a block diagram of the systems.

Upon application of power to the television system, cameras A and B begin shuttering alternately every 42.24 seconds. After shuttering, the impressed image on the face of the picture tube is scanned line-by-line each 60 milliseconds. The amplitude of the video signal is effectively sampled 18,900 times per second. The sampled video is then split into two channels. In the first channel, every seventh sample is digitized and recorded on the digital recorder. In the second channel, each sample is modified before being recorded on the analog recorder. The modification is such that small-scale variations are maintained and, in fact, enhanced at the sacrifice of precise relationships between points widely separated in the scene. The enhancement is like a commercial television picture in which the contrast setting is not proper, making the darker grays blacker and the lighter grays whiter. After receipt on Earth, the data are recombined to secure a high-quality picture of the original scene.

Table 1. Television Performance Characteristics

Characteristics	Camera A	Camera B
Effective focal length	50 mm	508 mm
Focal Ratio	f/3.0	f/2.5
Shutter speed	120 ms	12 ms
Angular field of view	11 x 14 deg	1.1 x 1.4 deg
Active scan lines per frame	704	
Active pictures elements per line	945	
Frame time between A and B	42.24	
Total picture elements per frame	665,180	
No. of gray levels per picture element	64	
Total picture bits per frame	3,991,080	
Minimum time to shutter 34 pictures	23m 13.92 sec	

Table 2. Data Return System Characteristics

Characteristics	Value
ATR* storage capacity	1.57×10^{8} bits
DTR** storage capacity	2.3×10^{7} bits
DTR record rate	16.2 kbps
Equivalent ATR Record Rate	113.4 kbps
ATR and DTR combined picture storage capacity	34 pictures
ATR and DTR Telemetry Playback rates	16.2 and 8.1 kbps
ATR and DTR running time	24 minutes

* ATR = analog tape recorder

** DTR = digital tape recorder

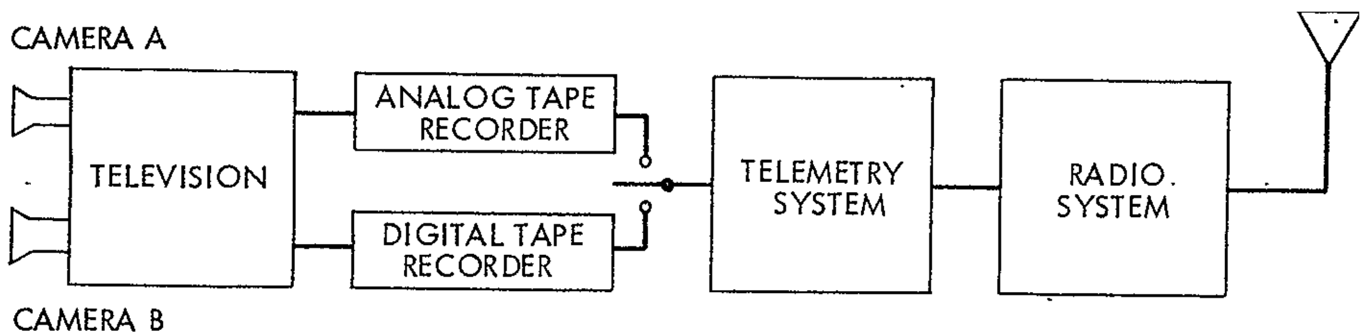

Figure 2. Combined Television/Data Storage and Transmission Systems

The recorders have a combined capacity to store 34 pictures, evenly divided between high- and low-resolution. Upon command from the CC&S or by the ground station, the recorders are played back sequentially via the telemetry and radio systems at 16,200 or 8,100 bps. At the 16,200 bps rate, the analog recorder is read out in 2 hours 42 minutes and the digital tape recorder in 24 minutes. At the 8,100 bps rate, these times are doubled. The analog recorder must be erased before re-recording. Start and stop commands can be sent to the recorders to record pictures at any time. However, the maximum record rate is one picture every 42.24 seconds.

2. Photographic Coverage

Pre-Encounter. At 73½ hours before orbital insertion, pre-encounter television operations are initiated. The photo/playback sequence is illustrated in Figure 3. This operation consists of three identical sequences wherein 32 pictures are recorded in a 21-hour period with narrow-angle camera B. Subsequent playback occurs in a 3-hour interval via the 16.2 Kbps link to Goldstone. Since Mars rotates at 24 hours per day, photographs of 7/8 of the planet are recorded in 10° increments of longitude. At I-72 hours, the planet will fill approximately half the field of view of the camera. At I-32 hours, the planet just completely fills the field of view. Pictures of three complete planet rotations will be recorded at resolutions from 22 km/tv line to 2 km/tv line. These pictures provide an excellent large-scale set for correlation with the pictures taken during orbital operations. Figure 4 illustrates the increase in resolution as the spacecraft approaches the planet.

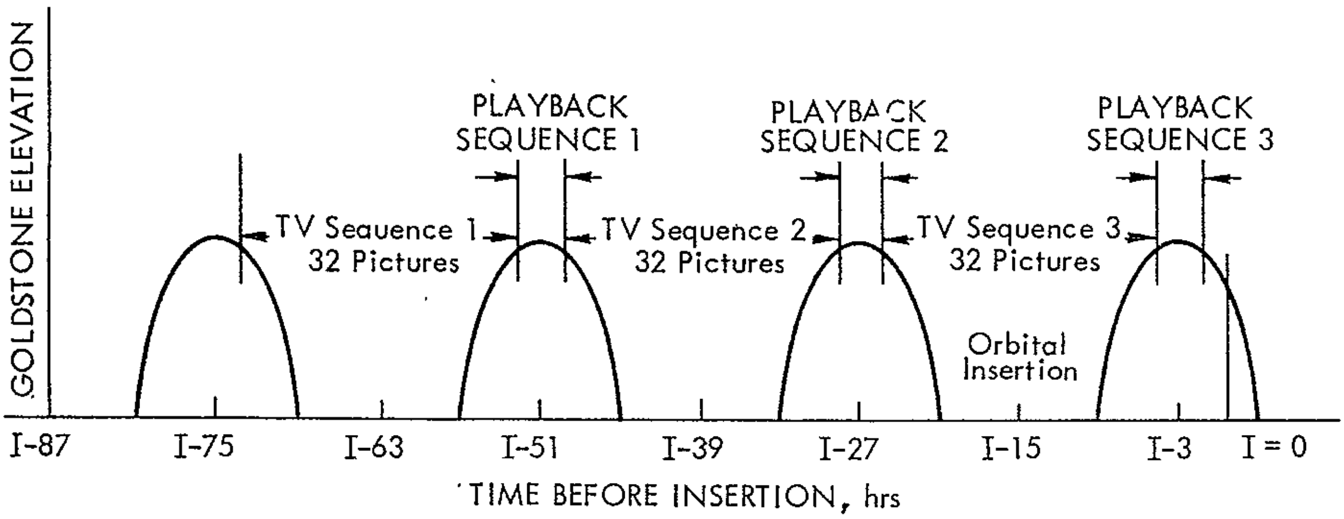

Figure 3. Pre-Encounter TV Sequence

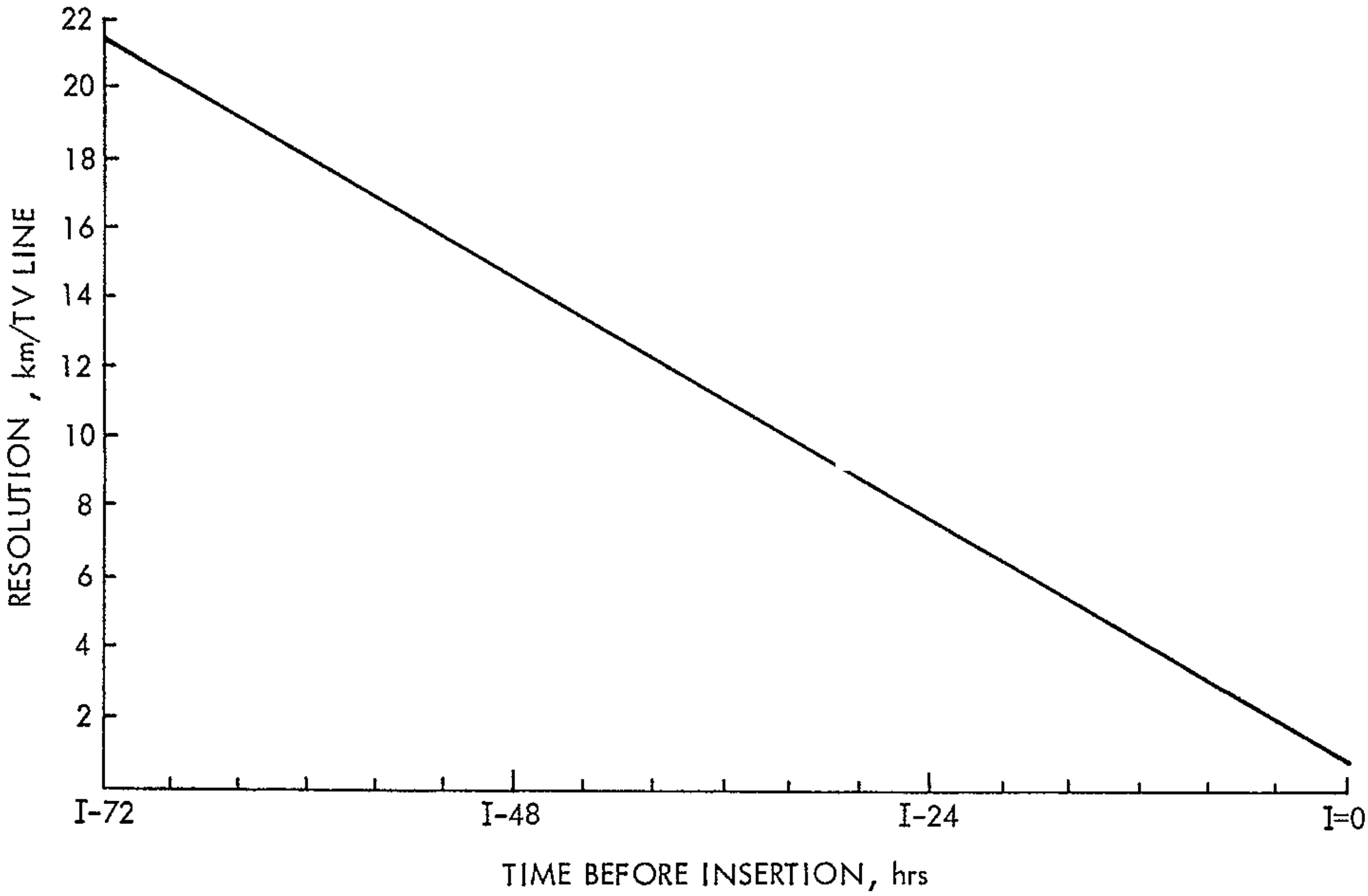

Figure 4. Pre-Encounter TV Resolution vs Time Before Insertion

Orbital Coverage. As seen in Figure 1, the spacecraft would be inserted into orbit a little after the beginning of summer in the southern Martian hemisphere. This season is near the maximum in darkening, particularly at the high southerly latitudes. Figure 1 also shows the need to conduct photographic operations for at least 90 Earth days. In fact, it is highly desirable to extend photographic operations to 150 days.

A strong factor in determining photographic coverage is the relationship between the orbital track over the surface, the lighting conditions along the track, and the altitude. Ideally, it would be desirable to always obtain pictures at low Sun elevation angles (10 to 40 degrees), when the spacecraft is near periapsis. Initially, it is possible to obtain a favorable match between these three factors by proper selection of orbital inclination. However, there is degradation as time-in-orbit passes because the favorable lighting band on the surface shifts relative to the inertially fixed orbit. Essentially, for this mission, there is observed a northerly progression of the favorable lighting band accompanied by a progressive increase in altitude when over the band.

The evolution of favorable lighting conditions toward the northerly latitudes as a function of time-in-orbit is illustrated in Figure 5 for a 60-degree inclination orbit. In this figure, solar illumination angle is the Sun elevation angle referenced to the local horizontal at the site. If we assume the minimum acceptable lighting is 10-degree illumination, the northerly progression of the lighting band can be obtained from Figure 5 and is illustrated in Table 3.

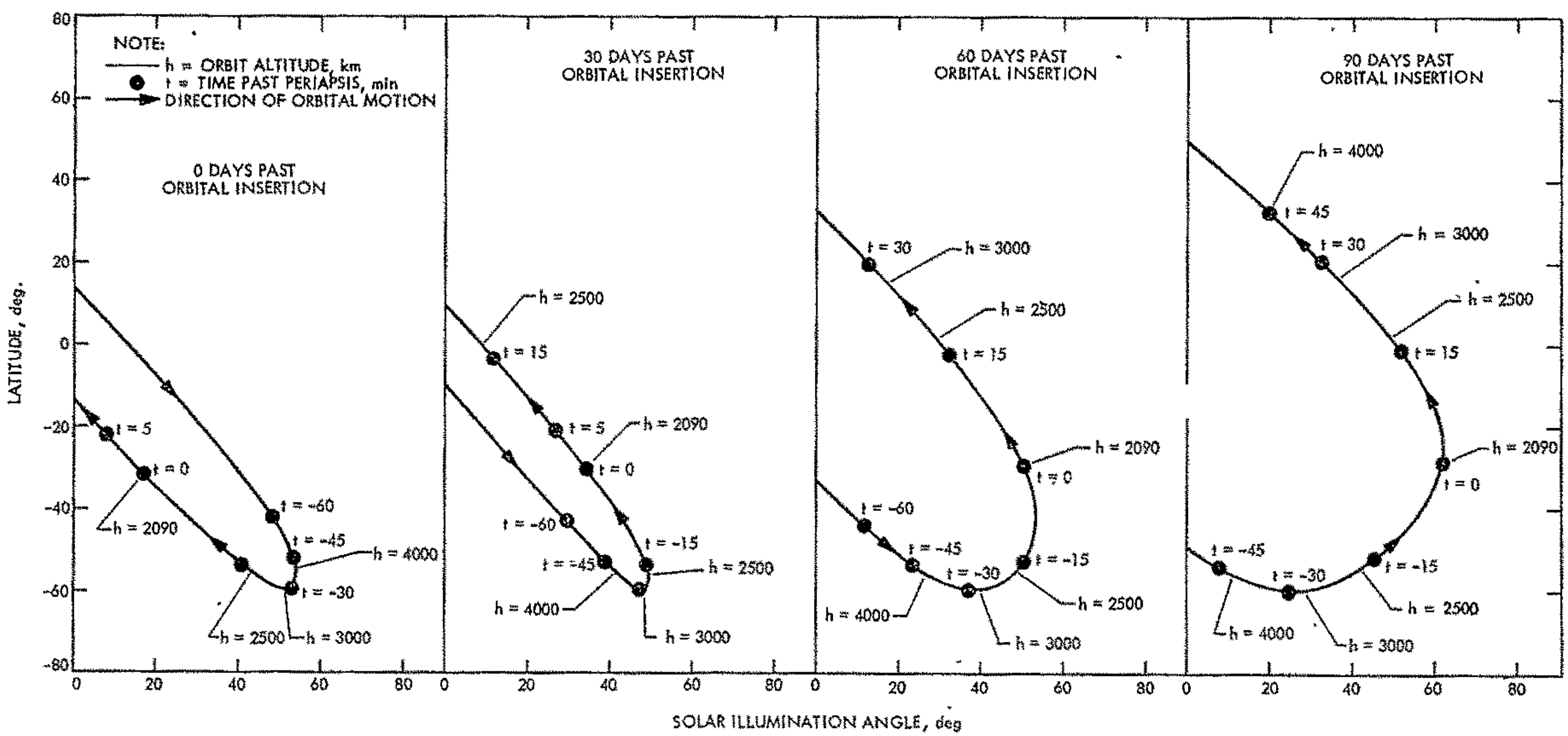

Figure 5. Lighting vs Latitude for Various Times in Orbit (60° Inclination)

610-3

Table 3. Northerly Progression of Lighting Band

Time in Orbit (days	Maximum Target Latitude at 10-degree Lighting
0	-24°
30	- 2°
60	+22°
90	+41°

However, it is also evident from Figure 5 that, although favorable lighting becomes available at the northerly latitudes as time progresses, the observation altitude increases, thus reducing resolution. This condition may be compensated for by using a trim maneuver to reduce periapsis altitude.

Based on this observation, a "follow-the-lighting band" policy of photographic coverage can be evolved. A typical coverage plan would be:

(1) Obtain three sets (i.e., three complete circuits in longitude) of contiguous coverage in the latitude bands of -60° to -24°, -39° to 3°, and -21° to 17°.

(2) After the third circuit, or after 54 days in orbit, perform a maneuver to drop periapsis to 1,000 km altitude.

(3) Obtain two more sets of contiguous coverage (i.e., two more circuits in longitude) covering the latitude bands of 0° to 30° and 18° to 41

(4) Upon completion of the above five circuits, 90 days in orbit would have elapsed. Considerable seasonal change would have occurred. At this time, one of two choices could be made: (1) return to the

high southerly latitudes and resume contiguous coverage, or (2) based on examination of previously obtained photography, re-photograph selected sites of interest (spot coverage).

The surface coverage for the first 90 days of orbit is shown in Figure 6. Successful execution of the photographic sequences would cover 40 million square miles or 72% of the planet's surface. Inspection of Figure 6 shows an approximate 50% latitude overlap between successive circuits. Thus, much of the area would be photographed twice. Typical television sequences for 0, 18, 36, 54, 72, and 90 days are given in Table 4.

Variation of lighting conditions as a function of latitude and time in orbit for a 70-degree inclination orbit are shown in Figure 7. Here, coverage is extended southward 10° to -70° latitude, and slightly north from 41 to 44°. Also observed is an approximate 10° reduction in the width of the lighting band relative to the 60-degree inclination orbit. These factors tend to indicate a preference for the more highly inclined orbit.

Data Return. The mission depicted above would return approximately 5,000 pictures in 90 days. To obtain this large return, it is necessary to fully utilize the high-performance capability of the Goldstone 210-foot antenna. After each photographic pass, both the analog and digital recorders must be played back. The alternating television and readout sequences are shown in Figure 8. The readout sequences consist of a 24-minute digital playback and a 2-hour 42-minute analog playback. A 6-minute erase cycle must follow each analog recorder playback. The readout and playback sequence for two spacecraft in orbit is shown in Figure 9.

NONSTANDARD

NONSTANDARD

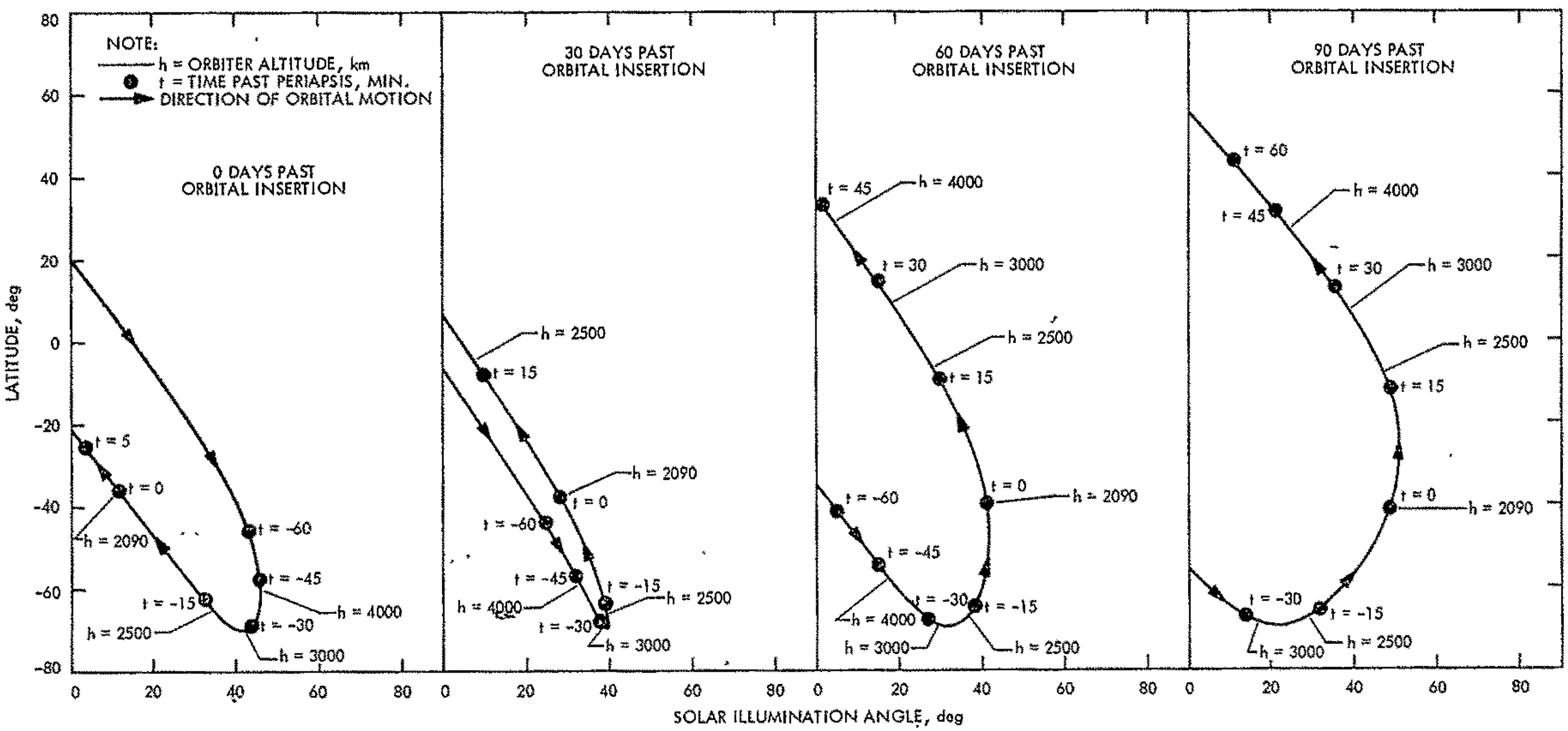

Figure 7. Lighting vs Latitude for Various Times in Orbit (70° Inclination)

6/0-3

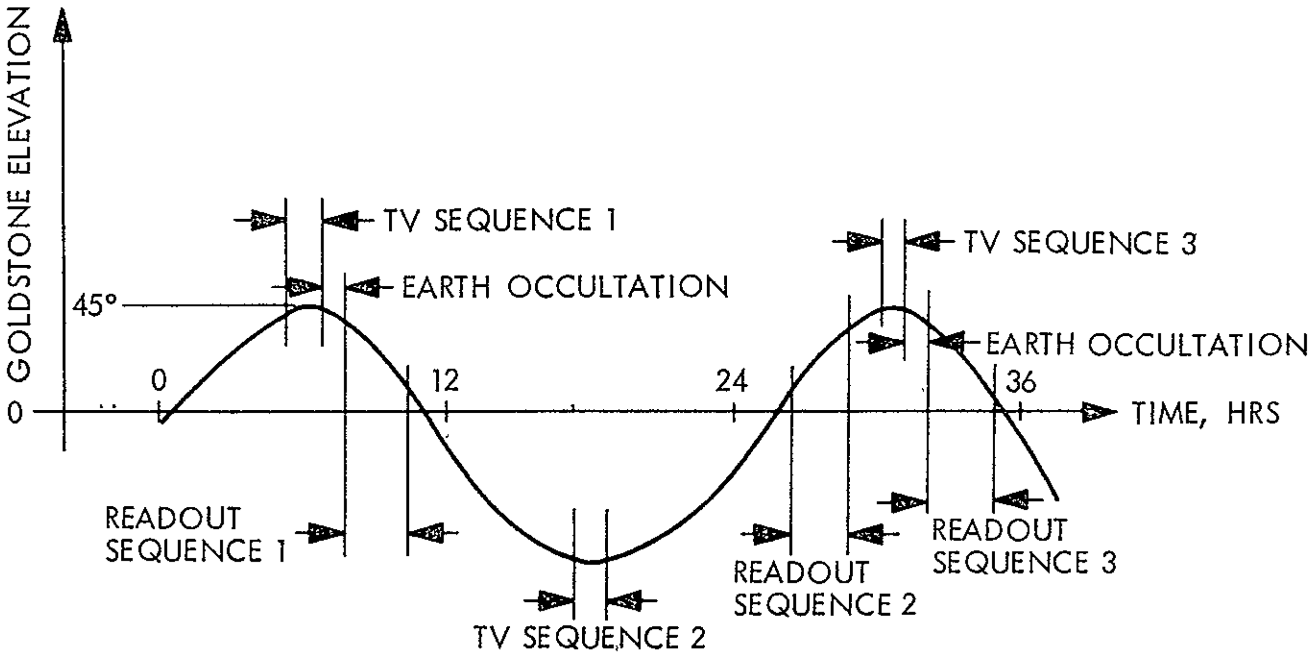

Figure 8. Readout During Goldstone Pass

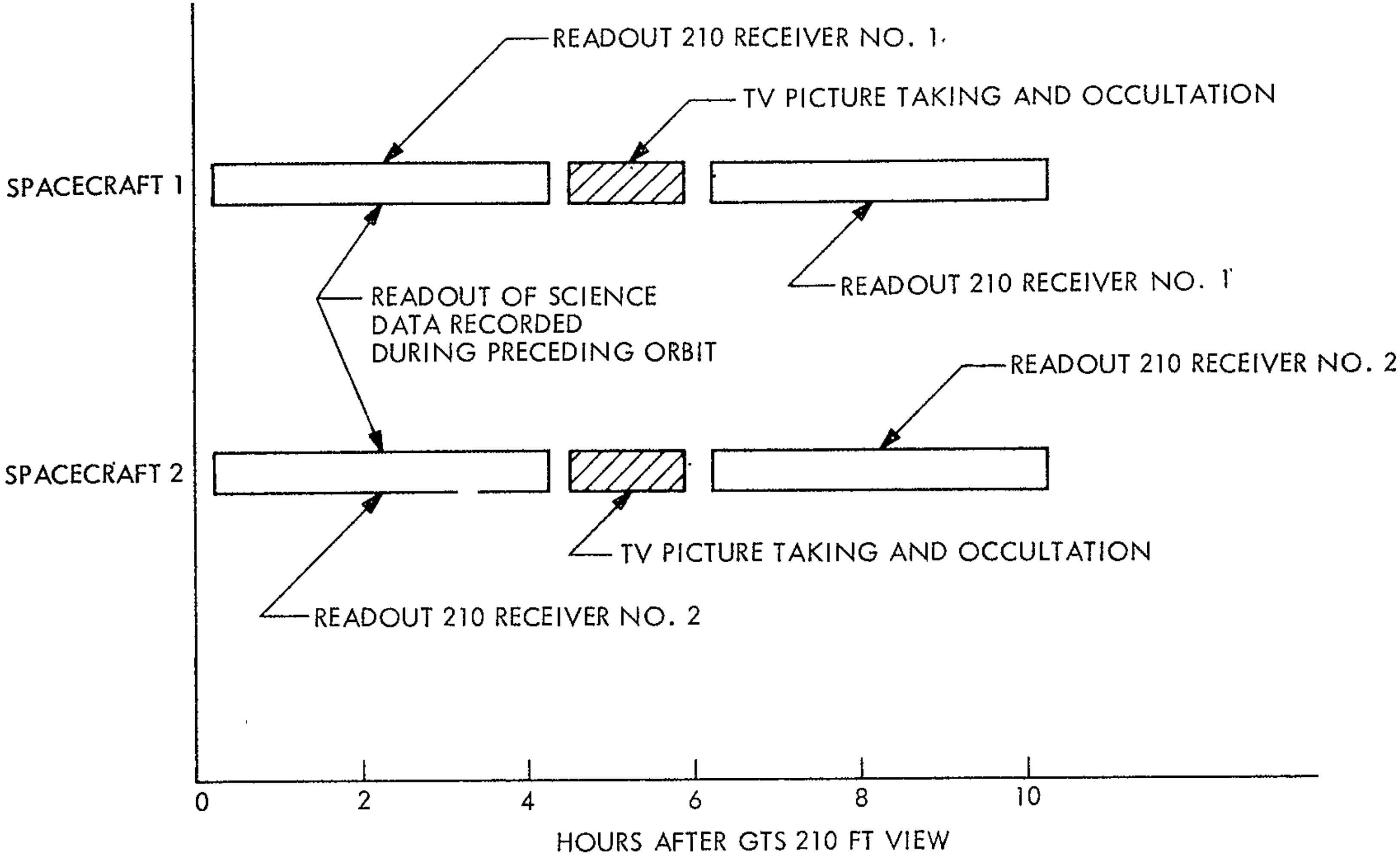

Figure 9. Typical Photo Sequence (Assuming One 210 Ft with 2 Receivers and 1 Transmitter)

610-3

IV. SYSTEMS ANALYSIS

A. Introduction

This section contains the systems analysis considerations upon which the gross spacecraft design and flight path selection were based. The following areas are covered:

(1) The payload capability of the selected launch vehicle.

(2) The velocity requirement necessary for the spacecraft propulsion system design.

(3) The selection of interplanetary trajectories.

(4) The selection of a suitable satellite orbit about Mars.

It is important to recognize that these topics are highly inter-related, so that, if consideration is given to changing the criteria or design of one area, it will most likely be necessary to re-evaluate some or all of the other areas. Because of this interdependence, several instances of cross-referencing will be found among the following four sub-sections, which treat each of the above topics in turn.

B. Launch Vehicle Performance and Payload Capability

1. Launch Vehicle Performance

The Atlas (SLV-3C)/Centaur performance used in this study is given in Figure 10. Spacecraft system weight is shown as a function of injection energy (C_3), with the following assumptions:

(1) 100 n. mi. parking orbit altitude.

(2) Launch azimuths ranging between 78° and 115° east of north.

(3) Minimum parking orbit coast time of 116 seconds.

(4) Mâximum parking orbit coast time of 25 minutes.

(5) Centaur I_{sp} = 442 seconds.

These assumptions are compatible with planned performance for Mariner Mars 1969.

Note that the weight given in Figure 10 is "Total Spacecraft Weight". This figure was computed assuming that all weight forward of the field joint is charged to the spacecraft system. The spacecraft performance, therefore, includes an 80-pound adapter, which remains attached to the Centaur after spacecraft separation. The total separated spacecraft weight capability may be obtained from Figure 10 by subtracting 80 pounds from the performance figure shown.

2. Gross Spacecraft Weight Breakdown

From an examination of the injection energy (C_3) requirements for the 1971 Mars opportunity, it was determined that a C_3 value of 10 km^2/sec^2 is required to ensure a 30-day launch period. From Figure 10, it follows that the spacecraft system weight must be no greater than 1,950 pounds. The system weight breakdown of the present spacecraft configuration is given in Table 5. Note that the total spacecraft weight of 1,971.6 pounds is 20.6

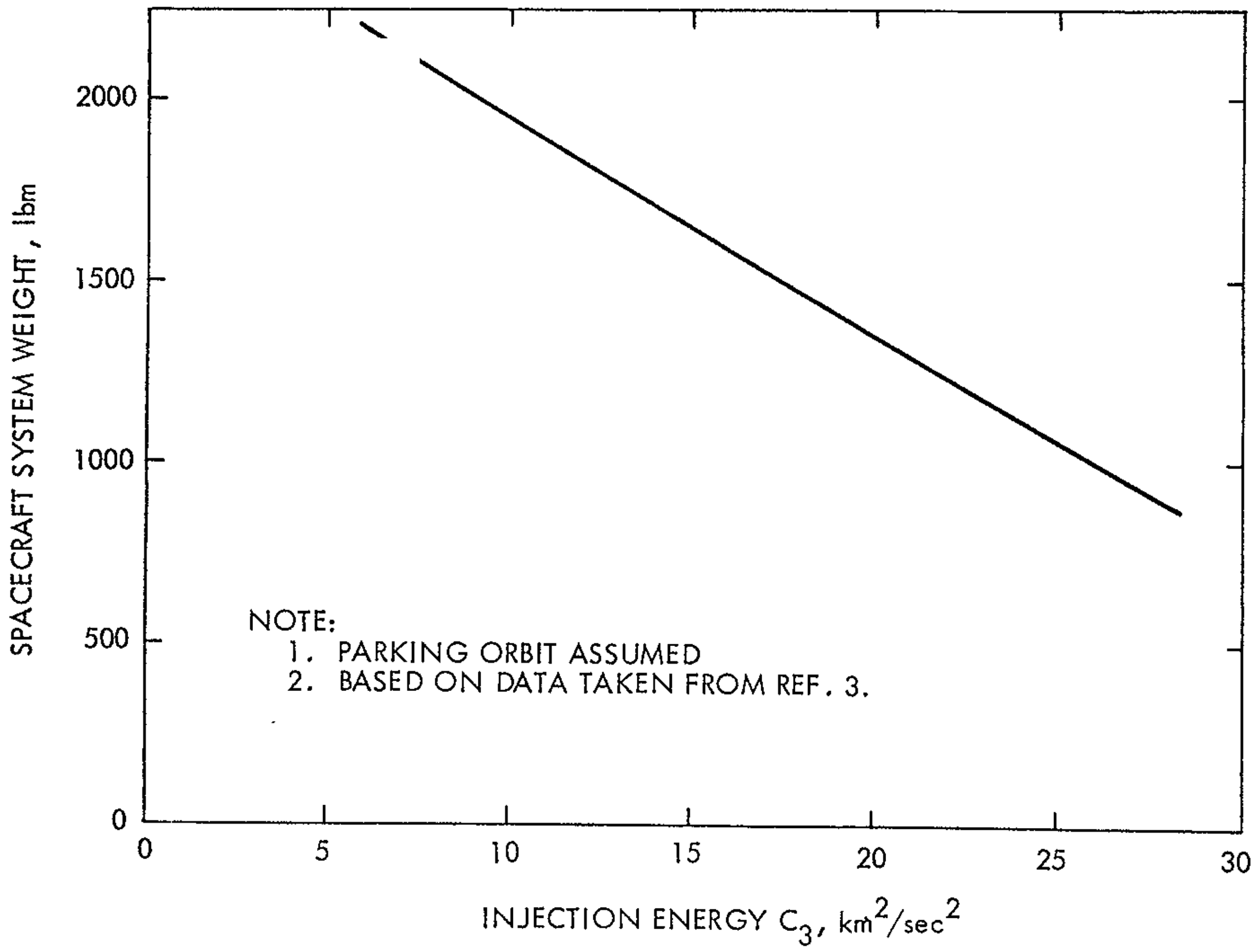

Figure 10. Spacecraft System Weight Capability vs Injection Energy

610-3

pounds greater than the 1,950 pounds available with a $C_3 = 10\ km^2/sec^2$. The reason for this disparity is that the spacecraft propulsion system sizing was based on the use of standardized Gemini propellant tanks.

The propulsion system has the capability of holding 907.6 pounds of usable propellant, representing a capability of 1,887 m/sec ΔV capability. As will be shown in the next section, this ΔV is larger than the velocity requirement for the presently planned mission profile. This suggests that by off-loading the propulsion system, the spacecraft system weight could be reduced by 20.6 pounds and therefore be in agreement with the $C_3 = 10\ km^2/sec^2$ payload capability. The 20.6-pound reduction in propellant reduces the total ΔV to 1,855 m/sec, a capability approximately equal to that required. Alternate methods of matching the spacecraft system weight with performance capability would be to: (1) Utilize a shorter launch period and thus lower the required C_3, and/or (2) Reduce spacecraft weight.

C. Spacecraft Propulsion System Velocity Increment Requirements

1. Orbit Insertion Velocity Increment

The orbit insertion maneuver requirement has been divided into two parts for convenience: (1) the impulsive velocity increment to transfer from the approach hyperbola into the desired elliptical orbit, and (2) a correction to account for the effects of the "gravity loss" characteristic of finite thrust propulsion systems.

Table 5. System Weight Breakdown

Separated Spacecraft Dry Less Payload	796.6 lbs
Payload	159.4 lbs
Propellant Reserves (3% of Usable Propellant)	27.2 lbs
Maximum Usable Propellant*	907.6 lbs
Total Separated Spacecraft Weight	1890.8 lbs
Adapter Weight	79.8 lbs
Total Spacecraft Weight**	1970.6 lbs

* Maximum Total Propellant - 934.8 lbs

** Includes All Weight Forward of Field Joint.

Impulsive Orbit Insertion Velocity Increment. The orbit selection discussed in Section IV-E results in a nominal orbit with a periapsis altitude of 2,090 km and an apoapsis altitude of 16,484 km, yielding a Goldstone synchronous orbital period of 12 hours. An examination of the interplanetary trajectory characteristics contained in Reference 4 revealed that the approach speed at Mars (V_∞), ranges between 3.0 and 3.5 km/sec for the trajectories of interest.

In order to determine the impulsive velocity increment required for a transfer into a given ellipse from an hyperbola characterized by fixed approach speed, it is necessary to specify the orientation of the line of apsides with respect to the approach hyperbola. A convenient way of doing this is with the parameter "ellipse orientation angle" (ψ), illustrated in Figure 11. It is defined as the angle between the negative approach asymptote vector and the ellipse periapsis radius vector, and is measured in the direction of orbital motion.

Figure 12 represents the minimum velocity increment required to inject into the nominal orbit as a function of ψ for various approach speeds. The minimum ΔV occurs at a value of ψ (which varies slightly with V_∞) corresponding to a periapsis-to-periapsis transfer. It is not desirable, however, to assume a nominal orbit insertion for ΔV calculations because of the inability to guarantee the required hyperbola periapsis altitude (h_{pa}) for the minimum ΔV insertion. Because of guidance and orbit determination uncertainties, an h_{pa} dispersion of ±300 km (3σ) has been assumed.

It has been found that, because of the rather large ΔV penalties associated with an h_{pa} dispersion 3σ low, an orbit insertion strategy that attempts

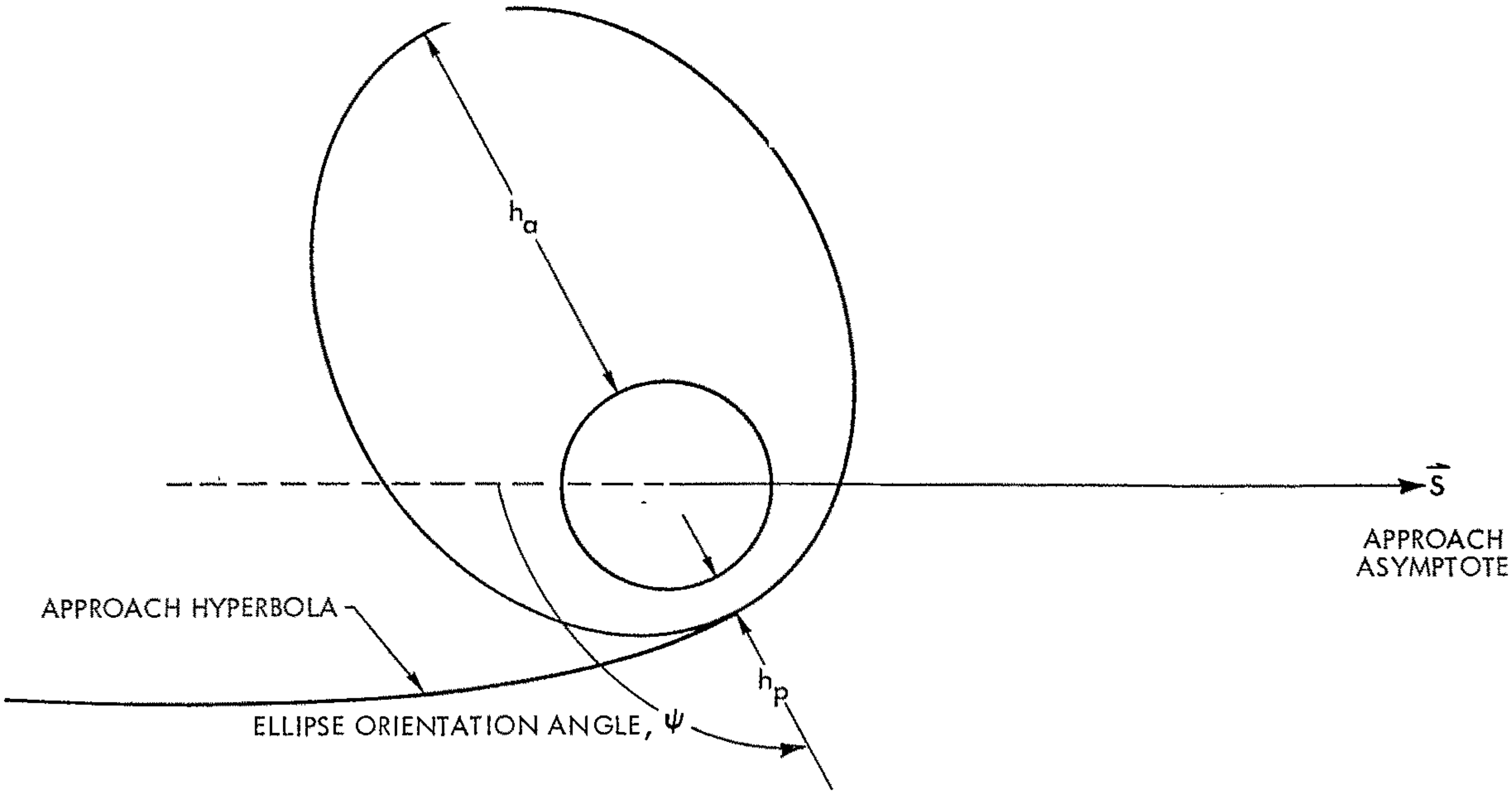

Figure 11. Definition of Satellite Orbit Parameters

610-3
45

610-3

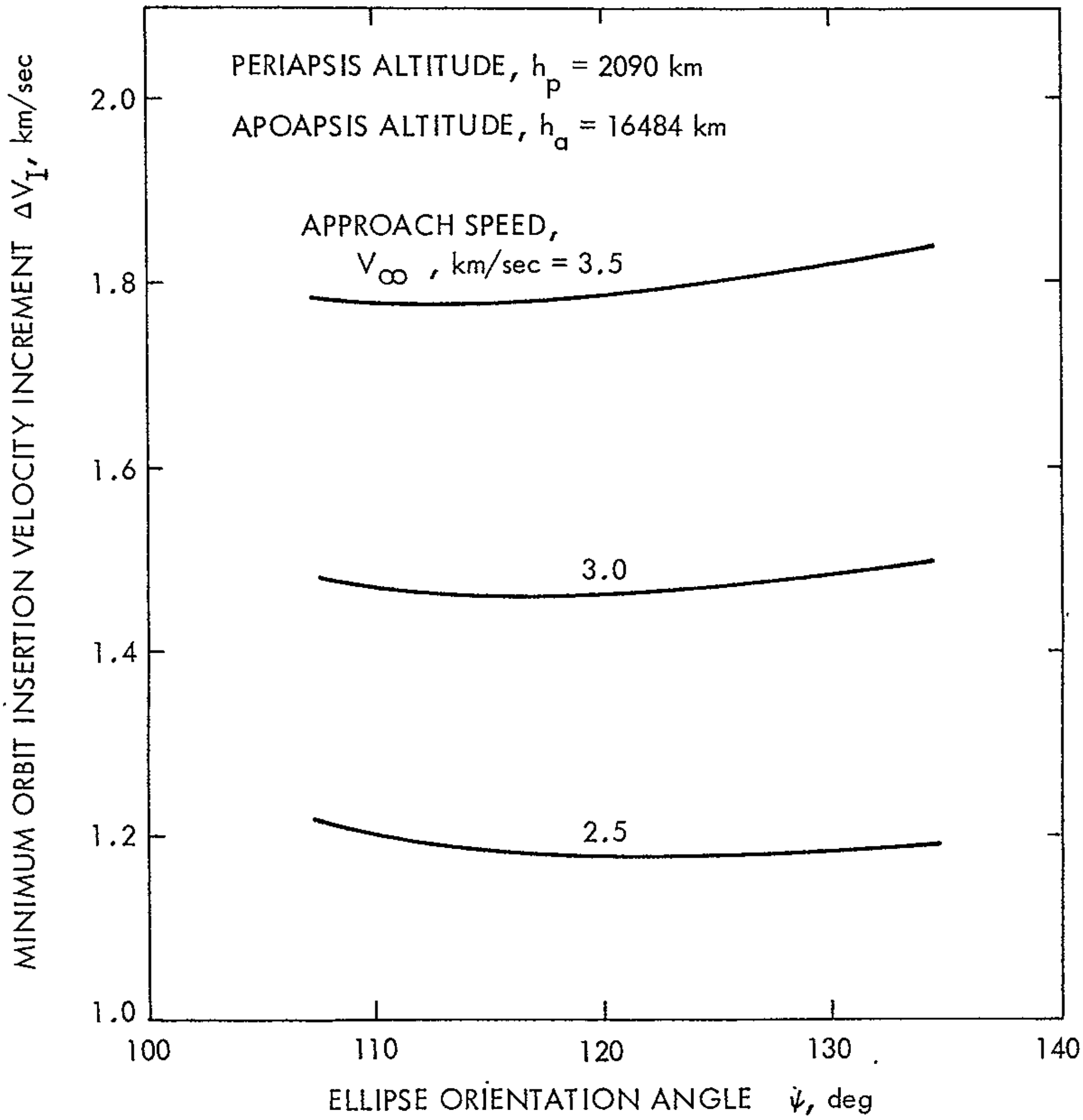

Figure 12. Minimum Orbit Insertion Velocity Increment vs Ellipse Orientation Angle for Nominal Orbit

46

to achieve the nominal ellipse directly is undesirable. An alternative policy, therefore, is to change the desired orbit periapsis in order to yield a minimum ΔV maneuver (the periapsis altitude would be corrected later with an orbit trim maneuver). Since the insertion occurs near periapsis, the ellipse periapsis altitude must be varied from approximately 1,790 to 2,390 km to cover the h_{pa} dispersions mentioned above. The largest insertion ΔV occurs for the highest periapsis altitude and it is, therefore, necessary to use the 2,390-km value for the orbit insertion ΔV computation. Figure 13 gives the minimum orbit insertion velocity increment for the 2,390-km periapsis orbit. Comparison of Figures 12 and 13 reveals that the higher periapsis causes a maximum increase of 36 m/sec for the range of ψ and V_∞ given.

Finite Thrust Effects. The additional velocity requirements that are associated with a finite thrust motor burn are sometimes referred to as "gravity losses". The magnitude of the losses depends upon the parameters of the approach hyperbola, the parameters of the elliptical orbit, and the propulsion system characteristics (largely the thrust-to-weight ratio). A parametric analysis of these losses is contained in Reference 5. Assuming an initial thrust-to-weight ratio of 0.16 (300-lb thrust and spacecraft weight of 1,970.6 lbs), $\psi \cong 120$ deg and $V_\infty = 3.5$ km/sec, the "gravity losses" for the previously described orbits amount to approximately 15 m/sec.

2. Midcourse Maneuver Requirements

A detailed orbit determination and midcourse guidance analysis has not been carried out for this mission. However, the Atlas/Centaur injection accuracy FOM (Figure of Merit) of 2-3 m/sec (1σ) ensures that an adequate adaptive midcourse policy of two (and sometimes three) maneuvers can be performed with a propellant allocation of 10 m/sec.

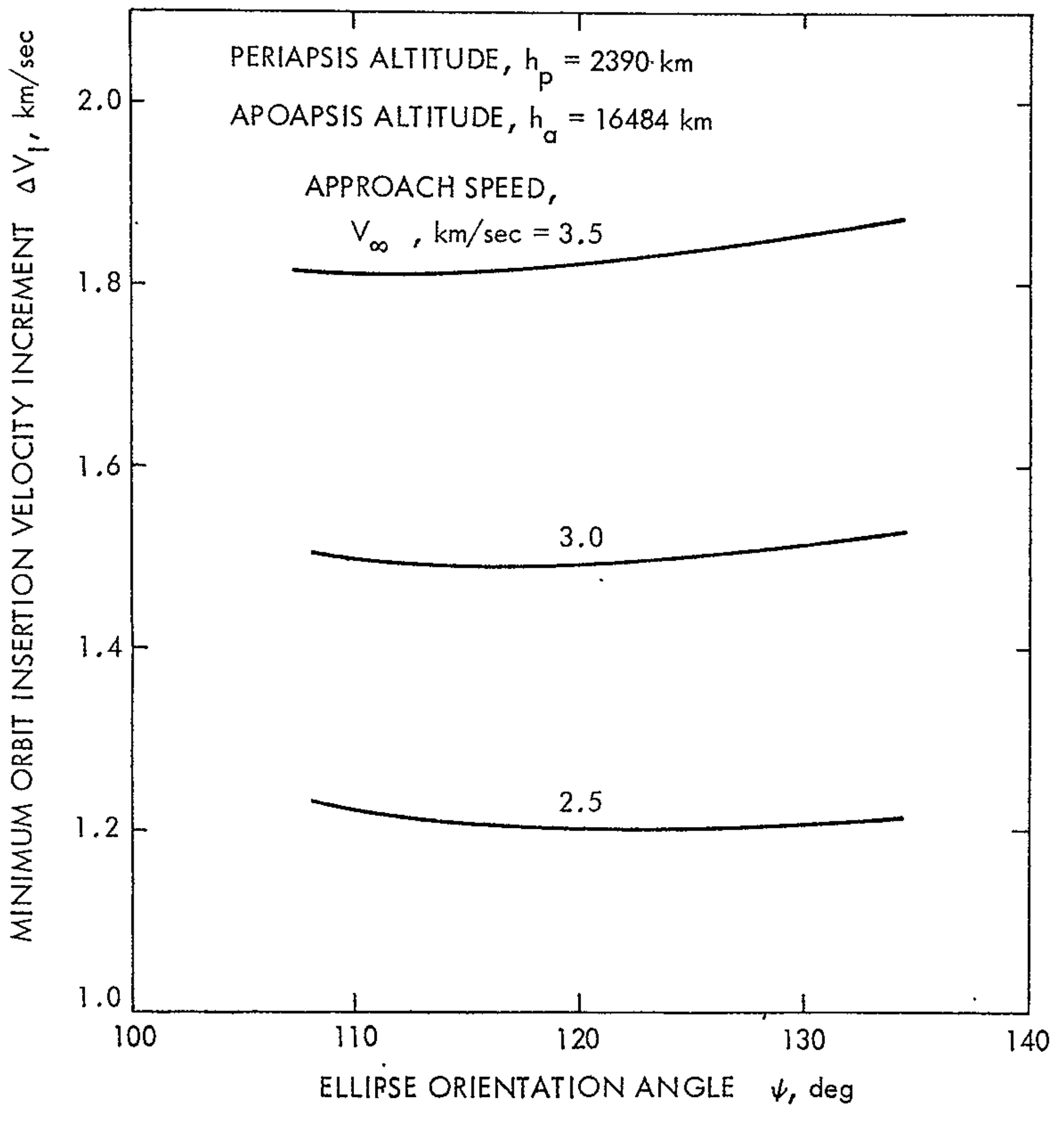

Figure 13. Minimum Orbit Insertion Velocity Increment vs Ellipse Orientation Angle for Nominal Orbit with 300 km Increase in Periapsis Altitude

3. Orbit Trim Requirements

The term "orbit trim" as used here includes all maneuvers that are performed while the spacecraft is in orbit about Mars. As discussed in Section III-D, at least three corrections would be required. The first burn would be used to correct periapsis to coincide with Goldstone zenith after one to six revolutions. For an estimated 3σ periapsis error of 300 km, a 21 m/sec correction capability would be required. A second trim to correct a 3σ orbital period error of 1.11 hr would require an additional 30 m/sec. The third correction maneuver, designed to lower periapsis altitude to 1,000 km, requires 75 m/sec. A fourth (optional) trim may be required if it is considered necessary to maintain a Goldstone synchronous orbital period after reducing periapsis altitude*. Maintenance of the 12-hour orbital period would require a 1,090-km increase in apoapsis altitude, which can be accomplished with 19 m/sec correction at periapsis.

Because of orbit trim execution errors, it may be necessary to perform one or more additional trim maneuvers to correct orbital period errors that cause periapsis to drift away from Goldstone zenith. These corrections, however, are expected to be quite small and, therefore, an additional trim ΔV allocation of 145 m/sec is sufficient to correct for probable guidance- and navigation-induced flight path errors, in addition to providing the orbit modifications that are included as part of the mission plan

* After 54 days in orbit, the time at which it is planned to lower periapsis, the larger communications distance may provide only an 8,100 bps data rate and, therefore, preclude the need for a Goldstone synchronous orbital period.

4. Total Velocity Increment Requirements

The total spacecraft ΔV requirements depend on four factors: (1) The midcourse maneuver allocation of 10 m/sec, (2) a "gravity loss" term of 15 m/sec, (3) The total orbit trim requirement of 145 m/sec, and (4) The impulsive orbit insertion ΔV requirement given in Figure 13.

Assuming a V_∞ of 3.262 km/sec, which is characteristic of the maximum approach speed trajectory discussed in Section IV-D, and the ellipse orientation angle (ψ = 130 deg) value given in Section IV-E, yields an orbit insertion ΔV requirement of 1,685 m/sec. Note that this ΔV allocation is based on the V_∞ for the last day of the first spacecraft arrival launch period. Since it is highly unlikely that this particular trajectory would actually be flown, the expected orbit insertion ΔV is smaller than the allocation. The breakdown, summarized in Table 6, reveals a total requirement of 1,855 m/sec, an amount exactly equal to the off-loaded spacecraft capability outlined in Section IV-B. Because the components of this breakdown all correspond to "worst case" or 3σ phenomena, further ΔV allocations for "contingencies" appear unnecessary.

D. Interplanetary Trajectory Selection and Characteristics

1. Trajectory Selection Criteria

The choice of transfer trajectories for the Mariner Mars 1971 Orbiter is governed by a number of factors related to the launch or near-Earth phase, the interplanetary transfer phase, and the Mars approach phase. Since the Atlas

610-13

Table 6. Spacecraft Velocity Increment Breakdown

Allocation		Velocity Increment (m/sec)
Midcourse Maneuvers		10
Orbit Insertion (impulsive)		1685
Gravity Losses		15
Periapsis Correction	21	
Orbital Period Correction	30	
Periapsis Altitude Reduction to 1,000 km	75	
Apoapsis Altitude Increase to Maintain 12-hr. Period	19	
Orbit Trim		145
Total Velocity Increment		1855

Centaur launch vehicle provides limited performance for a Mars orbiter mission, the resulting trajectory selection was influenced strongly by the desire to maximize orbiter mass.

Listed below are the various guidelines and constraints influencing the choice of the interplanetary trajectories:

Constant Arrival Date Interplanetary Trajectories. There are several reasons why constant arrival date trajectories are usually selected:

(1) The approach geometry (approach speed and angles to the Earth and Sun) are nearly constant over the launch period.

(2) The position of Earth in Sun-Canopus coordinates and communications range are constant at the time of encounter, simplifying the antenna pointing and communications system design and analysis.

(3) The Martian season is the same at encounter.

(4) The satellite orbit design problem is simplified. Because of (1) above, it is probably possible to design for a single inertially oriented satellite orbit for all launch days for a given arrival date, thus simplifying the scientific mission design and experimenter interface.

(5) There may be planning and scheduling advantages of having an *a priori* known arrival date and arrival date separation between the two spacecraft.

(6) There is a general simplification of communication between people and agencies.

Note that, for this launch opportunity, there are no particular advantages in using variable arrival dates.

Seven-Day Arrival Date Separation Between Spacecraft. This constraint was adopted in order to comfortably separate the encounter operations of the two spacecraft. The separation could possibly be reduced but the penalty resulting from this separation is not large (about a 15% decrease in the initial communications system performance).

Preference for Early Arrival Date Trajectories. This is a qualitative consideration which results from the shorter flight time, shorter communication distance, and greater Martian seasonal variations that result from early arrival date trajectories. However, the in-orbit payload capability decreases for earlier arrival dates so the arrival date must be compatible with payload requirements.

Interplanetary Trajectories. Good orbit determination properties are mandatory for interplanetary trajectories. Studies of interplanetary orbit determination capability have shown that the accuracy varies approximately inversely (for small angles) with the declination of the probe in Earth equatorial coordinates. When the probe is near Earth, the declination is given approximately by DLA, the declination of the outgoing asymptote. Near Mars, where it is necessary to have an accurate trajectory, the declination is approximately that of the planet. As a guideline, it is desirable to assure that $|DLA| > 5°$ and $|DEC| > 5°$, where DEC is the declination of Mars at arrival. It may be possible to use smaller values, but the orbit determination capability will have to be carefully examined.

2. Launch Phase

610-3

Launch Energy. On the basis of the discussion on launch vehicle performance given in Section IV-B, the launch energy C_3 will be limited to approximately 10 km^2/sec^2*. For a reasonable range of Type I arrival dates, this corresponds to a launch period duration of 30 days. Because of the high probabilities-of-launch characteristic of the Centaur launch vehicle, the 30-day period should provide adequate time for both launches with a minimum separation of six days to allow time for evaluation of the first spacecraft operations prior to the launching of the second.

Launch Azimuth. From Table 7, note that the delineations of the outgoing asymptote (DLA) range from -27.06 to -33.66 degrees. While southeast parking orbit launches are theoretically possible for this DLA range, they are characterized by either long coast times (approximately 90 minutes) with injections occurring off the west coast of the United States, or short coast times with injections far uprange. The minimum and maximum Centaur parking orbit durations are 2 minutes and 25 minutes, respectively, making southeast azimuths infeasible. Instead, if parking orbit trajectories are used, moderate northeast launch azimuths greater than 75° must be used to obtain adequate launch windows of approximately one-hour duration.

Near-Earth Communications Geometry. The near-Earth communications geometry may be related to the quantity ZAL, the angle between the outgoing asymptote and the Earth-Sun vector. This angle is approximately equal to the cone angle (Earth-spacecraft-Sun angle) of the Earth as seen from the spacecraft when it is on the asymptote of its hyperbolic Earth-escape trajectory (at about one day past launch). This angle then decreases at the initial rate of about one

* Some of the launch dates shown in Table 7 have energies slightly greater than 10 km^2/sec^2 because the dates were selected for energies that were closest to the 10 km^2/sec^2 value.

Table 7. Interplanetary Trajectory Parameters

Event	Launch* day	Launch date	Arrival date	C_3, km^2/sec^2	DLA, deg	ZAL, deg	Flight Time, days	Comm Distance at Encounter, 10^6 km	Mars-Sun Distance at Encounter, 10^6 km
1st S/C ARRIVAL	1	May 4	Nov 14	9.847	-32.59	108.21	194.0	120.836	211.20
	15	May 18	Nov 14	8.463	-29.29	89.44	180.0	120.836	211.20
	31	June 3	Nov 14	9.937	-28.18	63.85	164.0	120.836	211.20
2nd S/C ARRIVAL	1	May 3	Nov 21	10.209	-33.66	110.00	202.0	128.706	212.14
	17	May 19	Nov 21	8.275	-28.47	88.84	186.0	128.706	212.14
	35	June 6	Nov 21	10.257	-27.06	59.89	168.0	128.706	212.14

Event	Launch date	Arrival date	INC ecliptic, deg	SG1, km	SG2, km	V_∞, km/sec	ZAP, deg	ETS, deg	ZAE, deg	ETE, deg	LV1, deg	Arg. of Periapsis θ, deg
1st S/C ARRIVAL	May 4	Nov 14	2.2666	1067.3	400.8	3.124	111.88	178.26	154.76	172.34	-18.66	59.902
	May 18	Nov 14	1.5573	978.4	455.1	3.159	115.89	181.07	158.80	186.78	-14.06	60.271
	June 3	Nov 14	1.2093	1010.9	628.8	3.262	118.04	183.15	160.31	197.54	-11.37	61.323
2nd S/C ARRIVAL	May 3	Nov 21	2.4679	1575.6	383.1	3.004	104.13	178.25	147.20	172.08	-19.06	58.598
	May 19	Nov 21	1.4760	1293.5	429.6	3.008	108.86	180.85	151.99	186.73	-12.57	58.642
	June 6	Nov 21	1.0831	1298.8	610.8	3.113	111.09	182.61	153.54	195.42	-9.49	59.786

*Earliest and latest launch dates were chosen on the basis of having energies closest to 10 km^2/sec^2. For the two launch periods shown, 30-day launch periods are available with energies less than 10 km^2/sec^2

610-3

deg/day because of the changing positions of the Earth, Sun, and spacecraft.

As shown in Table 7, ZAL is approximately equal to 110 degrees at the beginning of the launch period. This means that the Earth is initially in the rear hemisphere of the spacecraft. This would have posed serious problems with the Mariner C spacecraft since near-Earth communications are achieved through the use of a low-gain antenna with a pattern covering the forward hemisphere of the spacecraft. For Mariner 1971, a low-gain antenna having a pattern with near-uniform coverage in the plane of the trajectory will be used, making the communications coverage essentially independent of ZAL.

3. Interplanetary Phase

Heliocentric Trajectory Characteristics. As can be seen from Table 7, the flight times are as short as 164 days for the early arrival date trajectories. The communication distance at encounter is only 121-129 million km, while for the Mariner IV and Mariner Mars 1969 missions they were approximately 216 and 103 million km, respectively. The Sun-Mars distance is about 212 million km. The smallest possible Sun-Mars distance is its perihelion distance of 206 million km. The distances for the 1971 arrivals are slightly larger than this value, with the arrivals occurring when Mars is just past perihelion. The location of the 1971 arrival period is illustrated in Figure 14, which contains a heliocentric plan view of the orbits of Earth and Mars, along with a typical 1971 Earth-Mars transfer trajectory. Also shown is the location of the Earth during the launch and arrival periods. The dots showing the relative positions of Earth and Mars at equal time intervals past encounter illustrate the effects of increasing communication distance and Sun-Mars

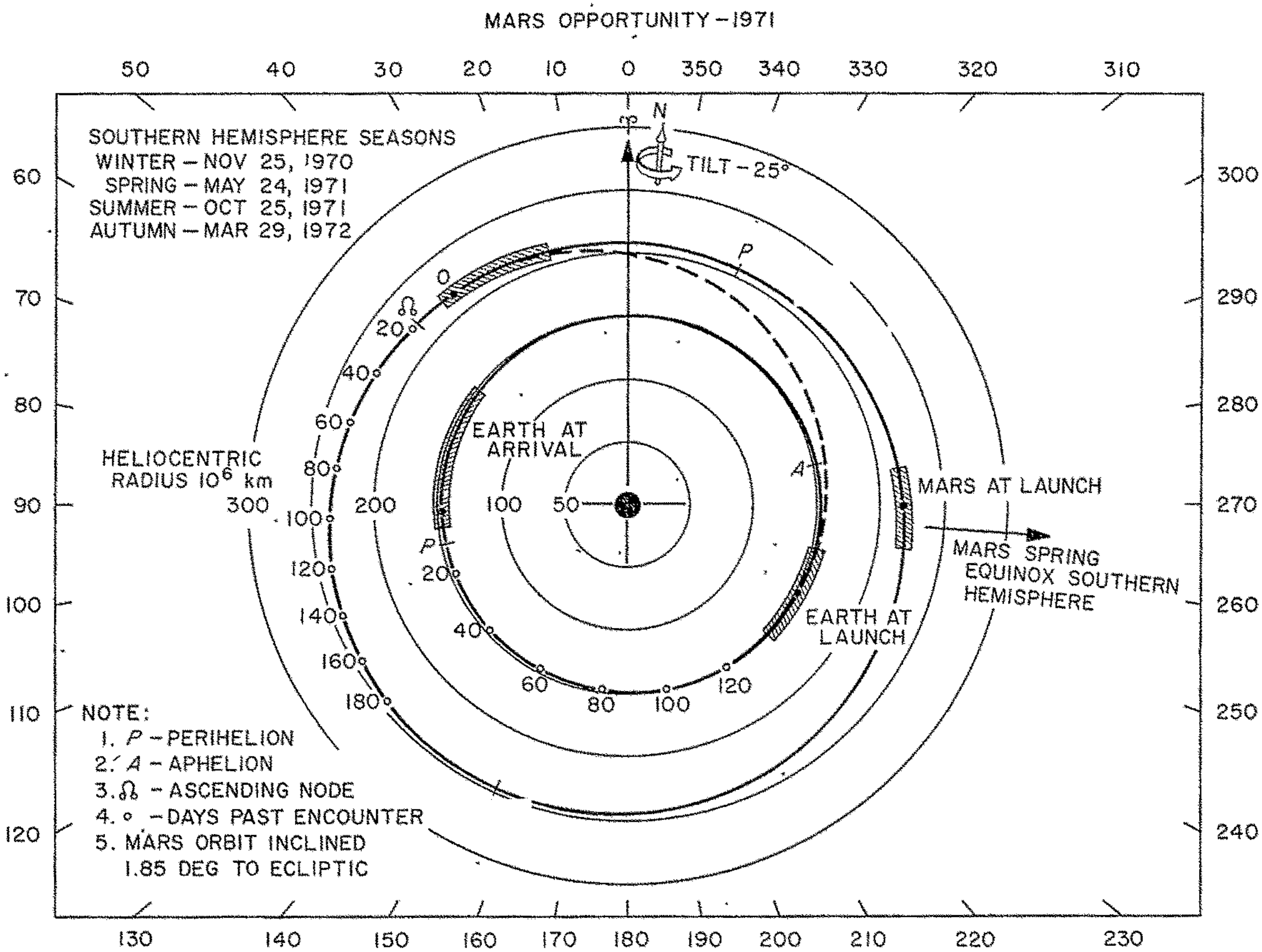

Figure 14. Plan View of Heliocentric Celestial Geometry

610-3

Table 8. Mission Characteristics During Orbital Operation

Event	Total Mission Operating Time, days			Communication Distance, millions of km			Sun-Mars Distance, millions of km		
	Encounter, E	E+30 days	E+90 days	Encounter, E	E+30 days	E+90 days	Encounter, E	E+30 days	E+90 days
1st S/C ARRIVAL	194	224	284	120.84	156.14	234.54	211.20	215.71	226.94
2nd S/C ARRIVAL	202	232	292	128.71	164.91	243.83	212.14	216.91	228.30

6/0-3

distance. The total mission operating times, communication distances, and Sun-Mars distances are given in Table 8 for both arrival dates and for three different satellite orbit operation lifetimes.

Figure 15 illustrates the changing position of the Earth in spacecraft coordinates as the spacecraft moves away from Earth. The tracks are shown for three different launch dates, utilizing the 14 November 1971 arrival. It can immediately be seen that the tracks--initially separated--converge at a communication distance of 120 million km, the Mars-Earth distance for this arrival date. From that point, it is assumed that the spacecraft will be orbiting Mars and result in the Earth track denoted by the dashed lines. The small amount of separation between the tracks at communication distances greater than 40 million km should simplify high-gain antenna pointing requirements. As shown in Reference 6, the use of a single-degree-of-freedom high-gain antenna enables the antenna boresight to be pointed within one degree of the Earth while the spacecraft is in Mars orbit.

One other factor pertaining to the heliocentric geometry bears mentioning. Note from Figure 14 that the arrival period occurs three Earth weeks after the start of southern summer. The 90-day orbiter operating lifetime extends almost to the beginning of fall. On the basis of the observed seasonal changes on Mars, the early arrival dates appear better suited for observation of these effects.

<u>Orbit Determination Properties</u>. References 8 and 9 show that the delineation of the outgoing asymptote (DLA) is an important paramter with regard to the redetermination of the trajectory after a midcourse maneuver from Earth. Small values of |DLA| (<5°) should be avoided. Table 7 shows that there is no problem for any of the trajectories considered.

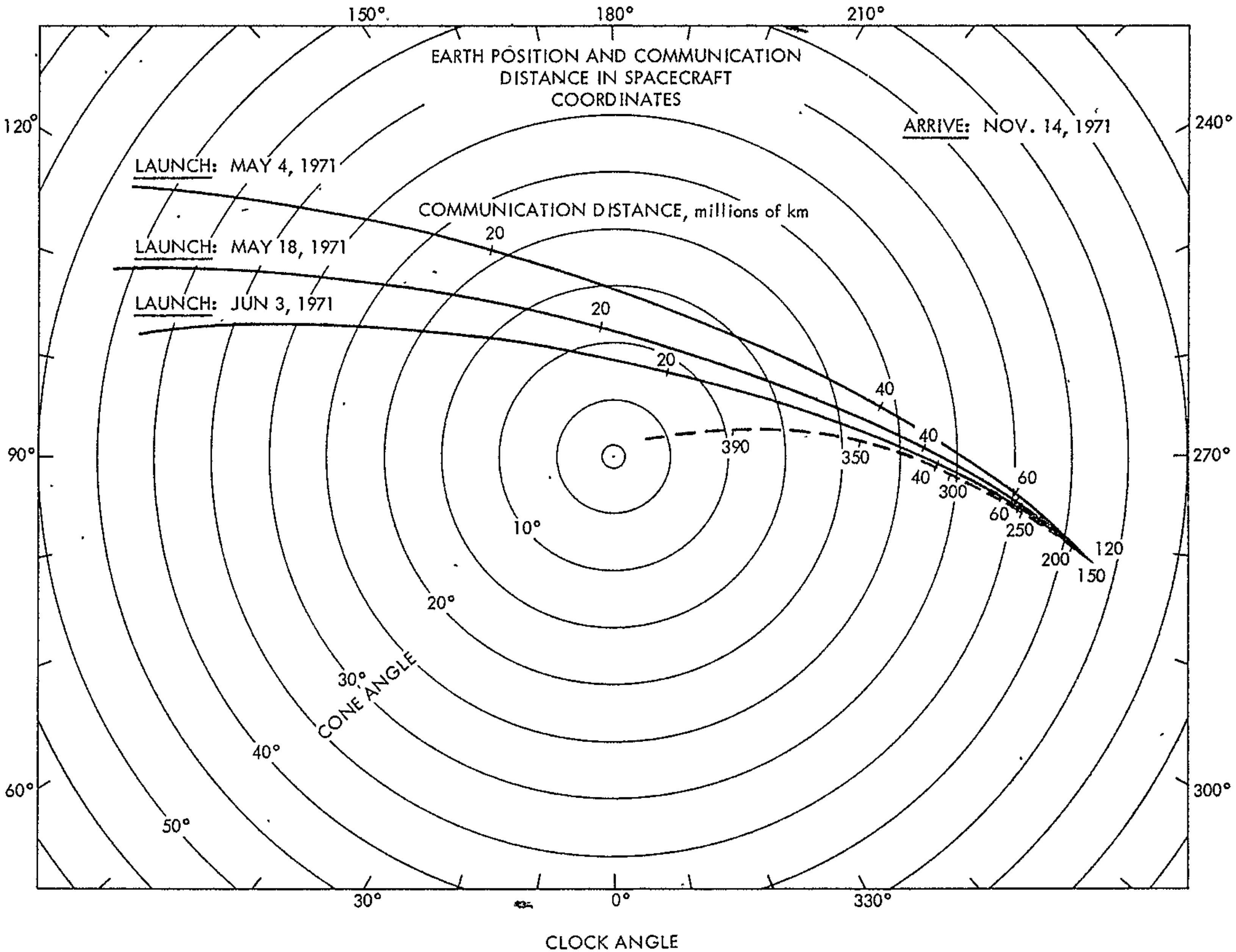

Figure 15. Atenna Pointing and Telecommunication Distance Requirements During Mission Lifetime

6/0-3

Similarly, the declination of Mars at arrival (DEC) is important for establishing the characteristics of the approach hyperbola before orbit insertion. Small values ($-5° < DEC < +5°$) should also be avoided. From a plot of DEC-vs-calendar date (Fig. 16), note that arrival dates between 9 December 1971 and 15 January 1972 yield undesirable orbit determination properties.

Midcourse Maneuver Error Sensitivity. The parameters SG1 and SG2 in Table 7 represent the semi-major and semi-minor axes of the dispersion ellipse at the planet caused by a 0.1 m/sec spherically distributed velocity error made at the time of the first midcourse maneuver (on the outgoing asymptote). The orientation of this dispersion is such that the semi-major axis maps into the miss parameter $\bar{B}$ (which affects the periapsis altitude of the approach hyperbola). Fortunately, the error sensitivity SG1 is quite small for the Type I trajectories under consideration. It can be seen that the errors are less for the earlier arrival date.

4. Mars Approach Phase

Approach Velocity. The hyperbolic excess velocity at Mars (V_∞) will be of primary concern in the mission design since it has a direct effect upon the orbit insertion propulsion system weight. The orbit insertion velocity requirements, which depend on approach speed, apsidal rotation, and orbit size, were discussed in detail in Section IV-C. An approximate "rule of thumb" for understanding the relationship between approach speed and orbit insertion ΔV is that an increase or reduction of 1 km/sec in V_∞ will result in a corresponding change of 0.6 km/sec in ΔV. From Table 7, it can be seen that the approach speeds for the early arrival dates reach a maximum of 3.262 km/sec. The selection of the 14 November 1971 date as the earliest possible arrival was based on the desire to limit the approach speed.

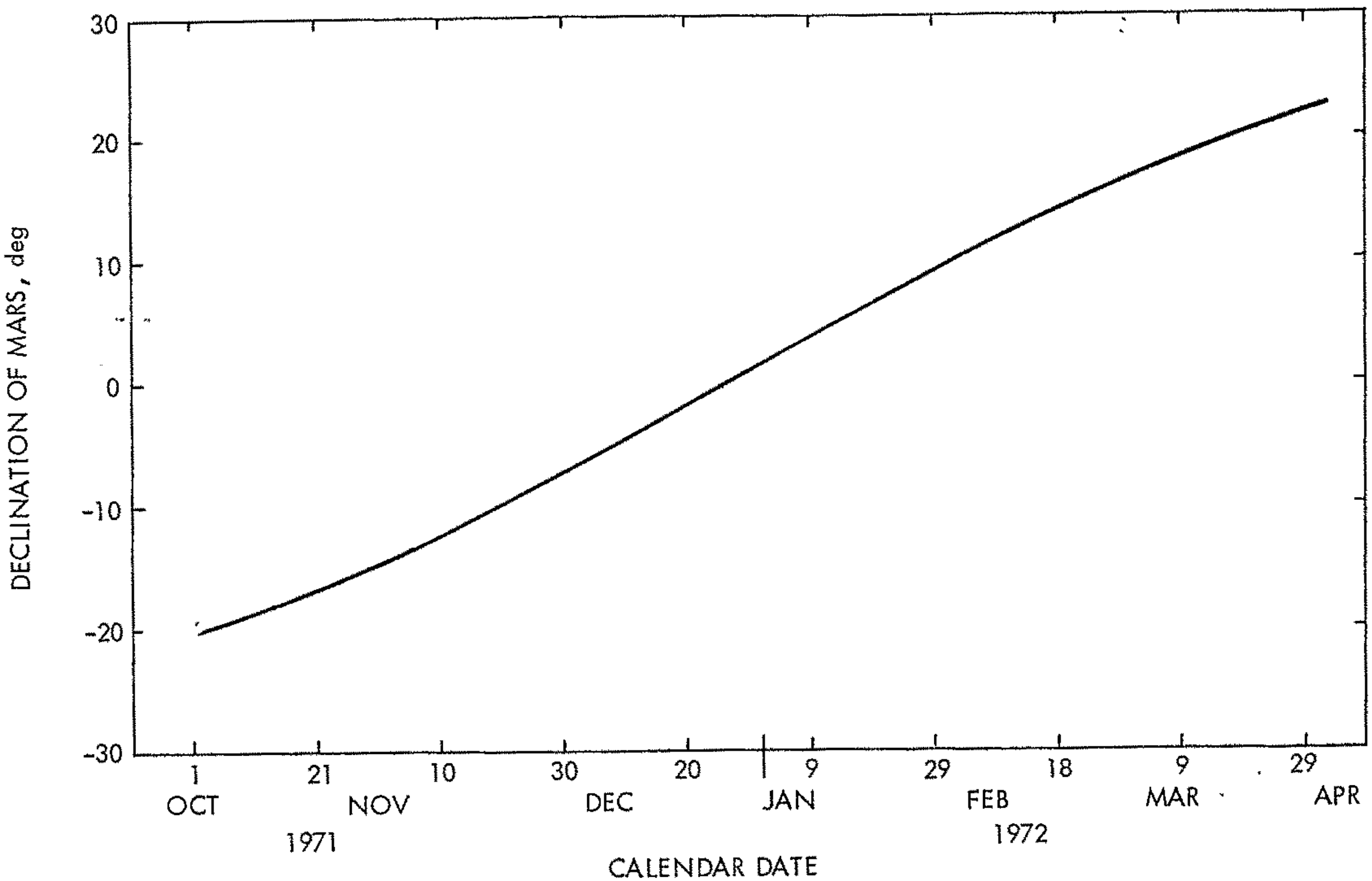

Figure 16. Declination of Mars vs Calendar Date

610-3

Approach Direction Relative to the Sun. For all feasible ballistic transfer trajectories to Mars, the spacecraft will approach Mars from its leading edge--the reason being that the spacecraft's heliocentric velocity is less than that of Mars near encounter. The approach direction can be described by the parameter, ZAP, which is tabulated in Table 7 for the various launch dates. It is defined as the angle between the Mars-Sun vector at encounter and the hyperbolic excess velocity vector. It represents the Mars-spacecraft-Sun angle at a few days before encounter. From observing this parameter, the approach direction relative to the Sun can be determined. Note from Table 7 that the range in ZAP is 104-118 degrees. In general, higher values of ZAP favor evening terminator orbits (periapsis located near the evening terminator), since they may be achieved with the use of smaller orbit insertion velocity increments. This may be visualized in Figure 17, which illustrates the incoming asymptote-related orbit geometry. The angle θ locates the periapsis ($\vec{R}_p$) of the approach hyperbola with respect to the approach asymptote $\vec{S}$. Its value depends largely upon V_∞. From the values tabulated in Table 7, its value is seen to be nearly 60 degrees for all launch dates. Referring again to Figure 17, note also that ZAP values of approximately 120 degrees provide hyperbolic periapsis locations ($\vec{R}_p$) with desirable television lighting angles (solar illumination angle, ILL = 30 deg). This is desirable since it permits a favorable elliptical orbit periapsis location with the utilization of minimum orbit insertion ΔV (periapsis-to-periapsis transfer). A decrease in the value of ZAP results in a correspond ing increase in the illumination angle. On the basis of the values of ZAP given in Table 7, it can be seen that good periapsis lighting angles can be achieved with a minimum apsidal rotation.

610-3

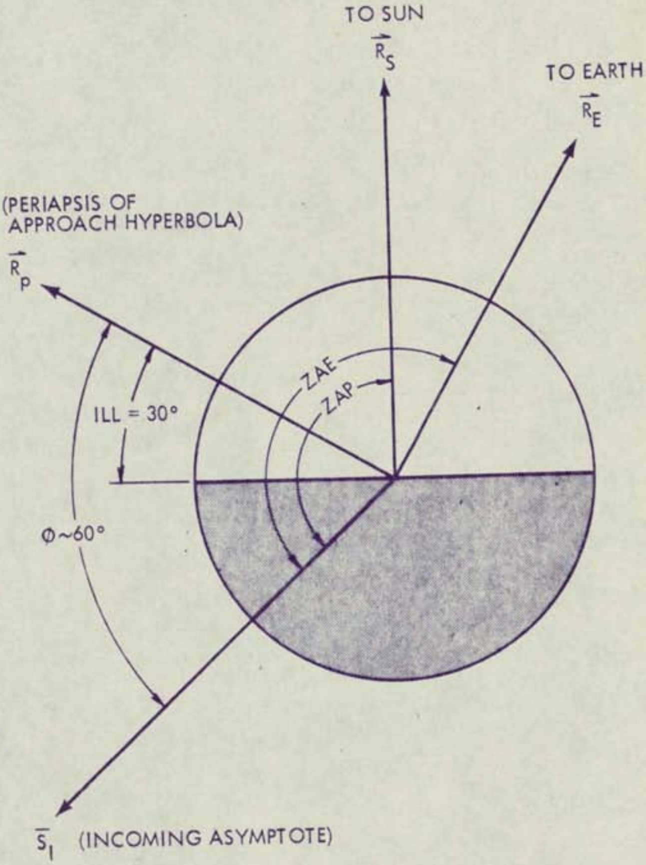

NOTE:
1. PLANE OF PAPER IS DEFINED BY $\vec{R}_S$ AND $\vec{S}_I$
2. $\vec{R}_E$ AND $\vec{R}_p$ DO NOT NECESSARILY LIE IN PLANE OF PAPER

Figure 17. Definition of Mars Approach Parameters

Table 4. TV Sequences for 60-deg Inclination Orbit

Days past insertion	0	18	36	54	72	90
Start TV						
Time, min	-19.15	-12.6	- 3.9	5.5	+15.5	26.9
Latitude, deg	-57.5	-50.0	-37.2	-19.9	0	17.0
True Anomaly, deg	-39.9	-25.3	- 9.5	+10.8	+35.0	53.4
Altitude, km	2590	2250	2150	2190	2360	3023
Illumination Angle, deg	45.3	43.8	42.3	40.9	39.3	36.0
Periapsis						
Latitude, deg	-31.6	-31.0	-30.4	-29.8	-29.2	-28.6
Altitude, km	2090	2090	2090	2090	2090	2090
Illumination Angle, deg	17.1	27.9	38.0	47.2	55.5	62.0
End TV						
Time, min	4.05	10.6	19.3	28.7	38.7	50.0
Latitude, deg	-24.2	-11.0	+3.8	+18.0	+30.9	+41.3
True Anomaly, deg	9.0	22.0	40.0	56.2	70.9	83.2
Altitude, km	2114	2265	2600	3140	3840	4660
Illumination Angle, deg	10	10	10	10	10	10

Approach Direction from Earth. At the time of Mars encounter, Earth will be ahead of Mars in its orbital position around the Sun. The angle between the direction to the Sun and Earth as measured from Mars will always be less than 45 degrees. Following encounter, this angle will decrease until it reaches zero degrees at the time of conjunction.

The parameter ZAE, which is given in Table 7 for various launch and arrival dates, is the angle between the Mars-Earth vector at encounter and the hyperbolic excess velocity vector. It represents the Mars-spacecraft-Earth angle as the spacecraft approaches Mars at a few days before encounter. For values of ZAE near 180 degrees, Earth occultation will occur for all aiming points (orbital inclinations) and apsidal rotations. From Table 7, it can be seen that the values of ZAE are close to 180 degrees, meaning that achievement of Earth occultation orbits is not difficult. Also associated with values of ZAE near 180 degrees is the possibility of the orbit insertion occurring while the spacecraft is in Earth occultation. It will be shown in the discussion on orbit selection that this phenomenon does not occur for the selected orbits.

Latitude of Vertical Impact Points. The latitude of vertical impact points on the surface of Mars, as measured from the equator of Mars, is also presented in Table 7 for the various launch and arrival dates; this parameter is labeled LVI. It is also closely equal to the latitude of the sub-vehicle point of the spacecraft a few days before closest approach to Mars. LVI also indicates the minimum achievable inclination of a satellite orbit about Mars which may be established without performing a yaw maneuver during orbit insertion.

610-3

E. Satellite Orbit Selection and Characteristics

1. Orbit Selection Criteria

The characteristics of the Mars satellite orbits that are available in conjunction with the approach geometry discussed in Section IV-D are treated in this section. Because of the interaction between the engineering design of the spacecraft and the selection of a suitable satellite orbit, it is necessary to define a series of considerations affecting the orbit design. Listed below are the scientific experiment requirements and spacecraft engineering considerations that are most relevant to an optimal mission design.

Provision for Television Experiment. The orbit required for this experiment should be nearly sub-synchronous to provide orbital tracks that are equally spaced in longitude, thus allowing side-to-side picture overlap and, hence, contiguous photographic coverage of a large region of the planet's surface. To achieve maximum picture resolution, the orbit periapsis altitude should be as low as possible and still be consistent with the capabilities of the Mariner Mars 1969 photographic system. The sub-satellite track near periapsis should also exhibit wide latitude variation and have solar illumination angles ranging somewhere between 10 and 50 degrees.

Provision for Earth Occultation Experiment. The Earth occultation experiment is designed to provide information about the atmospheric density profile, its locational variation, and the figure of the planet. Thus, an orbit is desired which provides for Earth occultation over a wide range of latitudes and solar illumination angles, and of short duration so as to maximize the telemetry data returned to Earth.

<u>No Sun Occultation for 90 Days</u>. This condition reduces the power system and thermal control requirements. It also allows continuous Sun acquisition, which should improve reliability. Ninety days is the design mission lifetime.

<u>Avoidance of Canopus Occultation, if Possible</u>. It is desirable, but not mandatory, to avoid Canopus occultation so that the roll attitude reference will not be lost.

<u>Avoidance of Earth Occultation During Orbit Insertion Maneuver</u>. It is desirable to avoid Earth occultation any time during the attitude turns or powered flight phases, allowing careful monitoring of the maneuver from Earth and permitting backup commands to be sent for critical events. The pre-insertion attitude turns, propulsion ignition, and propulsion shut-down are the most critical events.

<u>Choice of Orbit Period to Maximize Data Return</u>. Because of the data rate limitations associated with the large Earth-Mars communication distances, it is highly desirable to maximize the total number of tape recorder playbacks. The orbital period of revolution should provide a sufficient number of television sequences (periapsis passages) to take full advantage of the Goldstone 210-foot antenna communication capabilities.

2. Selection of Orbital Period

Because of the superior data rates available from the 210-foot antenna, it is desirable to have tape recorder readouts occur when the spacecraft is in view of the Goldstone station. At a data rate of 16,200 bps, one readout would require approximately 3 hours, suggesting that two readouts are possible during each view period. Because of the increase in ground station system temperature due to the Earth's atmosphere, however, the 16,200 bps data rate capability is limited to Goldstone elevation angles greater than approximately 15 degrees. Since this provides a Goldstone viewing period of 9 hours, careful orbital sequencing is necessary to guarantee two readouts. To accomplish this sequence, a Goldstone synchronous orbital period of 12 hours has been selected. The orbit would be phased to allow alternate television sequences (periapsis passages) to occur at Goldstone zenith. Data from Goldstone zenith television sequences would be read out during the second half of the viewing period while the first half of the viewing period would be used for the non-Goldstone zenith television sequence (preceding periapsis passage).

Because the Mars rotation period of 24 hours 40 minutes and the 12-hour Goldstone synchronous orbit are nearly sub-synchronous with respect to Mars, the satellite orbit tracks for alternate revolutions have longitude spacing that satisfies the requirement for side-to-side picture overlaps. Further discussion of side-to-side overlap is presented below.

3. Periapsis Altitude Considerations

The choice of periapsis altitude was influenced primarily by the desire to maximize picture resolution and to guarantee side-to-side overlap of the low-resolution television frames (11 x 14-deg field of view). The relationship between periapsis altitude (h_p) and the distance between alternate orbital tracks (d) is illustrated in Figure 18. For a given field of view ($\phi_L \times \phi_W$) and overlap ratio (OVL), the periapsis altitude is

$$h_p = \frac{d}{2\ (1 - \mathrm{OVL})\ \tan \phi/2} \qquad (1)$$

where $\phi = \phi_W$ or ϕ_L, depending on camera orientation.

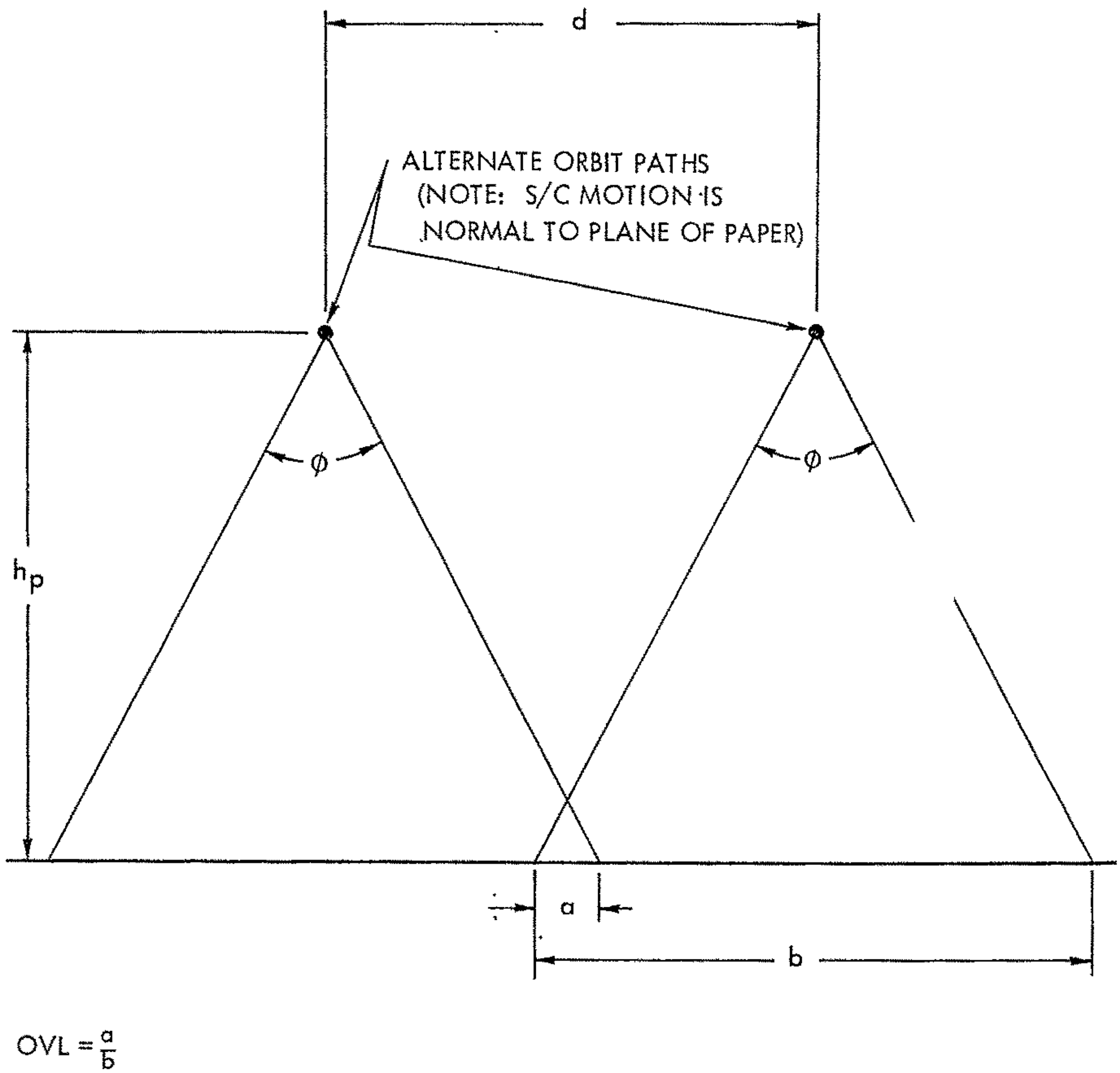

Figure 18. Relationship Between Camera Field of View and Altitude

The lowest periapsis altitude can be obtained by orienting the camera so that the larger field-of-view dimension (ϕ = 14 deg) is aligned normal to the track. The distance between orbital tracks (d) can be determined from the azimuth angle of the sub-satellite track at periapsis* (Σ_p) and the longitude difference between tracks ($\Delta\theta$). The relationship between these parameters (see Fig. 19) is given below:

$$d = R_m \sin^{-1}[\cos \Sigma_p \sin \Delta\theta] \qquad (2)$$

where R_m = Mars radius (3378 km).

Assuming a minimum overlap ratio of 0.06, an azimuth at periapsis of 35 degrees, and a $\Delta\theta$ value of 10 degrees (resulting from the 40-minute difference between the Mars rotation period and two satellite orbit revolutions), the periapsis altitude equals 2,090 km.

4. Orbital Inclination Considerations

To obtain a wide range of latitude coverage, it is desirable to choose an orbit with an inclination as large as possible with respect to the Mars equator. Another advantage of large inclination values is that they provide azimuths at periapsis (Σ_p) closer to zero degrees. This effect is illustrated in Figure 20, which gives Σ_p as a function of orbital inclination for ψ values of interest. Azimuth angles near zero or 180 degrees are desirable since they represent sub-periapsis traces with the greatest latitude variation. F southern hemisphere periapsis orbits, inclination angles greater than 6

---

* Thus quantity is a function of orbital inclination, which is discussed in the next sub-section. Σ_p is defined as the angle between the local meridian and the periapsis velocity vector measured east of north.

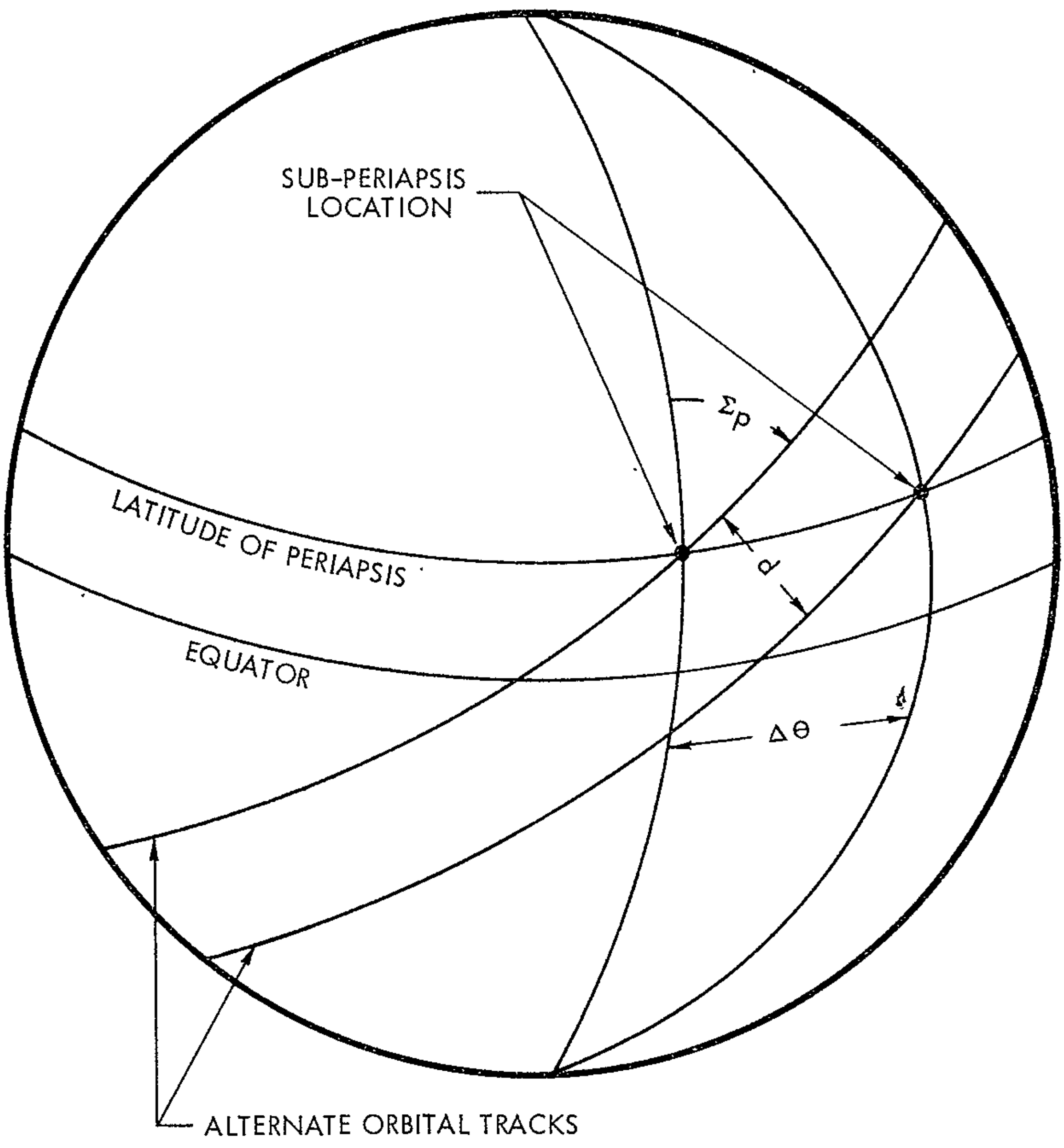

Figure 19. Sub-Satellite Trace Geometry

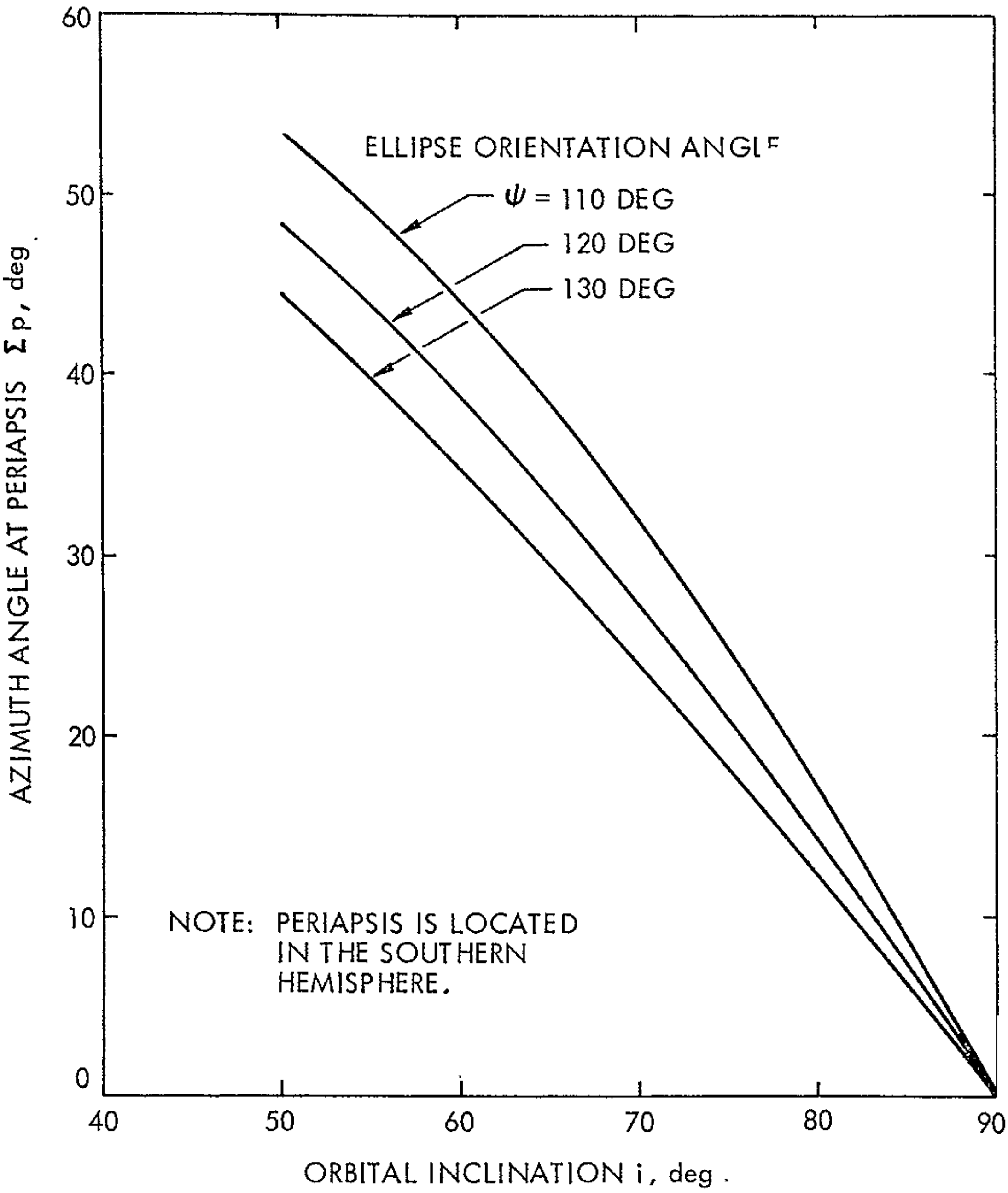

Figure 20. Azimuth Angle at Periapsis vs Orbital Inclination

degrees result in Canopus occultation and hence may be undesirable. Alternately, inclinations less than 40 degrees are disadvantageous since they cause Sun occultation sooner than 90 days past insertion.

A summary of the Sun, Earth, and Canopus occultation periods for three values of orbital inclination is given in Table 9. Also shown are the maximum durations per revolution for each of the respective occultations.

Northern hemisphere orbits, defined as having periapsis initially located in the northern hemisphere, are undesirable because Canopus occultation occurs for a wide range of inclinations, overlapping the inclination range exhibiting Sun occultation. In addition, moderately inclined northern hemisphere orbits have Σ_p values near 90 degrees and therefore have limited latitude variation near periapsis. Also disadvantageous are the low values of solar illumination angle at periapsis, necessary in order to avoid Earth occultation at orbit insertion. This characteristic is more predominant for large values of inclination.

5. Candidate Orbit

To satisfy the scientific objectives and engineering considerations discussed previously, a specific orbit was chosen. The selected orbit, which is established from an interplanetary transfer trajectory arriving 14 November 1971, has periapsis and apoapsis altitudes of 2,090 and 16,484 km, respectively, providing an approximate 1/2-Mars synchronous orbital period of 12 hours. The important characteristics of this orbit are summarized in Table 10. Note from the table that the ellipse periapsis location ψ was chosen to be 130 degrees, corresponding to an apsidal rotation of

Table 9. Orbital Characteristics for Various Inclinations

Orbit Inclination, deg	Engineering Characteristics: Canopus Occultation, min/rev — Days Past Insertion 0	30	90	Occultation — Sun: Time Period Past Orbit Insertion days	Sun: Maximum Duration, min	Sun: Fraction of Orbital Period, %	Earth: Time Period Past Orbit Insertion, days	Earth: Maximum Duration, min	Earth: Fraction of Orbital Period, %	Earth Occultation Experiment: Total Number of Days Exhibiting Earth Occultation*	Total Number of Occultation Measurements*	Latitude Range of Occultation Points
50	None	None	None	110 - 170	100	13.9	0 - 40, 140 - †	40	5.6	40	160	40° S to 70° N
60	None	None	None	130 - †	90	12.5	0 - 30, 165 - †	40	5.6	30	120	30° S to 70° N
70	None	None	55	145 - †	70	9.7	0 - 20	40	5.6	20	80	20° S to 70° N

* Assuming a 90-day mission lifetime.

† Greater than 180 days.

NOTE:

Southern hemisphere periapsis, (ellipse orientation angle, ψ = 130 deg).

610-3

610-3

Table 10. Summary of Orbital Characteristics

Orbital Parameters

Orbital period = 12 hrs (Goldstone synchronous)

Periapsis altitude = 2090 km

Apoapsis altitude = 16484 km

Inclination to Mars equator = 60 deg (periapsis in southern hemisphere)

Ellipse orientation angle, ψ = 130 deg

Canopus Occultation

None during 180 day time period past orbit insertion.

Sun Occultation

None for first 130 days past orbit insertion.

Maximum duration of 90 min at 150 days past insertion.

Earth Occultation

Exists for 30 days immediately following orbit insertion.

Duration of 40 min on 1st day (starts at 20 min past periapsis)

Occultation does not re-occur until 165 days past orbit insertion.

Orbit Insertion

Velocity Increment for nominal approach speed and periapsis altitude = 1,571 m/sec

Burn time = 12 min

De-boost starts at 16 min before periapsis

De-boost ends at 4 min before periapsis (24 min before Earth occultation) approximately 10 degrees in the direction of the evening terminator. The small ΔV penalty for this rotation allows for the natural migration of the terminator away from the relatively inertially stable orbit. This movement, caused by the orbital motion of Mars around the Sun, results in a 45-degree increase in solar illumination angle at periapsis during the 90-day mission lifetime.

This orbit geometry may be better understood by referring to Figure 21, which illustrates the initial orientation of this orbit as seen from the direction normal to the orbit plane. Periapsis is located above the southern hemisphere about 17 degrees from the terminator. Shown in this illustration are the Sun, Earth, and approach asymptote directions, the orbit insertion (de-boost) maneuver, and the data recording and Earth occultation sequences.

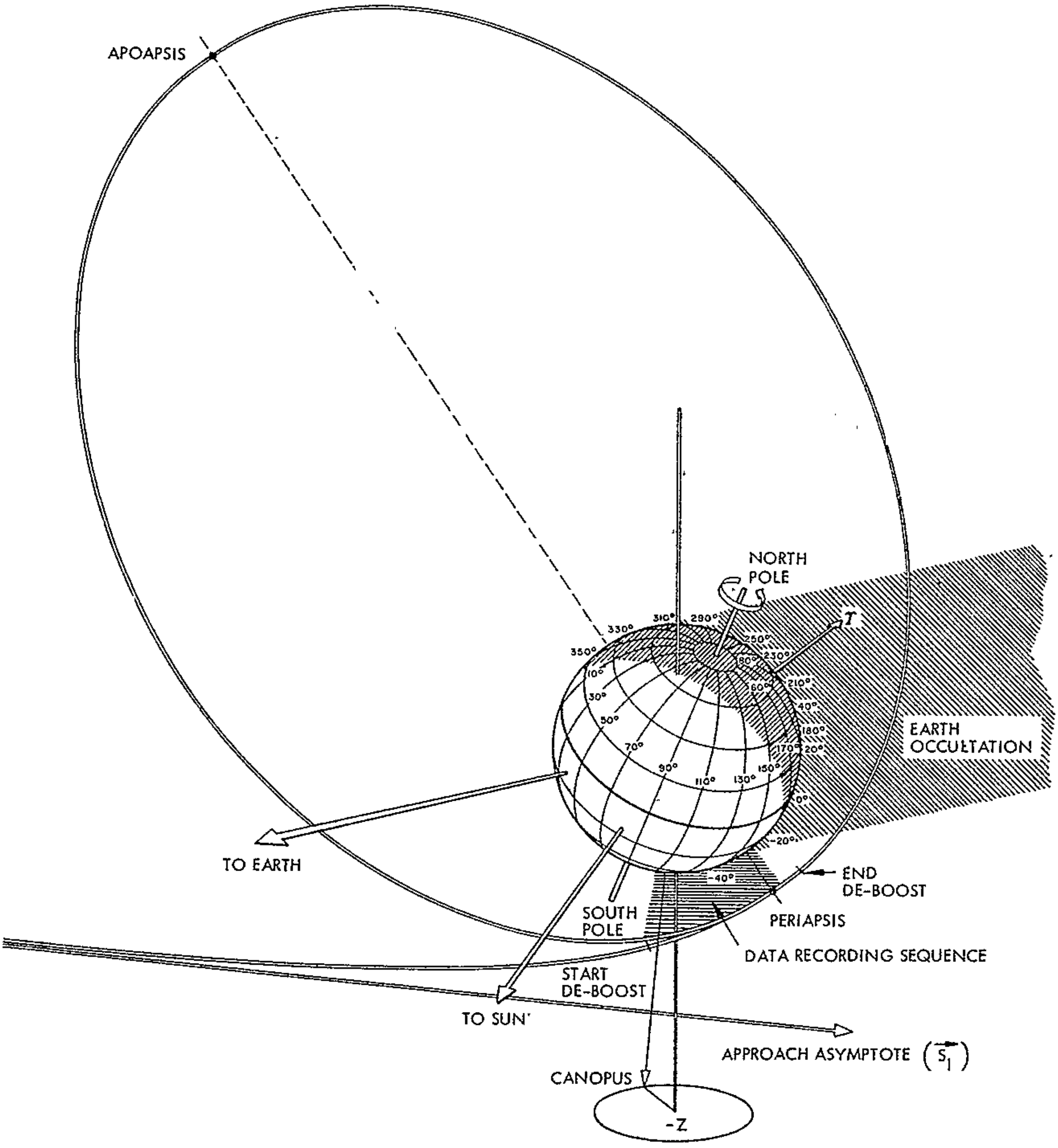

Figure 21. Mariner Mars 71 Orbit Profile As Seen From Direction Normal to Orbit Plane

V. SPACECRAFT DESCRIPTION

A. Functional Characteristics

1. Telecommunication Performance

Telemetry performance for encounter and playback during a Mariner 1971 Mars orbiter mission is considered here. The performance base is the Mariner Mars 1969 telemetry channel with the following major parameters:

(1) 20 watts spacecraft transmitter power.

(2) Fixed-position 40-inch circular aperture high-gain antenna with a peak gain of 25.6 db.

(3) High rate (designated CH C) block coded science channel at 16.2 Kbps, with a minimum bit and word error rate of 5 IN 10^3 and 1 IN 10^2, respectively. Medium rate (designated CH A) non-coded science channel at 270 bps, with a minimum bit and word error rate of 5 IN 10^3 and 3 IN 10^2, respectively.

(4) Ground 85-foot antenna for the 270-bps channel, 210-foot antenna for the 16.2 Kbps channel.

The performance goal is to achieve 90-day playback times at sufficiently high data rates that the spacecraft may photograph the Mars surface through the television camera over an extended period.

In light of this goal, an 8.1 Kbps rate (a block coded channel used with the 210-foot antenna after 16.2 Kbps threshold), a 48-inch high-gain, and multiple antenna positions were considered as modifications to the 1969 design and are reflected in the performance tables and curves.

Table 11 summarizes performance capability at 16.2 Kbps, 8.1 Kbps, and 270 bps for a Mariner 1971 mission. Based on an encounter date of 14 November 1971, performance at 8.1 Kbps is extended by switching to a second antenna position (Pos. II). The 270-bps, 85-foot ground antenna mode is considered a backup science mode. A 135-bps rate for this mode is possible (but not included here), using high-gain position II. Table 12 is a summary design control table providing a comparison between Mariner 1969 and 1971 channels using the 40-inch high-gain antenna.

The encounter range for 1971 (parameter 3, Table 12) is larger than the 1969 encounter range, resulting in a -1.9 db loss in performance. However, pointing the high-gain antenna for one 1971 encounter date (performance is compromised in 1969 by pointing the antenna for two bounding encounters) reduces antenna pointing loss and pointing loss tolerance and makes up 1.2 db of the 1.9 db loss.

The Earth position with respect to the spacecraft high-gain antenna is relatively fixed over a long enough period to allow sufficient playback times using one or two antenna positions. Figures 22 and 23 show Channel C telemetry margin after encounter for the 40-inch and 48-inch high-gain antennas, respectively. Both figures assume start of playback at 16.2 Kbps, using the first antenna position. When the margin reaches 0 (nominal threshold), the bit rate is changed to 8.1 Kbps. The antenna position remains unchanged. When 8.1 Kbps margin reaches the Σ neg tol, the antenna is moved to Position II to increase performance above the Σ neg tol curve for an additional period. The 48-inch antenna provides more time with the 16.2 Kbps margin above Σ neg tol, but actually less time at 8.1 Kbps above Σ neg tol for two antenna positions.

610-3

Table 11. Telemetry Performance (days after encounter)

	Antenna				
Bit Rate	48 In.		40 In.		Antenna Position
	Σ	Nom	Σ	Nom	
16.2 K bps	35	57	25	50	1
8.1 K bps	67	83	75	98	1 & 2
270 bps	40	60	37	57	1

Arrival Date: 14 November 1971

	Cone	Clock	Tolerance/Each Angle
Position I:	43°	283°	±0.85°
Position II:	39.8°	280.8°	±0.85°

610-3

Table 12. Performance Comparison Between 1969 and 1971

Channel Parameters	Parameter Values, Mars Encounter		
	8-1-69		11-14-71
	CH C	CH A	CH C
1 TX. Power $\left(17 {}^{+4}_{-0}\ w\right)$, dbm	42.3	42.3	42.3
TX. Antenna Gain, db	25.6	25.6	25.6
Size, in.	40 in.	40 in.	40 in.
2 Position, deg			
Cone	41.1	41.1	43
Clock	268.9	268.9	283
3 Space Loss, db	-259.4	-259.4	-261.3
Range (Encounter) x 10^6 km	96.6	96.6	120
4 Miscellaneous Channel Losses, db (See NOTES 1 and 2)	- 2.6	- 2.6	- 1.9
	1	1	2
5 RX. Antenna Gain, db	61.8	53.3	61.8
Size, ft	210	85	210
6 RX. Total Power, dbm	-132.3	-140.8	-133.4
7 Data Channel Power, dbm	-133.4	-143.4	-134.6
8 Data Threshold Power, dbm	-139.5	-152.5	-139.5
Bit Rate	16.2K	270	16.2K
Bit Error Rate (NOTE 3) in 10^3 bits	5	5	5
RX. Noise Temperature, deg °K (NOTE 4)	25	42	25
9 Nominal Margin, db	6.1	9.1	4.9
10 Σ Negative Tolerance, db	- 3.5	- 5.9	- 3.0
11 Margin Above Σ Negative Tolerance, db	2.6	3.2	1.9
12 Days of Playback	23	28	25

NOTES:

1. Parameter 4, 2.6 db = 1.8 db circuit loss +0.8 db pointing loss. Antenna pointed for 8-1-69 and 8-10-69 bounding encounter arrival dates.
2. Antenna pointed for one encounter only. Lessens antenna pointing loss and the pointing loss tolerance.
3. CH C: Science High Rate Block Coded Channel.
   CH A: Science Medium Rate Noncoded Channel.

   5 in 10^3 bit error rate = >1 in 10^2 word error rate for 6-bit biorthogonal code channels.

   5 in 10^3 bit error rate = >3 in 10^2 word error rate for 6-bit uncoded words.
4. The 25-deg noise temperature assumes an ultra cone/listen-only mode, less than 0.1 in. rain/hour and an elevation angle greater than 25-deg.

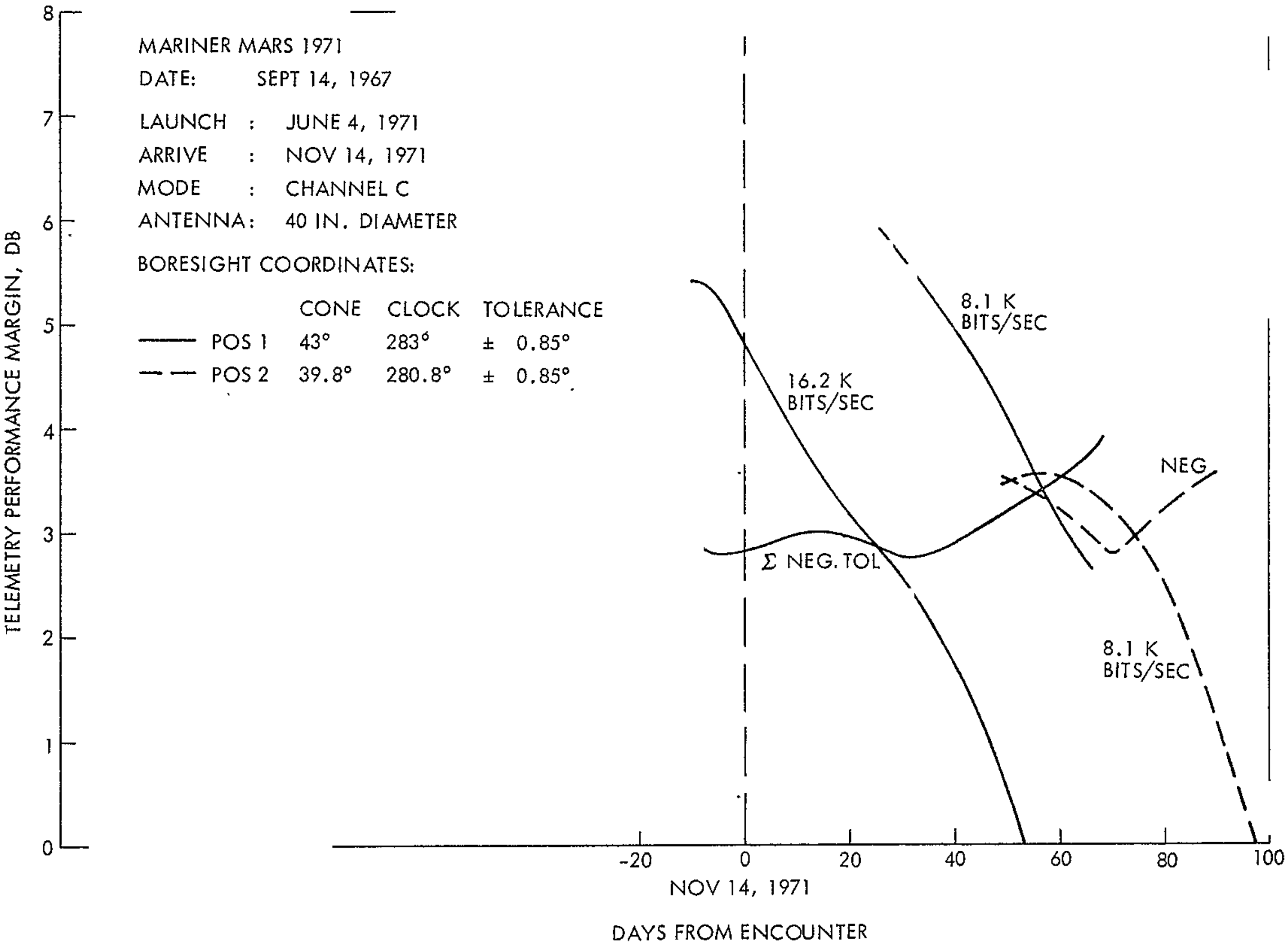

Figure 22. Post-encounter Channel C Telemetry Margins, 40-in. Antenna

610-3

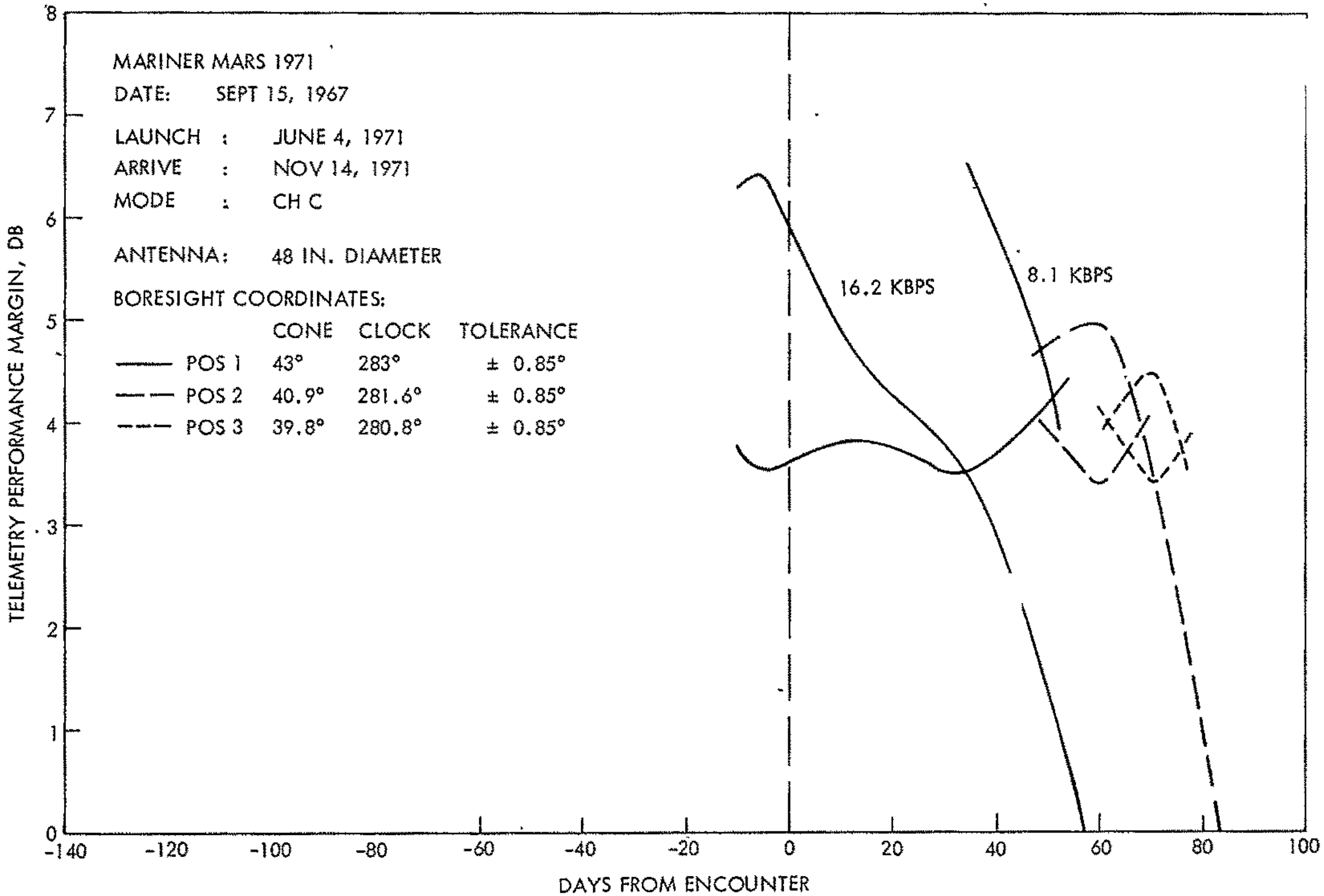

Figure 23. Post-encounter Channel C Telemetry Margins, 48-in. Antenna

610-3

A third position is included for the 48-inch antenna to show additional performance possibilities.

The larger 16.2 Kbps performance for the 48-inch antenna is due to higher peak gain and the relatively stationary Earth position with respect to the peak gain axis immediately after encounter. Lesser performance at 8.1 Kbps for two 48-inch antenna positions results from the narrower beamwidth. The Earth, during the 8.1 Kbps playback, is moving away from the peak gain axis at a faster rate. As a result, the narrower beamwidth causes a quicker loss of antenna gain. The 48-inch antenna must be pointed more accurately to achieve the benefit of its higher gain. Also, the 48-inch antenna is more sensitive to the 0.85-degree pointing tolerance, as indicated by the larger Σ neg tol curve for this antenna.

Figure 24 shows performance for the 40-inch and 48-inch antennas with no pointing loss. Comparison of Figures 22 and 23 with Figure 24 indicates the loss in performance due to the high-gain pointing system and the 0.85-degree pointing tolerance.

2. <u>Guidance Accuracy-Orbit Insertion</u>

An analysis was performed to determine whether the Mariner 1969 attitude control and autopilot performance capabilities would satisfy the orbit-insertion accuracy requirements for the Mariner 1971 mission. Of particular interest were the questions:

(1) Should accelerometer or timer shutoff be used?

(2) Is autopilot path guidance required?

(3) What accuracy improvement could be expected with the use of optical approach guidance?

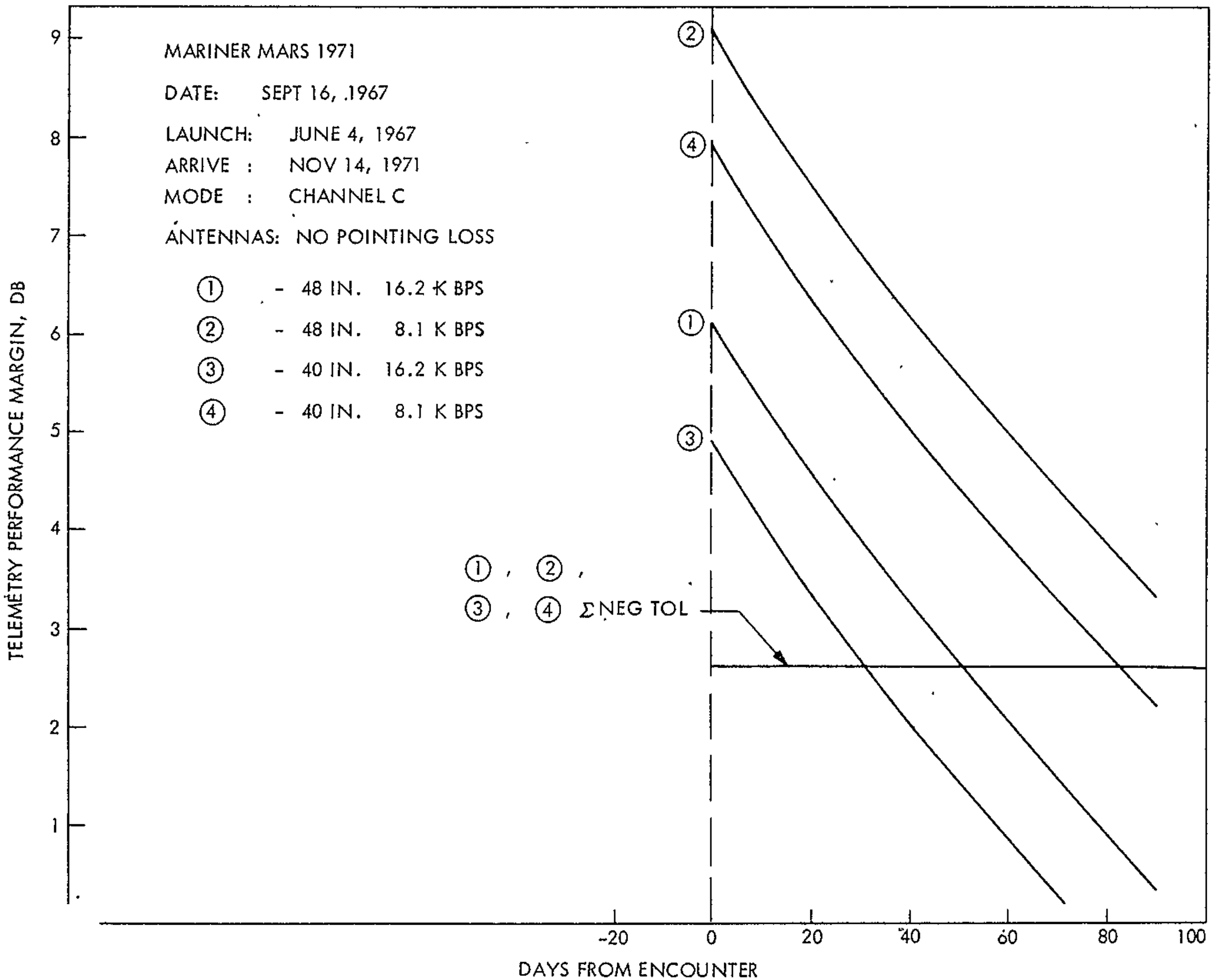

Figure 24. Antenna Performance With No Pointing Loss

610-3

The following sections cover the assumptions and error sources used and a discussion of the results of the orbit insertion accuracy analysis for the Mariner Mars 1971 orbiter mission.

Approach Trajectory and Planetary Orbit. The trajectory assumed for this analysis is characterized by a 4 May 1971 launch and 14 November 1971 arrival at Mars, with an approach speed of 3.124 km/sec. The assumed planetary orbit is characterized by a 1,000-km periapsis altitude and 20,000-km apoapsis altitude above Mars (μ = 42977.8 km^3/sec^2 and radius = 3,378 km). This orbit has a period of 13.76 hours. Changing the apoapsis to give a 12-hour orbit should not have a large effect on the accuracy results. Ellipse orientation, angle from asymptote to ellipse axis, is varied from 100° to 150° (periapsis-to-periapsis transfer is at $\approx$120°).

The approach trajectory miss parameter, b, is selected so that it is approximately tangent to the ellipse. The value of b is selected to be about 10 km inside the tangent orbit for the monte carlo analysis and on the tangent orbit for the linear analysis. This aiming point was changed for convenience in this short study.

It is assumed that the estimated approach orbit is the nominal orbit and the only uncertainty is the orbit determination error, the deviation of the actual orbit about the estimated/nominal orbit.

Orbit determination error is taken to be 50 km (1σ) for b and 10 sec (1σ) in time for radio O.D. Accuracy estimates were also made for 10 km and 0 km (1σ) errors in b. The 10-km accuracy is what could be achieved with optical approach guidance and the 0-km accuracy is included as a reference point for execution errors only (except that the 10-second error in time includes O.D. errors of time of periapsis as well as execution time errors).

Maneuver Execution Error Sources. The orbit insertion maneuver execution errors include thrust vector pointing, motor shutoff, and time of execution errors. Time error was covered in the last section since it is mainly an O.D. error. The other two errors are discussed below. Unless otherwise stated, all errors are 1σ.

(1) Thrust Vector Pointing. The thrust vector pointing error consists of three parts: maneuver turns error, center-of-gravity offsets, and motor angular misalignment.

The maneuver turns error was evaluated using the midcourse pointing error computer program with Mariner 1969 error sources and was found to be 7 mrad per axis. An angular misalignment due to gyro drift during motor burn is 0.43 mrad, the average angle offset for an 850-second burn and a drift rate of 0.2 deg/hr.

The center-of-gravity shifts are translational offsets between the center of gravity and center of thrust and include:

center-of-gravity offset 0.024 inch per axis from the relative alignment of the center of gravity and a single motor of 0.1 inch (3σ) split equally between the center of gravity and the motor locations.

center-of-thrust shift due to three motors with 0.024-inch location errors per axis = 0.014 inch.

center-of-thrust shift due to 1% (3σ) thrust error of three motors located 20 inches off the center line = 0.027 inch.

- center-of-gravity shift due to center of gravity of fuel being off the center line with progressive shift with fuel usage = 0.0083 inch for 10 in-lb mismatch among four tanks and 1,000 pounds of fuel and a 1,200-pound spacecraft

  center-of-gravity shift due to unequal fuel usage from the tanks = 0.017 inch from 1% (3σ) fuel flow from each tank.

These figures rss to 0.042 inch total offset. For a 20-inch distance distance from the plane of the three motors to the center of gravity, this is an angular offset of 2.1 mrad per axis. This is the predominant autopilot error when no path guidance loop is used.

The motor angular misalignment is 3.5 mrad per axis per motor for mechanical alignment and gimbal null offset, averaging to 2.0 mrad. This is the predominant error if a path guidance loop is used.

The rss of all angular offsets without path guidance is

$$[(7.0)^2 + (.43)^2 + (2.1)^2]^{1/2} = 7.33 \text{ mrad}$$

With path guidance, it is approximately the same.

(2) Shutoff Error. The cases of timer and accelerometer shutoff are both considered. In each, the resolution error is neglected since the maneuver can be designed to use an integral number of resolution steps. The tailoff uncertainty is neglected since it is small compared to the total impulse provided.

The timer error is due to the thrust level error of 1% (3σ) per motor. Averaged over three motors, this figure is 0.19%.

Two accelerometer errors occur: the scale factor of 0.1% and the null offset of 0.001 m/sec^2 (acting for 850 seconds to reach 1.5 km/sec total ΔV gives an error of 0.057%). The total error is 0.115%.

Table 13. Error Cases Considered in Accuracy Analysis

Error Case	Shutoff	Pointing	Time	Orbit Det.	Description
1	0.115%	7.33 mr	10 sec	50 km	Accelerom. & Radio O.D.
2	0.19	7.33	10	50	Timer & Radio O.D.
3	0.19	7.33	10	0	Timer & Perfect O.D.
4	0.115	7.33	10	0	Accelerom. & Perf. O.D.
5	0.19	7.33	10	10	Timer & Radio/Optical O.D.

Accuracy Analysis Results. Two methods of analysis were used in this study: the monte carlo program IRMA and a linear analysis program. Five error cases were considered, as shown in Table 13. Cases 1-3 were run by monte carlo and all by the linear method. Differences in the linear and monte carlo results are mainly due to the different maneuver points used and, to some extent, to the nonlinearities in the orbit transfer characteristics.

The results of these runs are tabulated in Table 14. The parameters of the ellipse considered are periapsis and apoapsis distances, ellipse orientation, and period. Selected cases are plotted in Figures 25 and 26. In all cases, the ellipse orientation accuracy is about 0.45°. Periapsis accuracy is determined by the O.D. accuracy and ellipse orientation and is about the same with timer or accelerometer shutoff. Apoapsis altitude accuracy is degraded by about 50 km when the timer shutoff is used instead of accelerometer shutoff and O.D. error is 50 km. The degradation is 100-150 km when there is no O.D. error, but the total error is still less than with the 50-km O.D. error.

The effect of adding spacecraft-based optical measurements to the radio tracking orbit determination is shown in Figure 26. Periapsis is improved by a factor of 2 to 5 and apoapsis is improved by up to a factor of 2, depending on the orientation.

Table 14. Results of Monte Carlo and Linear Analysis

Error Case	Ellipse Orientation	Monte Carlo 1σ Errors				Linear 1σ Errors		
		r_p, km	r_a, km	Period, hr	Orientation, deg	r_p, km	r_a, km	Orientation, deg
1	100	48.2	244.2	0.196	0.495	44.2	258.6	0.434
	110	49.2	285.2	0.238	0.446	44.1	327.5	0.430
	120	47.8	351.3	0.293	0.442	43.3	409.1	0.446
	130	47.4	422.6	0.347	0.443	43.4	443.7	0.462
	140	48.7	432.5	0.352	0.455	45.3	408.9	0.487
	150	51.4	368.8	0.301	0.478	48.8	323.5	0.517
2	100	47.0	285.6	0.225	0.513	44.2	310.9	0.442
	110	49.2	315.8	0.258	0.453	44.1	376.0	0.433
	120	48.9	389.3	0.320	0.449	43.3	450.8	0.446
	130	46.7	444.5	0.361	0.449	43.4	480.5	0.465
	140	47.7	453.1	0.365	0.443	45.3	442.8	0.476
	150	50.3	393.4	0.318	0.484	48.9	356.1	0.533
3	100	13.47	274.5	0.206	0.456	11.66	248.4	0.422
	110	7.05	260.1	0.194	0.442	5.87	232.9	0.423
	120	1.67	232.3	0.174	0.441	0.06	218.7	0.430
	130	5.53	210.4	0.156	0.420	6.07	233.6	0.422
	140	11.53	227.5	0.165	0.393	12.94	249.1	0.425
	150	19.77	236.3	0.170	0.418	22.38	234.6	0.468
4	100					11.66	178.2	0.413
	110					5.86	141.8	0.421
	120					0.06	109.4	0.430
	130					6.06	143.4	0.420
	140					12.86	182.1	0.415
	150					22.17	181.3	0.450
5	100					14.45	251.1	0.423
	110					10.53	240.2	0.423
	120					8.66	232.5	0.430
	130					10.52	248.2	0.425
	140					15.58	259.7	0.428
	150					24.01	240.6	0.471

610-3

ORBIT INSERTION ACCURACY ANALYSIS

ACCELEROMETER SHUTOFF
(ERROR CASES 1 AND 4)

ERROR SOURCES (1σ):

SHUTOFF	0.115%
POINTING	7.33 MRAD
IGNITION TIME	10 SEC
ORBIT DETERMINATION	50 KM ———
	0 KM - - - - - -

o o o MONTE - CARLO

x x x LINEAR

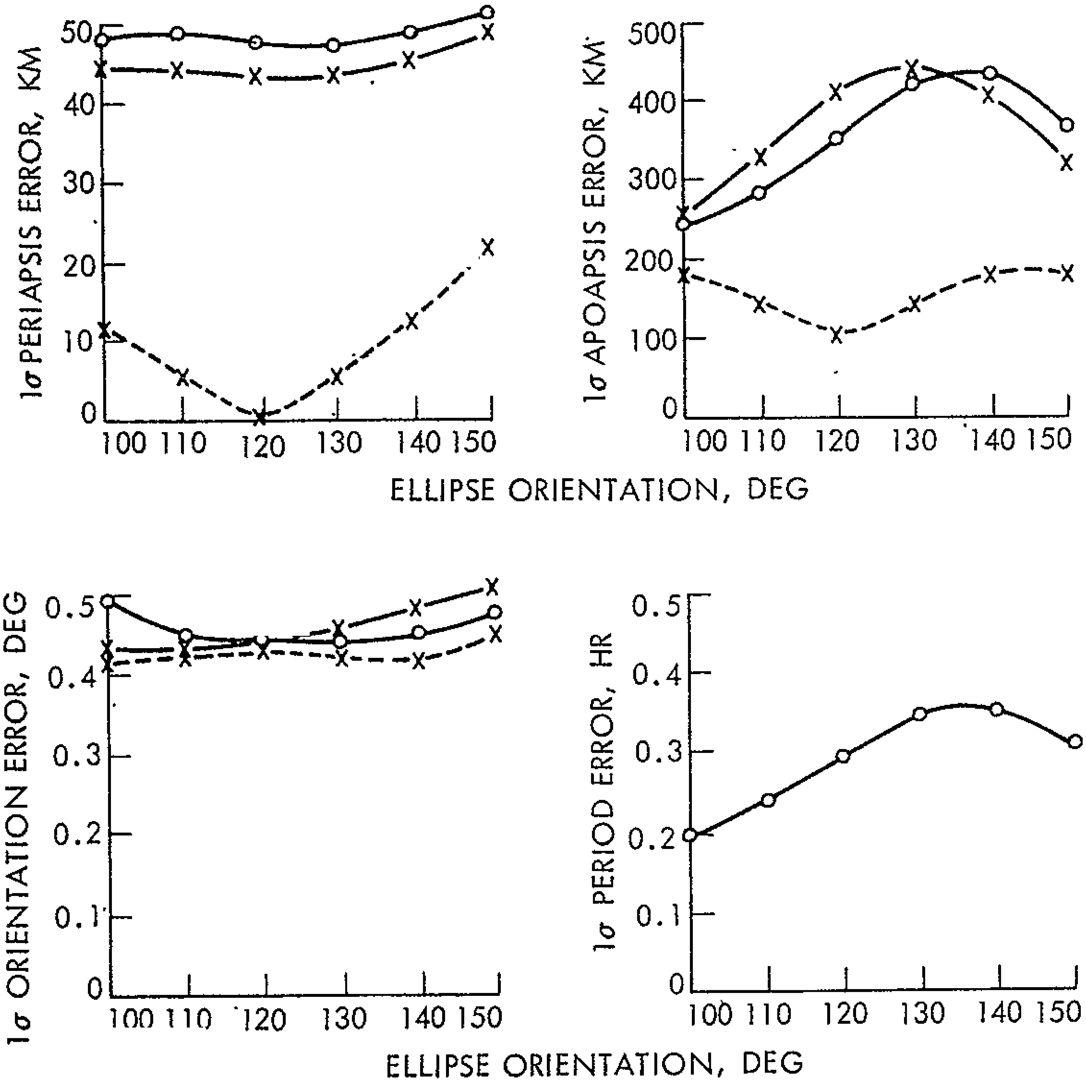

Figure 25. Orbit Insertion Accuracy Analysis

610-3

TIMER SHUTOFF
(ERROR CASES 2, 3 AND 5)

ERROR SOURCES (1σ):

SHUTOFF	0.19%
POINTING	7.33 MRAD
IGNITION TIME	10 SEC
ORBIT DETERMINATION	50 KM ———
	10 KM —·—·— (APPROACH GUIDANCE)
	0 KM - - - - - -

o o o MONTE CARLO

x x x LINEAR

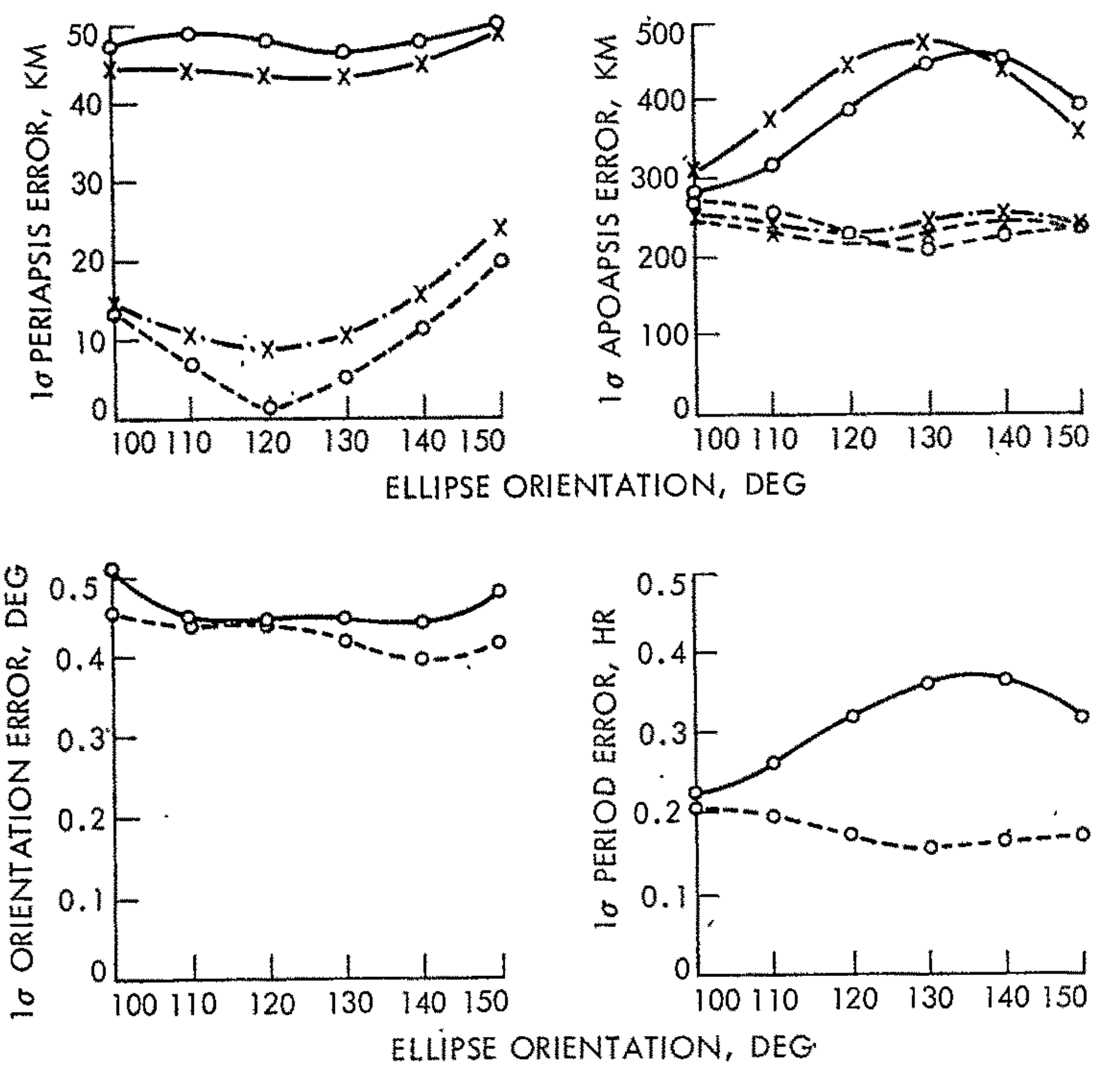

Figure 26. Orbit Insertion Accuracy Analysis

3. Power Margins

The Mariner 1971 electrical power requirements are satisfied by a power subsystem of Mariner 1969 design. Guaranteed 1969 solar array power exceeds 450 watts during the interplanetary trajectory phases of the 1971 Mars mission. In the orbital phase, the output of the solar array will decline to approximately 400 watts by the end of the 90-day period. A maximum Mariner 1971 spacecraft system load of 391 watts occurs during maneuvering. Two maneuvers are provided for trajectory correction and a third period of maneuver loads occurs at orbit insertion.

The power margin is 50-60 watts in excess of the load. During orbit, the margin will remain above 50 watts for normal operations, considering a maximum normal load of 348 watts during playback. A power profile of the Mariner 1971 Orbiter is tabulated below:

Phase	Power (watts)
Launch	348
Cruise	306
Maneuver	391
Orbit Insertion	391
Planet Scan	342
Orbit Playback	348
Orbit Cruise	306
Orbit Cruise (gyros)	325

Use of the traveling wave tube in the 20-watt mode is assumed only for orbit playback. During playback, science is assumed to be off. The temperature control subsystem requires 15 watts more than Mariner 1969, for a total of 47 watts.

The autopilot accelerometer was assumed to require 3 watts. CC&S relay hold was considered to require 4 watts extra during the launch phase, accounting for additional output relays.

4. Science Instrument Pointing Capabilities

The Mariner Mars 1971 Orbiter system uses the Mariner 1969 scan platform and scan control subsystem to accomplish pointing of the television cameras and the infrared radiometer during the science mission. Pointing is possible both in clock angle and cone angle within the physical restrictions of the platform-spacecraft configuration. Each axis of the platform is controlled by a position servo that follows an adjustable reference voltage. Adjustment of the references is made by the CC&S according to a preprogrammed sequence, or by quantitative commands from Earth. The scan program stored in the CC&S is updated by sending coded commands to the spacecraft. Quantitative commands are sent to scan to update the initial pointing angles. Sufficient flexibility exists to permit scan adjustments after each television picture, if needed.

B. Physical Characteristics

1. Configuration

Groundrules. For the purposes of this study, the following groundrules were used to develop an acceptable configuration:

(1) Use of the Mariner 1969 spacecraft design to the maximum extent which configurationally assumes the basic bus and electronics packaging are unchanged.

(2) Consideration of the Mariner 1969 scan platform as being modified only as required to reduce the science complement to television and infrared radiometer sensors.

(3) Integration of the proposed propulsion system defined as three bipropellant engines with a total system mass of approximately 1,100 pounds.

(4) Maintenance of the launch vehicle interface established for Mariner 1969 to the maximum extent. (This groundrule implies no change in shroud or shroud envelope and, if possible, no change to the Centaur mechanical interface.)

Within the above basic requirements, the configuration illustrated in Figure 27 was developed to demonstrate a compatible, minimum-modification system. Configurational changes are limited entirely to those required to integrate the propulsion subsystem with no additional revisions to functional requirements being anticipated. The following description summarizes, by subsystem, the extent of required modification to achieve the proposed configuration.

<u>Basic Structure</u>. The Mariner 1971 propulsion subsystem is mounted to the top of the bus at four existing structural tie points. To carry the additional load, the bus structure and spacecraft adapter must be resized by the use of heavier gauge material, but no change to the basic design is required.

The propulsion subsystem structure has the task of integrating the four 24-inch-diameter propellant tanks, two 10-inch-diameter pressure tanks, and three engines into a structurally independent module. In addition, the design must take into consideration numerous external interfaces--alignments for critical

NONSTANDARD

NONSTANDARD

hardware such as Sun sensors and motor gimbals, attachments for low- and high-gain antenna tiedowns and the routing of plumbing, cabling, and thermal shielding. Because of the size and degree of difficulty in developing an acceptable subsystem configuration, a certain number of minor compromises are conceded in the integration of the remaining subsystems.

Solar Panels. The power requirements for this mission are satisfied by solar cell areas achievable with four Mariner 1969 panels. As illustrated in Figure 27, the panels are required to hinge from outrigger supports to obtain clearance to the propulsion tankage and the shroud. However, the panels, the panel latching, and the deployment hardware can be used without change.

Antennas. The high-gain antenna considered for the 1971 Mariner Mars orbiter mission is a 48-inch-diameter dish of Mariner 1969 construction. Due to the size and location of the propulsion module, the antenna is relocated to a launch configuration above the module and deployed to a cruise position following spacecraft separation. Critical alignments are maintained by establishing the antenna interface at the bus structure and providing a mast-type support of sufficient stiffness to satisfy both structural and alignment requirements. The antenna deployment would be accomplished by a simple spring device.

The low-gain antenna must be positioned approximately perpendicular to the roll axis during cruise. Within the shroud envelope limitations, solar panels, and propulsion module restrictions, the 1969 wave guide antenna selected must be mounted on an outrigger structure and stowed like the high-gain antenna. Post-separation deployment by a spring device must be accomplished in sequence with solar panel deployment in order to avoid possible interference.

Attitude Control Subsystem. Of the attitude control sensors, only the primary Sun sensors are affected by the inclusion of the 1971 Orbiter propulsion module. To provide sufficient field of view, the primary sensors are relocated to attachments on the propulsion subsystem. This location assumes acceptable alignments can be achieved and thermal protection from propulsion engine radiation can be provided. If further study indicated an unacceptable compromise, an alternate primary sensor location on the solar panel outrigger supports could be implemented, using a network of sensors to obtain full coverage.

Configuration changes to the attitude control gas system include the addition of two more Mariner 1969 tanks but are otherwise limited to a revised mounting location on opposite solar panel support structures. Attachment interfaces for both the panel-mounted jets and the outrigger-mounted tank and regulator assemblies are unaltered, with the only anticipated hardware change being a revised routing of the low-pressure plumbing components.

Science. Although the science payload defined consists of an abbreviated Mariner 1969 complement, no changes are anticipated in the basic integration of this subsystem. Existing platform structure and scan hardware would be utilized with only minor modification to take advantage of the decreased payload.

2. Summary of Mariner 1969 Subsystem Changes

Structure Subsystem. The Mariner 1971 spacecraft uses a 1969 octagon structure modified to limit test accelerations at the propulsion tankage assembly. The 1969 propulsion subsystem is removed from Bay II. The large Mariner 1971 propulsion subsystem is mounted on top of the bus, replacing the former superstructure. Support structure is added for the new propulsion subsystem. A new support structure is required for the low-gain antenna and a new aperture design is required. A new high-gain antenna structure having a 48-inch circular aperture and integral reinforcement is used on Mariner 1971. A mounting boom for the high-gain antenna and provisions for deploying both antennas are included in the structure subsystem. The spacecraft adapter structure is redesigned for the greater weight of the 1971 orbiter, its different weight distribution, and for the associated changes in the motions the spacecraft will experience during launch. Outrigger support structure is added to provide an outboard mounting of solar panels that will clear the large propulsion tanks in a stowed configuration.

Radio Frequency Subsystem. The Mariner 1969 design is used, except for additional cable assemblies for the low- and high-gain antennas.

Flight Telemetry Subsystem. Only minor modifications to the 1969 design are required for the Mariner 1971 system.

Attitude Control Subsystem. The Mariner 1969 design is used with two additional tanks of nitrogen, a new autopilot, and gimbal drives for the three rocket engines in the propulsion subsystem.

Pyrotechnic Subsystem. Redesign is required to provide for firing the new propulsion valves. A new V-band release device will be required because of the increased V-band tension required to accommodate the heavier spacecraft. Additional pyrotechnic devices are provided for release of the deployable antennas.

Cabling Subsystem. The 1971 cabling involves some increase in propulsion and pyrotechnic wiring; otherwise, the mechanical design of the cabling and the cabling configuration will be unchanged from 1969.

Propulsion Subsystem. Propulsion is a new subsystem, using three Marquardt R-4D engines, all three of which are gimballed for thrust vector control. The propellant (934.80 lbs for $C_3 = 10\ km^2/sec^2$) is stored in four tanks mounted on top of the octagon bus.

Temperature Control. The Mariner 1969 design is used with some additional weight for the upper thermal shield and rocket radiation shields.

Devices. Using the modified 1969 structural criterion, the V-band assembly is retained for Mariner 1971. In addition to the Mariner 1969 devices, a high-gain antenna boom deployment and positioning mechanism is required. A mechanism for deploying the low-gain antenna is also added. Outboard mounting of solar panels requires a new cruise damper and latch designs.

Data Storage Subsystem. The Mariner 1969 design is modified to provide the digital recorder with additional playback speeds of 16,200 bps and 8,100 bps.

Data Automation Subsystem. The Mariner 1971 Data Automation subsystem is essentially the same as for 1969; only minor hardware changes are needed.

Unchanged Subsystems. The following Mariner Mars 1971 subsystems are unchanged from the 1969 design: flight command, power (with possibly extra output relays), CC&S, scan control (with far-encounter planet sensor deleted) television, and infrared radiometer subsystem.

Deleted Subsystems. Both the Mariner 1969 ultraviolet spectrometer and infrared spectrometer are deleted from the Mariner 1971 Orbiter design.

3. Weight Breakdown

The Mariner 1969 launch weight is estimated to be 881.92 pounds in November 1967. The weight of the Mariner 1971 spacecraft design is 1,971.6 pounds. Thus, the 1971 spacecraft weighs 1,089 pounds more than Mariner 1969 in the launch configuration.

The changes required to implement the Mariner 1971 from the 1969 subsystem designs were described in the preceding section. Most of the weight adjustments associated with these changes are minor. The new propulsion subsystem used in Mariner 1971 accounts for 92% or 1,003 pounds of the total weight increase. Propellant alone weighs 934 pounds for the 1971 mission.

Other changes of significance are: a growth of 50% in the weight of the structure, from approximately 200 to 300 pounds; attitude control increase to 86 pounds from 62; and, the omission of the ultraviolet and infrared spectrometers from the 1971 science payload, which removes 67 pounds.

4. Propulsion Subsystem

Introduction. The Mariner 1969 propulsion subsystem is inadequate for an orbiter mission because its total impulse capability is far short of that required to establish orbit. A new propulsion subsystem design is presented, based on maximum usage of existing designs and hardware from current and near-past space programs.

The following assumptions were made regarding propulsion subsystem design criteria:

(1) The spacecraft design mass (exclusive of propulsion) would be 780.6 lbm. The design ΔV would be ≤ 1.9 km/sec.

(2) A single propulsion unit would be used for both the midcourse and orbit insertion maneuvers.

(3) Only existing, flight-qualified, bipropellant liquid engines would be considered.

(4) Six propulsion starts were required (two midcourse, one orbit insertion, and three orbit trim), and eight would be desirable.

Note at the outset that the available thruster options are severely limited by assumption (3) above, while the propulsion feed system design is heavily influenced by assumption (4).

In the remainder of this section, the rationale for the bipropellant system selection is given, followed by a description of the characteristics of the selected system. Some considerations of a propellant substitution for increased payload capability are given in Appendix B. Examination of an alternate solid propellant system is also presented.

Propulsion Subsystem Selection Rationale.

(1) Rocket Motor Selection. It would be desirable for this application to provide a propulsion subsystem with a single gimballed engine in the thrust range of 300 to 1,000 lbf. A survey of current technology satisfying the flight-proven hardware constraint failed to reveal any satisfactory engines in the applicable thrust range. The selection was therefore limited to lower-thrust engines.

The choice between a single low-thrust engine and multiple low-thrust engines is influenced by several factors. A single low-thrust engine such as the Marquardt Corporation R-4D Apollo Reaction Control engine (100 lbf thrust) would be suitable from engine lifetime considerations, since it is radiatively cooled and is designed for deliverable total impulse of up to 10^6 lbf-sec. There are, however, several generally undesirable characteristics which can be attributed directly to such a mechanization.

First, the low-thrust capability dictates a rather large burn time requirement--of the order of 50 minutes. This means that the spacecraft must be designed for full attitude stabilization, using internal references (gyros) for a time period in excess of one hour. This is normally not considered desirable.

Second, the spacecraft power supply must be designed to provide all the power normally required by the spacecraft, plus a peak load demand by the propulsion subsystem for this same time period (greater than one hour). This consideration places an undesirably large battery design capability requirement on the spacecraft.

In addition to the two considerations mentioned above, preliminary analysis of 1971 Mars orbit insertion trajectories revealed a definite possibility of Earth occultation during the orbit insertion maneuver if such a long burn time were to be accommodated. Analysis also revealed that gravity-burn-time losses would be significant for these long burn times, thereby resulting in decreased spacecraft performance capability. For instance, with a periapsis altitude of 1,000 km and a V_∞ of 3.5 km/sec, the gravity losses for a velocity increment of 1.5 km/sec were estimated to be about 53 m/sec, or of the order of 8%. Gravity burn-time losses for a three-engine system (300 lbf total) are negligible for the same conditions assumed above. On the basis of the above considerations, it was decided that a three-engine configuration would be more appropriate for the application under consideration.

Figure 28 shows the ideal velocity increment available and required burn time for a three-engine system as a function of useful propellant mass. It was assumed that the spacecraft bus mass is 780.6 lbm and that the propulsion system specific impulse is 294.5 lbf-sec/lbm. It was further assumed that the propulsion subsystem mass fraction was 0.83 (mass of useful propellant/total propulsion system mass). It is shown in Figure 28 that, for a design ΔV of 1.9 km/sec, about 900 lbm of useful propellant would be required. This was chosen as the design propellant mass for this study. It can also be seen from Figure 28 that, for this design point, the burn time will be about 880 seconds.

Two engines are qualified for this application: (1) the Marquardt Corporation Model R-4D Apollo Reaction Control engine, and (2) the Thiokol (Reaction Motors Division) Model TD-339 engine used in the Surveyor vernier application. The TRW Systems throttleable MIRA 180, designed as the Surveyor vernier backup, would also appear to be acceptable, with the exception that it has not been used on a flight program. The Thiokol (RMD) Model C-1 engine is also a candidate for this application. This engine is partially regeneratively, partially radiatively cooled and has some design characteristics similar to the Surveyor engine. The C-1 has not been flight-qualified. The C-1, like the Marquardt R-4D, is not currently designed for throttling capability.

Engine selection, then, was limited to a choice between the Marquardt R-4D and the Thiokol TD-339. The R-4D is not a throttled engine but rather, is designed for gimballed applications. The TD-339 is designed for throttled applications (e.g., Surveyor). Thus, the thrust vector control mechanization would be quite different for the two engines. The three-engine throttled

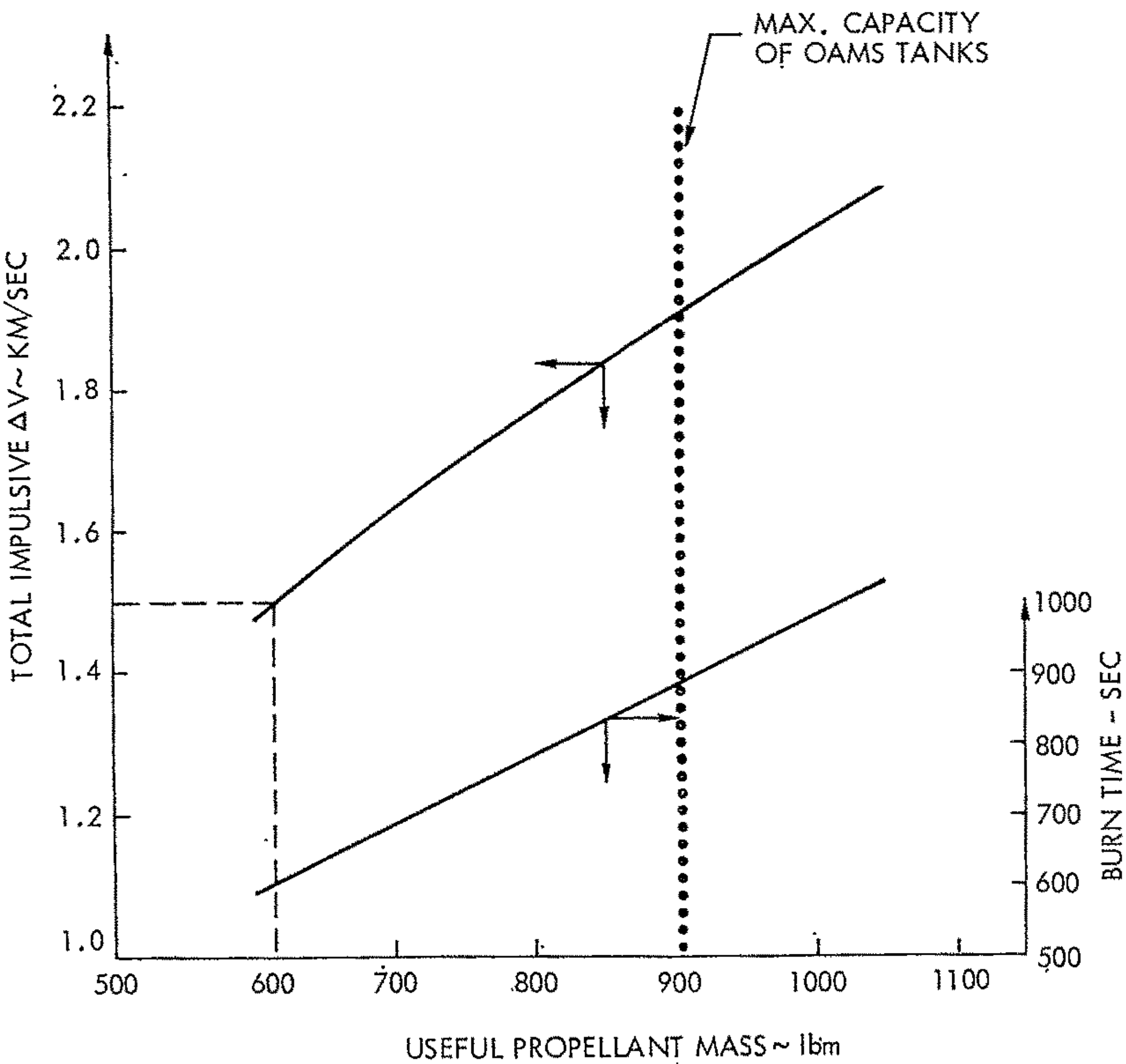

Figure 28. Impulsive ΔV and Burn Time vs. Useful Propellant Mass

concept has been used on Surveyor and is a familiar autopilot mechanization The three-engine gimballed mechanization has not been previously used in spacecraft applications, although launch vehicles with multiple gimballed engines are the rule rather than the exception.

There is a flight velocity increment bias associated with center-of-gravity offsets in the case of gimballed engines. Adjusting for this bias adds complexity to the autopilot mechanization. The throttled engines would not require the adjustment because the thrust vector in this case is translated until it extends through the spacecraft center-of-gravity, rather than the vector being rotated. On the other hand, the three-engine throttled syst is a more complex propulsion system than the three-engine gimballed system.

The TD-339 engines operate at relatively high (250 psia) chamber pressure and also require a high pressure drop across the throttle valves and injector. This condition manifests itself primarily in the larger mass of propellant tankage, feed system, and pressurization system required for proper operation of the TD-339. The R-4D engine operates with a nominal 96.5-psia chamber pressure and, because it is not throttled, has a relatively low pressure drop across the injector.

On the basis of the above considerations, the R-4D engine was selected for the purposes of the current study.

(2) Propellant Acquisition. Nearly vapor-free propellants must be supplied at the tank outlets prior to initiation of a propulsive maneuver. Three methods for zero-g propellant acquisition were considered: start tank, auxiliary thrusters, and main tank gas-liquid separation.

A small metal bellows start tank was considered. This concept appears to be somewhat more complex than the others but has been successfully used on the Gemini Docking Target Vehicle. A metal bellows start-tank would provide positive expulsion for engine starting and, once propellant settling was accomplished, the engines would be "switched over" and fed from the main tankage.

Auxiliary cold gas settling jets were also considered. The thrust levels required to settle propellants in a reasonable time may be above those used for spacecraft cruise mode attitude control; a separate settling system would be required in this case. This option requires further study and may be competitive with the propellant acquisition concept chosen.

Two classes of gas-liquid separators were considered: plastic bladders and metal diaphragms. Bladders, although allowing propellant permeation into the pressurizing circuit and permitting some pressurizing gas to diffuse into the propellants, are a common type of spacecraft propellant acquisition device. Their salient feature is that they allow a large number of expulsion cycles without a compromise in expulsion efficiency or weight. Metal diaphragms can be designed for essentially zero permeation but suffer from a lack of recycleability for checkout and an increase in weight over a comparable bladder.

Plastic bladders were chosen as the method for positive propellant acquisition. This decision was influenced by the fact that flight-qualified propellant tanks that appear to be capable of satisfying the Mariner 1971 propulsion subsystem design requirements are available from the Gemini Program. These tanks are currently equipped with bladders and are discussed in more detail below. The pressurizing gas circuit was designed to prevent possible mixing of different fuel and oxidizer vapors.

(3) Propellant Tanks. The Gemini Orbiting and Maneuvering System (OAMS) propellant tanks appear to be satisfactory for this application. These tanks are spherical in shape and have a 22-inch diameter. The OAMS propellant tanks are fabricated from 6Al-4V titanium and have an available propellant volume of approximately 5550 in^3. The tanks have a 0.010-inch-thick laminated TFE/FEP Teflon bladder. The normal operating pressure for these tanks is suitable for the R-4D engine application. The OAMS tanks, therefore, can be used in their present Gemini configuration with the Marquardt R-4D engine.

Large reductions in bladder permeation rates, likely to be needed for the extended planetary missions, can be achieved through the use of the new laminate configurations already tested in advanced development programs.

(4) Auxiliary Hardware. The Surveyor regulator, although not optimum for this propulsion design, would be adequate for the Mariner 1971 application The squib isolation valves would be identical or quite similar to those used on Surveyor or Mariner. The helium pressurization tanks would most certainly reflect the current Apollo program technology, if not actual Apollo hardware, although the latter point has not been pursued in depth during this study.

Propulsion System Characteristics. Figure 29 shows a schematic of the propulsion subsystem design; a summary of its characteristics is presented in Table 15. The operating characteristics of the Marquardt R-4D are shown in Table 16.

Unlimited start capability for this system is provided by the solenoid-actuated valves, which are part of rocket motor assemblies. However, in order to assure leak-free operation over the mission lifetime, the starts are restricted to occur during the propulsion firing periods. The maximum

610-3

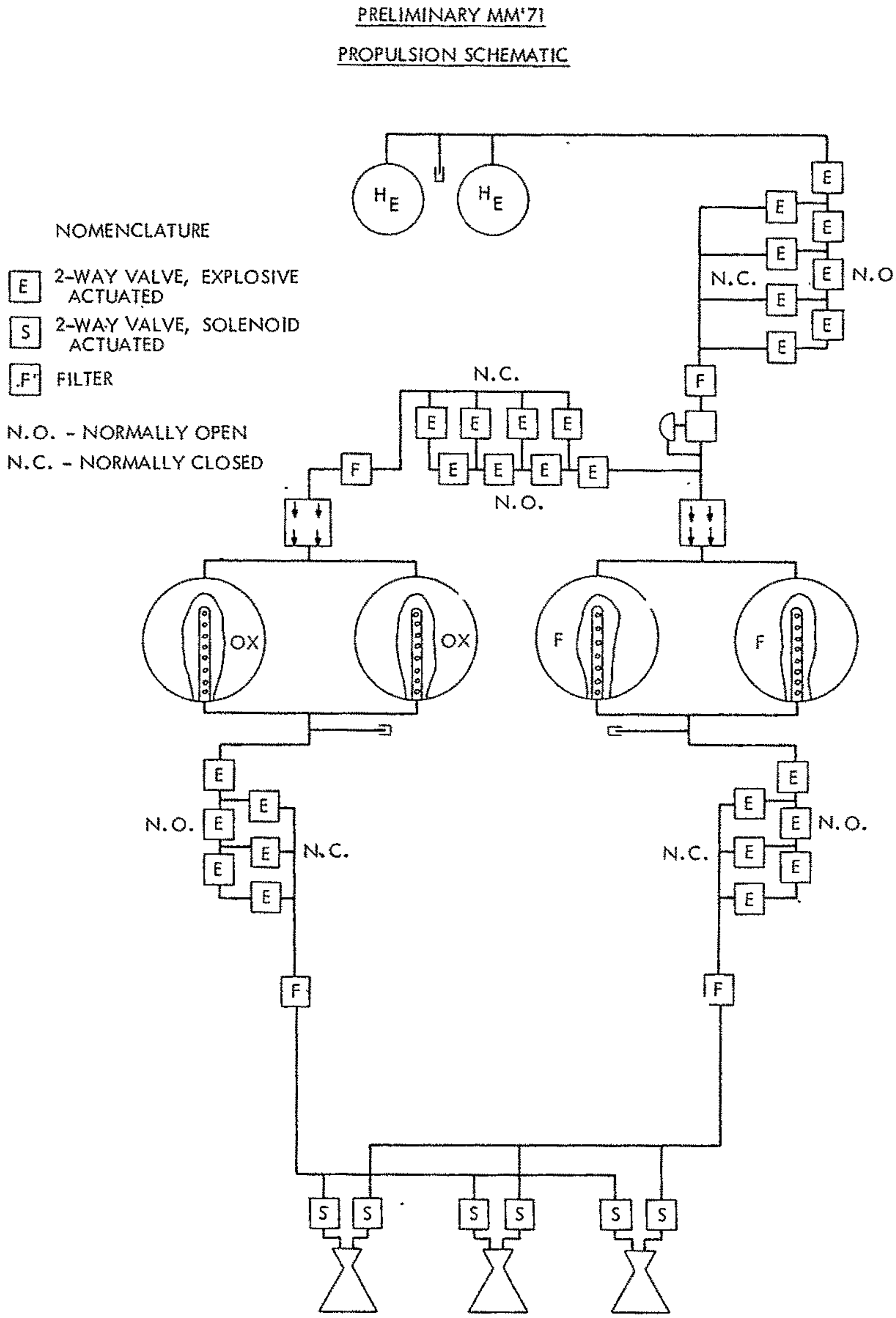

Figure 29. Preliminary MM'71 Propulsion Schematic

610·3

Table 15. MM1971 Orbiter Propulsion System Design Characteristics

	lbm	lbm
System Mass Estimate		
Usable Propellant	907.6*	
Residual Propellant	27.2	
Total Propellant		934.8
Helium Tanks (2)	27.9	
Helium Gas	2.3	
Pressurization Lines, Regulator, & Fittings	10.0	
Pressurization Valves (16)	8.0	
Total Pressurization System		48.2
Propellant Tanks and Bladders	41.0	
Propellant Feed System Valves (12)	6.0	
Propellant Feed System Lines and Fittings	5.0	
Total Propellant Feed System		52.0
Thrust Chamber Assemblies		14.6
Structure and Thermal Control (Assumed)		75.0
Total Propulsion System (Fully Loaded)		1,124.6
Propellant Mass Fraction		0.81
Nominal Propulsion Firing Periods		3
Minimum Impulse Bit ~ lbf-sec		1.53 ± 0.54
Total Impulse Capability ~ lbf-sec		267,288

* Maximum propellant load

610-3

Table 16: Estimated Operating Characteristics of R-4D Apollo Reaction Control Rocket Motor for MM 1971 Application

Performance	
Thrust (Vacuum) - lbf	100
Chamber Pressure - psia	96.5
Specific Impulse (nominal) $\frac{\text{lbf-sec}}{\text{lbm}}$	294.5
Mixture Ratio (O/F)	1.6:1
Dimensions	
Length (overall) in.	16.7
Width (overall) in.	7.3
Throat Diameter - in.	0.868
Throat Area - in.^{2}	0.592
Exit Diameter - in.	6.72
Exit Area - in.^{2}	35.52
Combustion Chamber Diameter - in.	1.77
Combustion Chamber Area - in.^{2}	2.46
Expansion Area Ratio	60:1
Contraction Area Ratio	4.16:1
Miscellaneous	
Propellants	N_2O_4/50% N_2H_4 + 50% $(CH_3)_2$ NNH_2
Cooling Method	Combined fuel film cooling and radiation cooling
Thrust Vector Control	Gimballed
Dry Weight - lbm	5.0
Required Voltage (VDC)	27 ± 3
Reliability (90% conf.)	0.997 (goal) 0.97 (demonstrated)

Table 17. Firing Period Starts and Times of Occurrence

Firing Period	Propulsion Start	Time of Occurrence
First	1st Trajectory Correction 2nd Trajectory Correction	Launch + 2 to 10 days Launch + 10 to 30 days
Second	3rd Trajectory Correction* Orbit Insertion 1st Orbit Trim 2nd Orbit Trim	Encounter -30 to -10 days Encounter Insertion + 1 day Insertion + 2 days
Third	3rd Orbit Trim 4th Orbit Trim*	Insertion + 54 days Insertion + 50 to 80 days

* Optional--if warranted by Orbit Determination

allowable length of these periods is not yet fixed but probably would be on the order of one month. Explosively actuated valves serve to isolate these separate firing periods by locking the system, thus avoiding any possibility of leakage during the intervals between firing periods.

Table 17 shows the propulsion starts allocated to each firing period and the approximate time of occurrence of each.

Figure 29 shows the two fuel and two oxidizer OAMS tanks required. Two helium pressurization tanks are packaged symmetrically in the spacecraft to maintain center-of-gravity control. Four pairs of isolation valves are shown between the helium pressurization tanks and the regulator, and another four pairs between the oxidizer and fuel systems. The first set of valves isolates the pressurizing gas between propulsive maneuvers, thus preventing leakage int the propellant tanks. The second set prevents mixing of propellant vapors should the check valves fail during the long coast periods. Three pairs of each set are required for the nominal propulsion firing periods. The fourth pair is provided as a backup should any of the other three pairs fail. The fourth valve pair also allows an additional firing period, providing that no previous failures are encountered. Further reliability studies should be performed in order to ascertain the necessity of the propellant isolation explosive valves, in light of projected reliability estimates for quad-redundant check valves. Quad-redundant valving was also considered, but was felt to be an unnecessarily penalizing concept in terms of added weight and complexity, in light of the high reliability of the squib valves envisioned for the Mariner 1971 design. Explosively actuated isolation valves are also shown in both the fuel and oxidizer feed lines.

For clarity, no instrumentation or test points are shown in Figure 29. These would, of course, be required on the flight units. It should also be mentioned that a reliability analysis should be performed during future Mariner 1971 studies in order to determine the trade-offs between the single regulator shown and possible redundancy applications.

As can be seen from Table 15, the total estimated mass of this design is 1,124.6 lbm, which includes 934.8 lbm of propellant (907.6 usable), 114.8 lbm of dry propulsion mass (including inerts), and an allocation of 75 lbm for the propulsion mounting structure and propulsion thermal control. These estimates yield a propellant mass fraction (mass of usable propellant/total propulsion subsystem mass) of 0.81.

Solid Propellant System Alternate. Despite the constraining assumptions listed above, some considerations have been given to the use of the Applica-

610-3

Table 18. Design Parameters for ATS Apogee Motor

Burning Time (sec)	43.5
Maximum Chamber Pressure (psia	260.0
Maximum Vacuum Thrust (lbf)	,250.0
Total Weight (lbm)	837.5
Propellant Weight (lbm)	760.0
Propellant Mass Fraction	0.91
Maximum Diameter (in.)	28.2
Overall Length (in.)	54.6
Throat Diameter (in.)	4.08
Expansion Ratio	35:1

tions Technology Satellite (ATS) Apogee Motor against Mariner 1971 design requirements. This motor uses a solid-propellant formulation, and is designed in its current application to place a 1,625-lbm spacecraft into a synchronous Earth orbit. The propellant is a conventional polyurethane ammonium perchlorate-aluminum system. Pertinent design parameters are shown in Table 18.

Use of the ATS motor for the Mars orbit insertion maneuver would, of course, require an auxiliary propulsion unit on the spacecraft to perform the required midcourse and orbit trim maneuvers and to provide thrust-vector control for the solid orbit insertion motor. The ATS motor has sufficient performance capability to provide the velocity increment needed at the planet. The progressive burning characteristics of this motor indicate that a maximum acceleration level of greater than 4.5 g could be expected. This acceleration level places a serious constraint on the use of Mariner 1969 subsystems and hardware (e.g., solar panels), since these items are designed to withstand only 1 g with the solar panels extended. For this reason, the ATS motor was dropped from further immediate consideration.

610-3

REFERENCES

1. Focas, J. H., "Seasonal Evolution of the Fine Structure of the Dark Areas of Mars," Planetary and Space Science, Vol. 9, pp. 371-381, January-February 1962.

2. Neugebauer, G., "A Proposal for a Surface Temperature Measurement for the Mariner Mission to Mars, 1969," California Institute of Technology.

3. "Centaur Configuration, Performance, and Weight Status Report," Report GDC 63-0495-49, Contract NAS 3-8711, August 1967, General Dynamics-Convair.

4. Kohlhase, C. E. and Bollman, W. E., "Trajectory Selection Considerations for Voyager Missions to Mars During the 1971-1977 Time Period," EPD 281, Jet Propulsion Laboratory, September 15, 1965.

5. Stavro, William, "A Study of Finite Burn Gravity Losses," Technical Memorandum 213-1, Voyager Interim Project Office, MA&E, April 17, 1967.

6. Dahlgren, J. B., and Committee, "Antenna Pointing Mechanization Study," Section Report 349-1, Jet Propulsion Laboratory, April 15, 1966.

7. Kliore, A. and Tito, D. A., "Radio Occultation Investigations of the Atmosphere of Mars," Technical Report No. 32-1157, Jet Propulsion Laboratory, May 1967.

8. Hamilton, T. W. and Melbourne, W. G., "Information Content of a Single-Pass of Doppler Data from a Distant Spacecraft," Space Programs Summary 37-39, Vol. III, Jet Propulsion Laboratory, May 31, 1966.

9. Light, Jay O., "Orbit Redetermination Following First Midcourse Maneuver," Technical Memorandum 312-552, Jet Propulsion Laboratory, May 3, 1965.

APPENDIX

A. Performance and Payload Capability for Related Missions

This section of the Appendix compares the trajectory and performance characteristics for alternative orbiter missions to Mars and Venus. Table A-1 presents a comparison of the interplanetary trajectory characteristics for the Mars 1971, Mars 1973, Venus 1972, and Venus 1973 launch opportunities. In all four missions, a 30-day launch period was assumed. An arrival period of six to seven days was used except for the Mars 1973 opportunity, where only a three-day separation was allowed because of limited range of acceptable trajectories.

A comparison of the Mars 1971 and 1973 opportunities immediately reveals the superior nature of the earlier opportunity. While the maximum approach speeds (V_∞) are equal, there is a substantial difference between the required launch energies (C_3). Quite striking also are the larger flight time, communication distances, and Sun-Mars distances for the 1973 period. The Venus 1972 and 1973 opportunities, however, do not exhibit such large overall differences. The most significant characteristic revealed in comparing these two opportunities is the smaller approach speeds existing for 1973.

The orbit insertion velocity increments that result from the approach speeds, together with the midcourse maneuver and orbit trim ΔV's, are summarized in Table A-2, which also includes lunar information. For the Mars 1971 mission, a 12-hour orbit with a ±10-degree apsidal rotation capability was assumed.

Table A-1. Interplanetary Trajectory Characteristics

Mission	Launch dates	Arrival dates	C_3 max, km^2/sec^2	V_∞ max, km/sec	Flight Time, days	Communication Distance, 10^6 km			Distance from Sun, 10^6 km		
						E	E +30	E +90	E	E +30	E +90
Mars '71	5/4/71 - 6/4/71	11/14/71 - 11/21/71	10.0	3.26	164 - 200	129	164	244	212	217	228
Mars '73	7/12/73 - 8/12/73	2/9/74 - 2/12/74	16.6	3.26	180 - 200	185	215	300	235	240	248
Venus '72	3/20/72 - 4/20/72	9/20/72 - 9/26/72	9.5	5.50	160-182	130	165	210	108	108	108
Venus '73	10/20/73 - 11/20/73	4/9/74 - 4/17/74	8.6	4.40	145 - 170	110	145	210	107	108	108

610-3

Table A-2. ΔV Requirements (m/sec)

	Mars '71	Mars '73	Venus '72	Venus '73	Moon
Insertion	1500	1450	1750	1500	900
Gravity Losses	15	15	15	15	15
Maneuver	15	15	15	15	15
Trim	200	100	100	100	270
TOTALS:	1730	1580	1880	1630	1200

Because of payload limitations resulting from the high C_3 requirement for the 1973 Mars opportunity, a 24-hour orbit was necessary as a result of the restricted ΔV capability. A ±20-degree apsidal rotation capability was allocated, however, because of periapsis lighting requirements. For the Venus missions, a 20-hour orbit was assumed for the 1973 opportunity. Because of the restricted ΔV capability available during the 1972 opportunity, a 60-hour orbit had to be used. Note that the trim allocation of 200 m/sec for the Mars 1971 opportunity resulted from the greater ΔV availability and not from any specific mission requirements.

Certain inconsistencies between the results discussed here and those associated with the Mariner 1971 Orbiter mission and shown in Section IV, should be ignored. These differences can be attributed to the many simplifications required in order to compare the variety of missions considered in this Appendix. An accurate comparison of the Mariner 1971 Orbiter with the various Mars and Venus missions would require more detailed studies to determine the payload and performance requirements more precisely.

Table A-3 summarizes the weight breakdowns for each of the five missions. Note that the variations in energy requirements allow for a variety of scientific payload weights that can be traded-off with spacecraft propulsion system velocity increment capabilities. This option is illustrated in Figure A-1, which shows a curve of spacecraft science payload as a function of C_3 for the fully loaded propulsion system. Lines of constant ΔV are also shown to illustrate the C_3 increase resulting from decreased science weight and propellant loading.

This discussion leads to the conclusion that all of the various missions outlined in this Appendix are feasible. However, strong preferences exist as to the year selected for Atlas/Centaur-launched orbiter missions to Mars and Venus. For the Mars missions, the 1971 launch opportunity is highly superior because of the increased mission capabilities afforded by the larger ΔV capability, lower communication distances, and more pronounced Mars seasonal changes during the orbiter lifetime. A Mariner orbiter in 1973 would be handicapped by a higher orbital period (resulting in fewer television sequences), limited ability to perform orbit modifications such as those discussed in Section IV, smaller arrival time separation and flexibility in arrival date choice, and lower data rates. For similar reasons, the 1973 opportunity appears to be much more suitable for a Venus orbiter mission.

610-3

Table A-3. Performance Summary

	Lunar	Mars '71	Mars '73	Venus '72	Venus '73
ΔV (M/S)	1200	1730	1580	1880	1630
S/C wt (lbs)	797	797	797	797	797
Prop wt (lbs)	915	875	660	935	865
Science wt (lbs)	888	198	13	168	288
TOTAL SEPARATED WT (lbs)	2600	1870	1470	1900	1950
C_{3E} (km^2/sec^2)	0	10.0	16.6	9.5	8.6

610-3

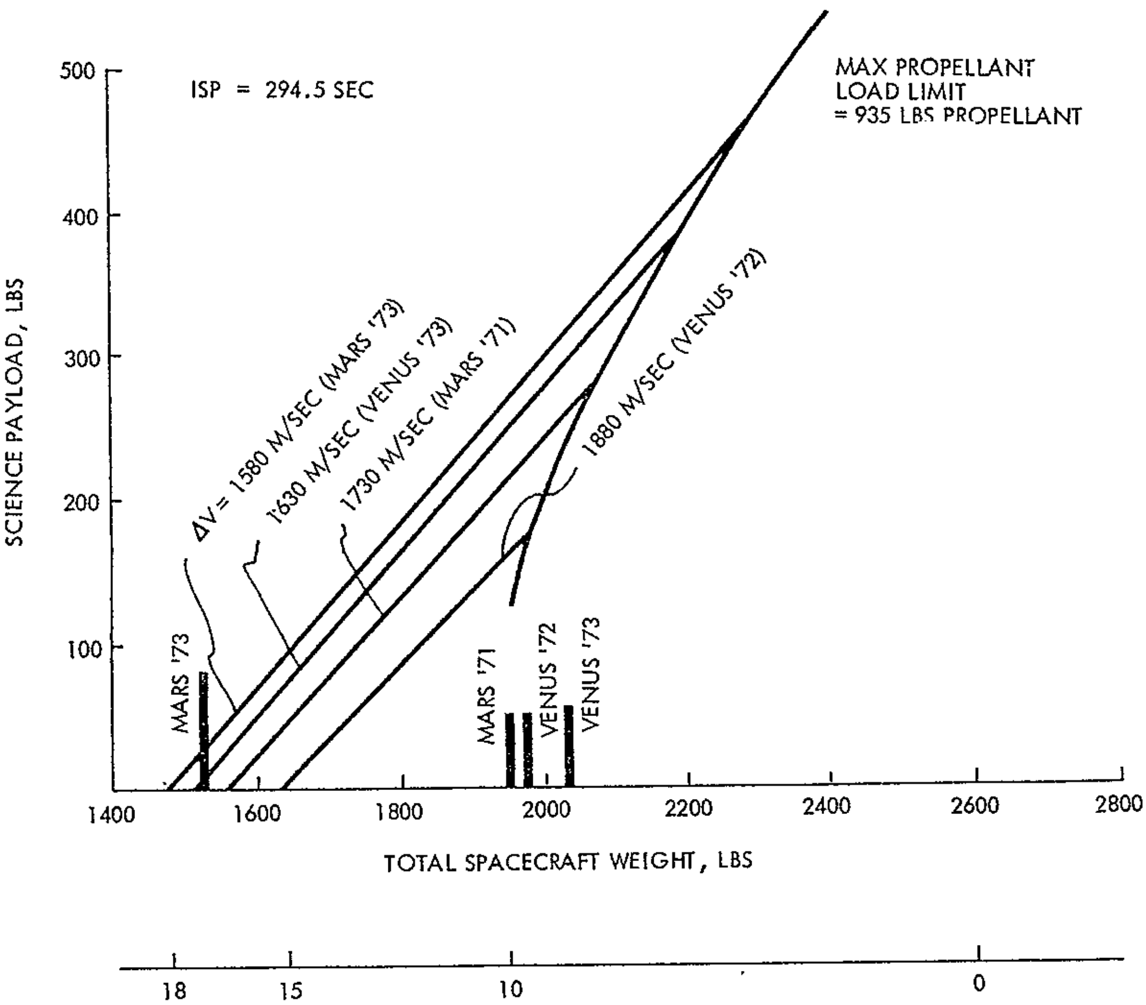

Figure A-1. Science Payload as Function of Injected Weight and ΔV

B. Propellant Substitution for Increased Payload Capability

While not integral to the Mariner 1971 mission study, the following comments bear on the desirability of the mission when viewed in terms of follow-on missions. Payload capability can be substantially increased through the use of space-storable propellants (OF_2-B_2H_6). This feature increases development costs and complexity of launch operations; however, in some cases, the payload increase represents the difference between a mission and none at all.

Much of the cost of development of a substitute space-storable propulsion module may be borne by Supporting Research and Advanced Development programs already underway and scheduled for maturity in Fiscal Years 1970 and 1971. Development of a complete system of a similar scale is a part of the present plan. Thus, the option of switching to a higher-performance propulsion module with nearly identical spacecraft interfaces is reasonably attainable for, say, the Mars 1973 mission opportunity.

With the exception of the Venus 1972 study, the total separated weight and the ΔV of each mission were kept constant, and the payload computed assuming space-storable propellants. The spacecraft mass (dry mass of the injected vehicle less the payload) was increased by 30 lbm to account for the increase in propulsion system dry mass due to the change from Earth- to space storable propellants. The theoretical I_{sp} of the space-storable combination at a mixture ratio of 3.75 is 430 lbf-sec/lbm. This value was corrected for an anticipated I_{sp} efficiency of 0.9. Furthermore, it was assumed that the

610-3

Table B-1. Comparison of Payload for Earth-Storable and Space-Storable Propellants

	Payload Mass, lb_m	
Mission	Earth-Storable Propellants	Space-Storable Propellants
Lunar	888	1034
Mars '71	198	335
Mars '73	13	122
Venus '72	168	293
Venus '73	288	417

propellant tanks used for Earth-storable propellants could also be used for the space-storable propellants. Table B-1 compares the attainable payloads for Earth-storable and space-storable propellants.

The Table clearly shows a significant payload increase for all missions and, notably, the 1973 Mars opportunity. Conceptually, propulsion module interactions with the rest of the spacecraft systems would be unaffected by the change from Earth- to space-storable propellants. All of the required structural (mounting) provisions and thermal control provisions could be accommodated in the propulsion module.

Thus, the use of space-storable propellants provides a significant increase in mission capability at the outset, or, provides a significant uprating capability if Earth-storable propellants are initially selected.